TRACE ELEMENTAL DISTRIBUTIONS WITHIN ORGANOPHOSPHATIC BRACHIOPOD SHELLS: IMPLICATIONS FOR GROWTH, PRESERVATION AND PALEOENVIRONMENT

by

TRISTAN JOSHUA BETZNER

B.S., University of Georgia, 2012

A thesis submitted to the

Faculty of the Graduate School of the

University of Colorado in partial fulfillment

of the requirement for the degree of

Master of Science

Department of Geological Sciences

2014

This thesis entitled:

Trace Elemental Distributions within Organophosphatic Brachiopod Shells: Implications for Growth and Paleoenvironment

written by Tristan Betzner

has been approved for the Department of Geological Sciences

_____

Karen Chin, Advisor

_____

David Budd

_____

Thomas Marchitto

Date_____

The final copy of this thesis has been examined by the signatories, and we

Find that both the content and the form meet acceptable presentation standards

Of scholarly work in the above mentioned discipline.

ABSTRACT

Betzner, Tristan Joshua (Department of Geological Sciences)

Trace Elemental Distributions within Organophosphatic Brachiopod Shells: Implications for Growth, Preservation and Paleoenvironment

Thesis directed by Associate Professor Karen Chin

The initial incorporation of elements into the accretionary hardparts of marine invertebrates is controlled by prevailing seawater chemistry and vital effects. While trace-element signatures of invertebrates accreting carbonate hardparts have been examined extensively, the shells of phosphatic organisms have largely been ignored. In this study, major and trace elements of fossil organophosphatic brachiopod shells are investigated to determine the fidelity with which their shell chemistry may be preserved, and to evaluate their potential as paleoenvironmental archives.

Trace elements within the shells of lingulid brachiopods from the Kanguk Formation of Devon Island, Arctic Canada and the Blufftown Formation of Stewart County, Georgia, USA were analyzed via electron microprobe. Elemental maps revealed spatial distributions, and element concentrations were measured within dorso-ventral transects proceeding toward the shell interior. The distributions of Mg, Na and Sr are similar among all lingulids, and absolute values of Mg and Na were similar between all fossil specimens. Concentrations of Mg and Sr are similar between fossil lingulids and modern calcitic brachiopods, suggesting that their signatures may be preserved.

Ca, Fl and P are zoned within fossil shells from Stewart County and a modern lingulid, but are heterogeneously distributed in Devon Island specimens. While Mn and Fe concentrations

are orders of magnitude greater in fossil lingulids than in modern calcitic brachiopods, they exhibit opposite distributional trends between fossil sites. Among fossil assemblages, elemental concentrations along dorso-ventral transects exhibit pronounced correlations between element pairs. Fossil specimens show a positive correlation between Na—Mg (80% of shells) and Fe—Mn (60% of shells). These trends suggest that elements observed to occur in the same zones in element maps and those that commonly substitute for one another are most likely to exhibit positive correlations. Ratios of mean concentrations of Mg/Ca and Sr/Ca decline sharply with shell length, suggesting that rates of biofractionation decreased with age. The chemical signatures analyzed in this study indicate that all of the fossil lingulids are diagenetically altered, but that the Devon Island specimens are more altered than those from Stewart County. Ultimately, reliable paleoenvironmental information was not extracted from these samples.

For my family both lineal and chosen, and for my grandmother *in memoriam*.

ACKNOWLEDGMENTS

I would like to convey my appreciation to Dr. Karen Chin for her great patience and for her steadfast and compassionate support of my research and, at times, eccentric endeavors. Karen has encouraged me to pursue research and learning opportunities that have contributed to my growth as both a person and as a scientist during my time at CU Boulder. I shall remain deeply grateful for her guidance.

I would also like to thank my committee members who were instrumental in the completion of this work. Dr. Tom Marchitto's geochemical expertise has influenced both my research methodologies as well as inspired my own interest in marine geochemistry. Dr. David Budd provided me with the petrographic skills needed for my thesis research and future endeavors.

I extend much gratitude to all of my committee members for their review of this thesis and support of my academic aspirations. The responsibilities of professors are many, and their time often limited. I am deeply grateful to all of my committee members for investing their time and efforts in this project and in serving as role models to me through their own teaching and research.

Technical support and advice provided by Dr. Julien Allez while analyzing the shell chemistry of lingulid specimens was invaluable. I am indebted to Drs. Susan Kidwell and Adam Tomašovỳch for their gift of modern *Glottidia sp*. specimens for comparative analyses as well as much-valued advice. I am also grateful to my colleague, Dr. David Schwimmer, for providing initial fossil specimens from Georgia and for his assistance in field collections. Charles Magovern's assistance with fossil preparation provided valuable insight. I am appreciative of Dr.

Christian Emig for his contributions to my understanding of lingulid evolution, morphology, and ecology. I am also grateful to Dr. Doug Jones for his insights and encouragement.

I am most grateful to both Dr. Sally E. Walker and George Betzner for their enduring support of all of my endeavors; without them, this thesis would not have been possible. My dearest friends, Aya El-Attar, Mohammed Al-Qattan, and Tuba Evsan made my time in Boulder one of great joy, love, and self-discovery; I cannot express my love for you all.

Many thanks to my friends, especially those at CU Boulder and the University of Chicago: Allison Vitkus, Omkar Pradhan, Katie McComas, Lindsay Walker, Leighanna Hinejosa, Nicole Ridgwell, Evan Anderson, Rick Levy, Rhiannon LaVine, Nadia Pierrehumbert, Marites Villarosa-Garcia and Madeline Marshall. Jared Foust and David "Davison" Hogan, thank you for always cheering me up regardless of the circumstance. Yasmine Ghojehvand, you were my light for eight years; you made me come alive. Mathias Shaw, you have helped me to find the best of myself. To the faculty, staff, students and *Triopha catalinae* of Friday Harbor Laboratories, I will forever be grateful.

Dr. Bruce Railsback has been both my friend and my guide in times of elatedness and existential crisis; he is truly a gentleman and a scholar. Dr. Rob Hawman remains a constant source of support and friendship. Drs. Dena Smith, Talia Karim, Chris Jenkins, Roy Plotnick and Seth Finnegan have all provided guidance, encouragement, great conversation and compassion. I am grateful to Dr. David Jablonski for his willingness to help me achieve academic advancement, and for his enthusiastic approach to complex questions in paleontology.

Funding for this research was generously provided by the University of Colorado Department of Geological Sciences Kenneth Allen Johnston Memorial Scholarship and Museum of Natural History William H. Burt Fund. Travel assistance was provided through the

Department of Geological Sciences Student Travel Grant. Support for my time at CU Boulder was generously provided by the Department of Geological Sciences through a Graduate Fellowship and Graduate Teaching Assistantship. My studies at Friday Harbor Laboratories were permitted through the Alan J. Kohn Endowed Fellowship.

CONTENTS

ABBREVIATIONS

1. Canadian Museum of Nature (Invertebrate Fossil collection) – CMN(IF)
2. Nunavut Invertebrate Fossil collection – NUIF
3. University of Colorado Museum of Natural History – UCM
4. Columbus State University - CSUK
5. Devon Island lingulid(s) – DIL
6. Stewart County lingulid(s) – SCL/ GA
7. California specimens - CA

TABLES

FIGURES

ELEMENTAL DISTRIBUTIONS WITHIN ORGANOPHOSPHATIC BRACHIOPOD SHELLS: IMPLICATIONS FOR GROWTH, PRESERVATION AND PALEOENVIRONMENT

Introduction

Biogenic hardparts of marine invertebrate taxa that exhibit accretionary growth commonly record changes in physicochemical conditions via differential incorporation of environmentally-sensitive trace elements (Brand et al., 2003, Lee et al., 2004; England et al., 2007; Brand et al., 2007; Perez-Huerta et al., 2008; Powell et al., 2009; Angiolini et al., 2012; Zabini et al., 2012). Most sclerotized invertebrate marine taxa (mollusks, corals, and brachiopods) produce hardparts of calcium carbonate ($CaCO_3$) or, in the case of lingulid brachiopods, the calcium phosphate ($CaPO_4$) mineral francolite [$(Ca, Mg, Sr, Na)_{10}(PO_4, SO_4, CO_3)_6F_{2-3}$] (Benmore et al., 1983; Kocsis et al., 2012), both of which form in approximate equilibrium with prevailing seawater conditions as they are incorporated through the process of accretionary growth (Lowenstam, 1961; Popp et al., 1986). This is particularly significant as preserved elemental signatures of growth features (e.g., growth increments, shell laminae, etc.) may record the geochemical fingerprint of past environmental conditions, similarly to tree-rings in terrestrial ecosystems (Jones and Quitmyer, 1996). While direct quantification of original seawater chemistry may not be possible due to the effects of chemical diagenesis upon original mineralogy, qualitative trends in relative abundances and distributions may be preserved through geologic time (Grossman et al., 1996; Rodland et al., 2003; Kocsis et al., 2012).

Paleoenvironmental conditions have been inferred from variations in the abundances and distributions of trace elements, including rare-earth elements (REEs), and stable oxygen and carbon isotopes observed in the carbonate hardparts of mollusks and articulated brachiopods (Carroll et al., 2002; Lee et al., 2004; England et al., 2007; Angiolini et al., 2012). However,

substantially fewer studies have focused upon the organophosphatic shells of inarticulated brachiopods, particularly the longevous and morphologically conservative Lingulidae (Kowaleski et al., 1997; Williams et al., 2004; Kocsis et al., 2012; Zabini et al., 2012). Limited research suggests that biogenic apatite, such as that comprising the shells of lingulids, may offer a valuable proxy for understanding paleoenvironmental conditions (Kocsis et al., 2012; Zabini et al., 2012). However, others note that early diagenesis and conversion from francolite to fluorapatite ($Ca_5(PO_4)_3F$) may alter geochemical values (Elliot et al., 2002; Rodland et al., 2003; Lecuyer, 2004). It therefore seems pertinent to continue evaluating the geochemistry of ancient biogenic apatites and to consider the fidelity with which original shell chemistry may be preserved.

Trace elements, including rare-earth elements (REEs), can provide insights into paleoenvironment conditions such as temperature, oxygenation and food supply, growth rates, chemical diagenesis and provenance (Grossman et al., 1996; Picard, 2002; Lecuyer, 2004; Sturresson et al., 2005). Trace elements may be incorporated into the crystalline lattices of biogenic minerals through three dominant processes: replacement, substitution, and biogenic uptake, all of which may vary between layers of differing original shell chemistry (i.e., chitinous or mineralized laminae, primary and secondary layers) (Grossman et al., 1996). Replacement occurs during diagenesis when original constituents are dissolved due to pressure or fluid influx (e.g., contact with meteoric water, etc.) (Putnis, 2009). Areas from which minerals are dissolved may then serve as nucleation sites for new mineral phases provided that after dissolution, they represent sites of reduced chemical and physical stress (Putnis, 2009). Substitution of elements under a given physicochemical regime may occur either during skeletal accretion or diagenesis (Grossman et al., 1996; Elliot et al., 2002). With regard to $CaPO_4$ minerals, both Sr and Mg

commonly substitute for Ca within the apatite lattice. Substitution rates during skeletal formation often reflect prevailing temperature regimes, with high Sr substitution suggesting increased temperatures and high Mg substitution suggesting decreased temperatures (Freitas et al., 2006). Such substitutions are possible due to the similar size of these cations as well as their equal charges (Elliot et al., 2002).

Biogenic uptake of trace elements is determined both by vital effects and environmental conditions. Trace elements may be taken in through feeding and through direct mineral precipitation as the shells of marine invertebrates grow (Lowenstam, 1961; Lee et al., 2004). Where elemental distributions appear uniform among members of a single taxon but vary in other taxa within a given environment, one may assign taxonomic significance to them (Grossman et al., 1996); however, concentrations may be expected to vary throughout ontogeny (Lee et al., 2004). Conversely, distributions of elements exhibiting a high degree of variation among individuals of a single species may be attributed to changing availability or uptake of these elements during shell growth (England et al., 2007). Element uptake can change either during the organism's life history (Lowenstam, 1961; Grossman et al., 1996), or due to changing physicochemical conditions (Grossman et al., 1996; Freitas et al., 2006; England et al., 2007).

Before assessing the utility of organophosphatic brachiopods as (paleo) environmental archives, it is useful to turn to the more widely-utilized calcium carbonate archives of bivalve mollusks and articulated brachiopods. Stable oxygen and carbon isotope profiles preserved within the shells of calcitic mollusks are frequently utilized in the study of paleoenvironment (Jones et al., 1988, Schöne et al., 2002, 2006). In these studies, $\delta^{18}O$ and $\delta^{13}O$ are used as proxies for temperature and paleo-productivity, respectively. While isotopic data from calcitic mollusks and brachiopods may provide crucial insights into paleoenvironmental conditions,

these data are not always available (i.e., may not be preserved in environmental settings under-saturated with respect to carbonate) and may be altered during diagenesis (Rodland et al., 2003; Kocsis et al., 2012).

While overall growth is similar between mollusks and brachiopods, important differences should not be discounted. Both mollusks and brachiopods grow through accretion of mineralized and organic laminae along a ventral margin (Williams et al., 1994), and growth in many marine invertebrates may be interrupted during spawning or unfavorable environmental conditions (e.g., extremes in temperature, reduced food supply, etc.) (Brockington and Clarke, 2001). However, brachiopods grow by accreting stratiform laminae (Fig. 1) while bivalve growth intervals are accreted at an acute angle relative to the dorso-ventral midline (2). The result of these differences in growth is that growth lines in the cross-sectioned shells of brachiopods, particularly organophosphatic taxa, occur as roughly perpendicular truncations of these laminae, which are often difficult to observe

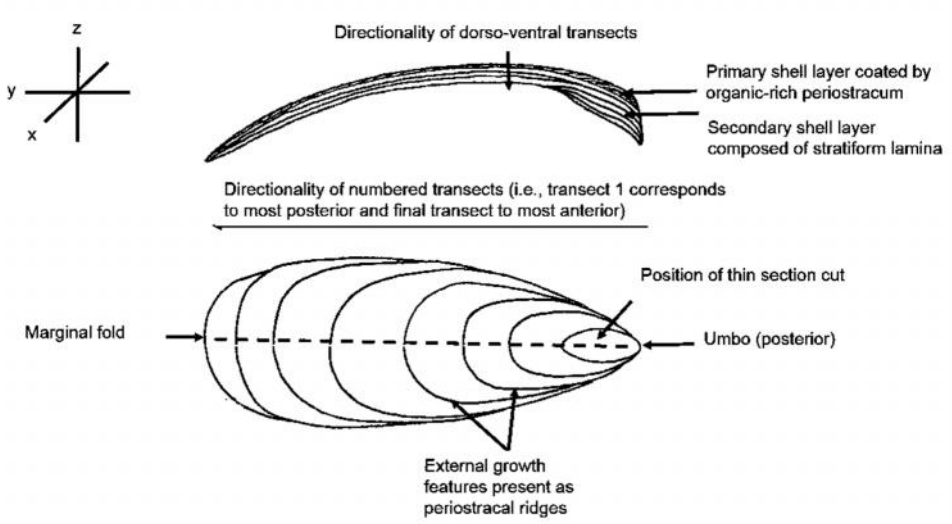

Figure 1: Labeled schematic of a generalized lingulid shell with axes and analytical points illustrated.

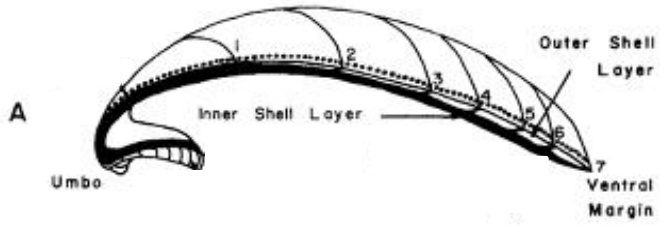

Figure 2: Labeled schematic of bivalve shell after Jones et al., 1984.

in thin section. This appears to be at least partially responsible for the paucity of geochemical observations in organophosphatic brachiopods that would be analogous to those from more robust articulated brachiopods and calcitic bivalve mollusks.

When examining trace-element distributions in the shells of articulated brachiopods, England et al. (2007) found that Mg varied longitudinally and dorso-ventrally through the shells of modern articulated brachiopods. They postulated that the variations along the axis of maximum growth (longitudinal) were due to variable incorporation of these elements throughout ontogeny; these conclusions were supported by the differing Mg/Ca profiles between brachiopod genera from a single locality. Additionally, the finding that concentrations of Mg and Ca differ between shell lamina may suggest that differential incorporation within the shells of brachiopods in driven by changes in (paleo) environmental conditions.

In one of the few studies examining trace element geochemistry in the stratiform shells of organophosphatic brachiopods, Zabini et al. (2012) found that profiles of Fe, Ba and S varied both longitudinally and vertically through the shells of Devonian lingulids. Furthermore, these variations were found to correspond with changes in shell microstructure, suggesting that as with mollusks (see Schöne et al., 2005 for one case study), trace elements may be useful in determining seasonality. Other workers have found that the $\delta^{18}O$ of lingulid shells varies both with longitudinal extension and dorso-ventral thickening (Rodland et al., 2003). Brachiopods grow approximately continuously except when interrupted by spawning or extreme changes in environmental conditions (Brockington and Clarke, 2001). It may be possible to correlate changes in shell chemistry with shell microstructures indicating either cessation or renewal of growth induced by either biotic or environmental changes.

The purpose of this study was to investigate the utility of distributions of trace elements within the shells of lingulid brachiopods as indicators of variations in physicochemical conditions between two Late Cretaceous shallow marine environments from different latitudes. The hypotheses were that: 1) elemental values should be substantially different between localities, 2) the dorso-ventral distributions of elements within each locality should not be substantially different, 3) those elemental concentrations and distributional trends that do not vary between fossil sites might be assumed to reflect incorporation due to vital effects rather than differences in physicochemical setting (Grossman et al., 1996), and 4) differences in the concentrations of redox-sensitive elements should reflect differential diagenetic alteration in fossil lingulids. To investigate these questions, fossil lingulids from the Late Cretaceous of Arctic Canada and western Georgia, USA were analyzed with an electron microprobe. Elemental concentrations were measured via point analysis, and elemental maps were produced for specimens from each locality. Elemental maps were also generated for both major (Ca, P and F) and trace (Fe, Mg, Sr, S, Mn and Na) elements for a modern lingulid specimen for use as a diagenetic control. By understanding how trace elements are distributed within the shells of lingulids, we may begin to differentiate between chemical signatures resulting from vital effects, environmental change, or chemical diagenesis.

Geologic Setting of Fossil Materials

Fossil lingulids examined in this study were collected from two contemporaneous and latitudinally-disparate localities (Fig. 3): Eidsbotn graben, Devon Island, Nunavut, Canada (76° 17’ N, 91° 12’ W; Chin et al., 2008) and Hanahatchee Creek, Stewart County, Georgia, USA (32° 8’ N, 84° 57’W; D. R. Schwimmer, *pers. comm.,* 2014). Modern specimens were collected

from offshore of San Pedro, California, USA (A. Tomašovỳch, *pers. comm.*, 2014). Twenty-three specimens were available from Devon Island, thirty-three were available from the Stewart County site, and four from the modern locality. Not all could be utilized, however, as thin section preparation for microprobe analysis required destruction of sections of the specimens.

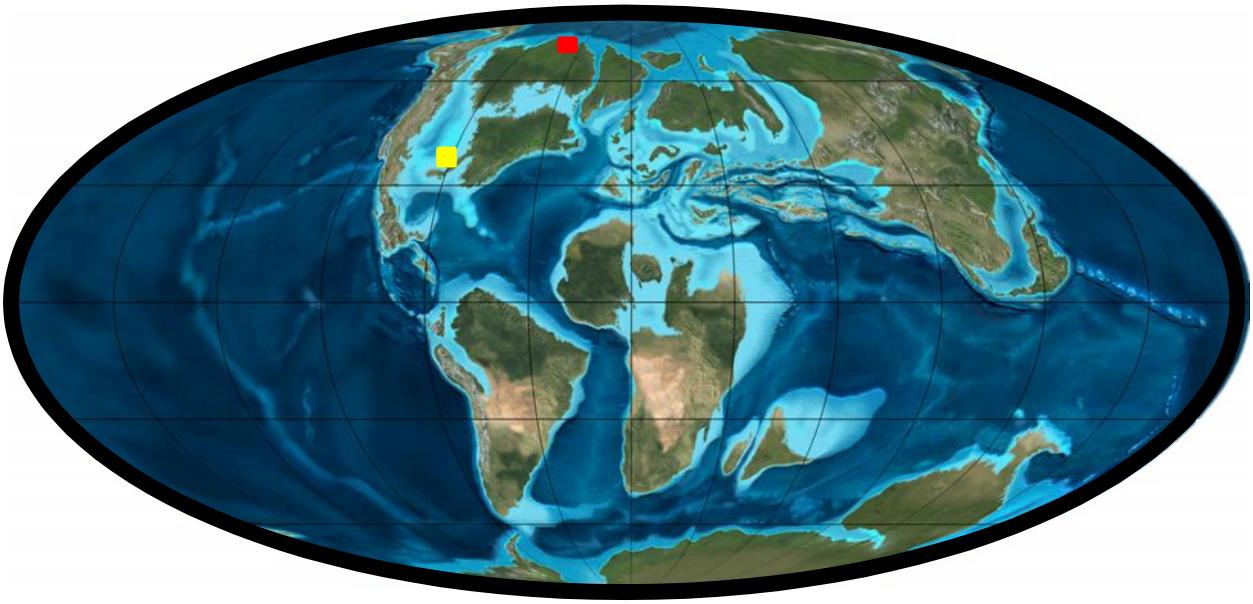

Figure 3: Map of Late Cretaceous (90 MYA) Earth with fossil localities indicated by squares (Devon Island, red; Stewart County, yellow); squares are not to scale. After Blakey (2011).

Upper Kanguk Formation, Devon Island

Devon Island, Nunavut, Canada represents the depositional margin of the Sverdrup Basin, which forms part of the Arctic Platform, a thick succession of Lower Paleozoic strata overlain unconformably by Mesozoic and Paleogene deposits (Fortier et al., 1963; Miall, 1979, 1991; Embry et al., 1991). Lingulids were found within exposures of Late Cretaceous sediments at Eidsbotn graben on Devon Island (Fig. 4), and were collected in expeditions to the site in 1998 and 2003 (Chin et al., 2008). The unit has been correlated with the Kanguk Formation (Mayr et al., 1998), and siliceous microfossil evidence indicates that the rocks are Campanian to

Santonian in age (Chin et al., 2008; McCartney et al., 2011; Witkowski et al., 2011). At the time of their deposition, the materials were at a paleolatitude of ~70°N (Tarduno et al., 1998; Blakey, 2014) (Fig. 3).

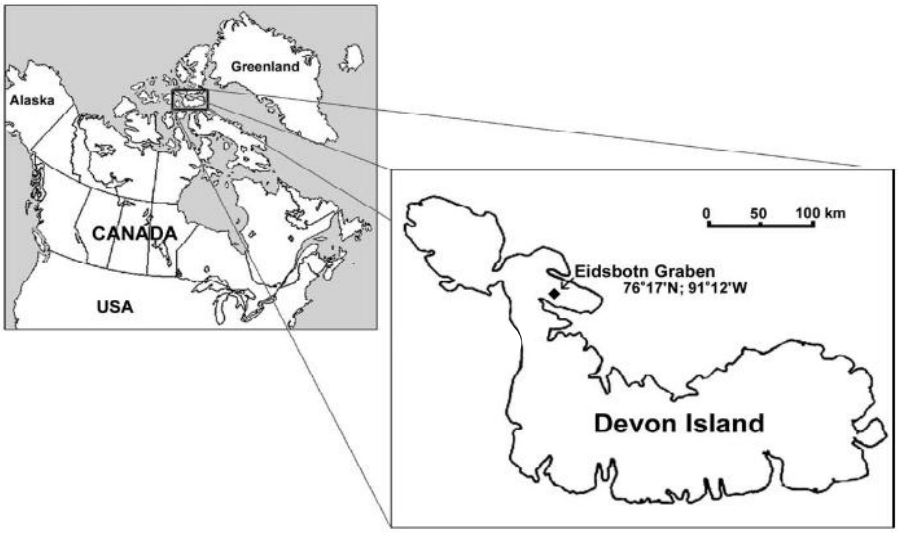

Figure 4: Map of Arctic fossil locality and its position within the Canadian Archipelago from Chin et al. (2008).

The exposure of the Kanguk Formation from which fossil lingulids were collected is comprised of poorly-indurated glauconitic sands that are interbedded with layers of mudstone and bentonite. The outcrops preserve a regressive sequence of marine sediments, including dark shales overlain by tens of meters of unconsolidated glauconitic greensands (Bloch et al., 2004). The unit is gradationally overlain by the deltaic Expedition Fjord Formation (Fig. 5). Lingulids were found exclusively within greensand deposits and coprolites within these sediments (Chin et al., 2008).

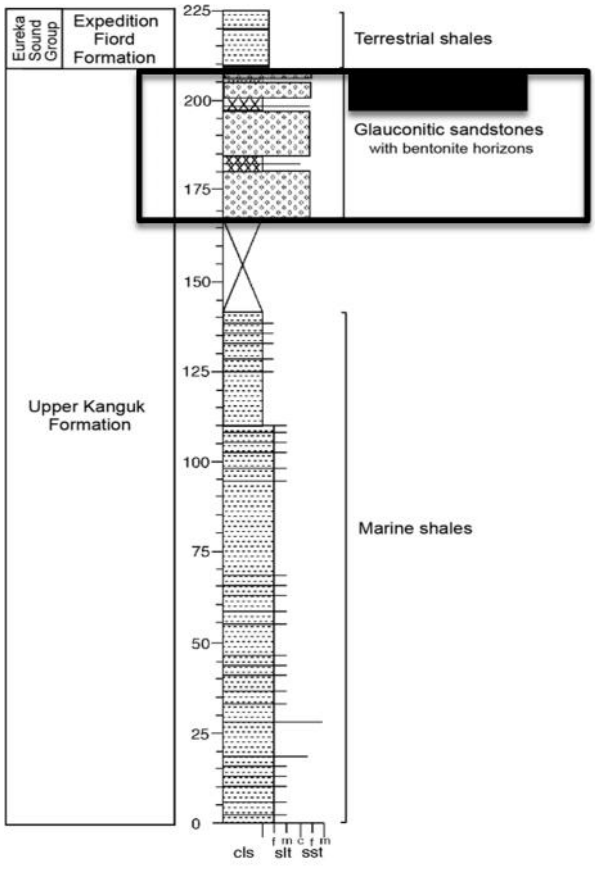

Figure 5: Composite stratigraphic section of Upper Kanguk from Devon Island, Canada with study interval shown in box. After Chin et al. (2008).

Upper Blufftown Formation, Stewart County

The Hanahatchee Creek fossil site (Fig. 6) is located in western Stewart County, Georgia, USA. Lingulid fossils were recovered in 2004 and 2013 from the uppermost 1 m of the lower Campanian Blufftown Formation, which is overlain by the sandy Cusetta Formation (Case and Schwimmer, 1988; Fig. 7). Lingulids were collected from a gray to green, micaceous, poorly-indurated sandstone with abundant molluscan shell debris. Evidence for substantial reworking from within the Blufftown exists in the form of disarticulated and crushed shells and abundant molluscan and vertebrate debris (Case and Schwimmer, 1988). The entire Blufftown section is interpreted to represent a regressive sequence, ranging from back-barrier marine in the lower units to estuarine with substantial fluvial input in the uppermost units (Schwimmer, 1986; Case and Schwimmer, 1988). At the time of their deposition, the materials were at a paleolatitude of 30-40°N (Blakey, 2014; Fig. 3).

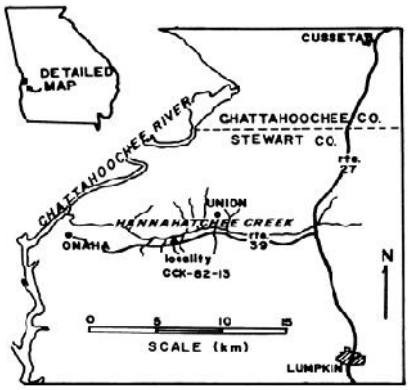

Figure 6: Hanahatchee Creek fossil site in Stewart County, western Georgia, USA. From Schwimmer et

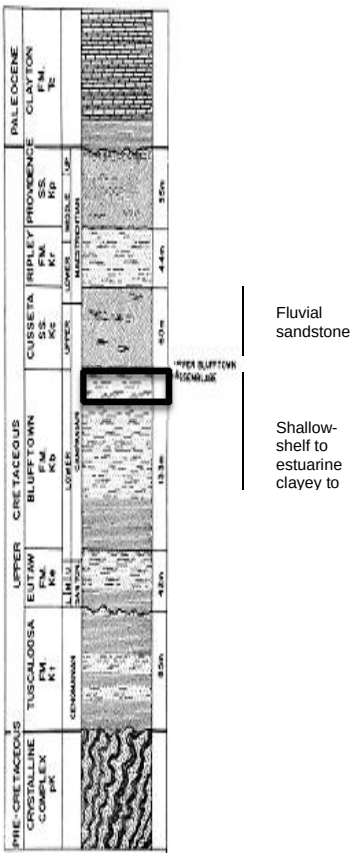

Figure 7: Stratigraphy of Hanahatchee Creek fossil site with Upper Blufftown study interval shown in black box. After Schwimmer et al. (1988) and based off of Eargle (1955).

Methods

Thin Section Preparation and Microscopy

Three fossil lingulids from Devon Island (specimens DIL-8/CMNIF 245, DIL-12/CMNIF 245, and DIL-25/CMNIF 166), two from Stewart County (specimens SCL-25/UCM 79789 and SCL-29/UCM 79790) and one recent lingulid from the Gulf of California (CA 4232) were selected for electron microprobe analysis (Fig. 8). A complete list of fossil materials examined in this study is given in Appendix A. The lingulids from Georgia occur as single valves in

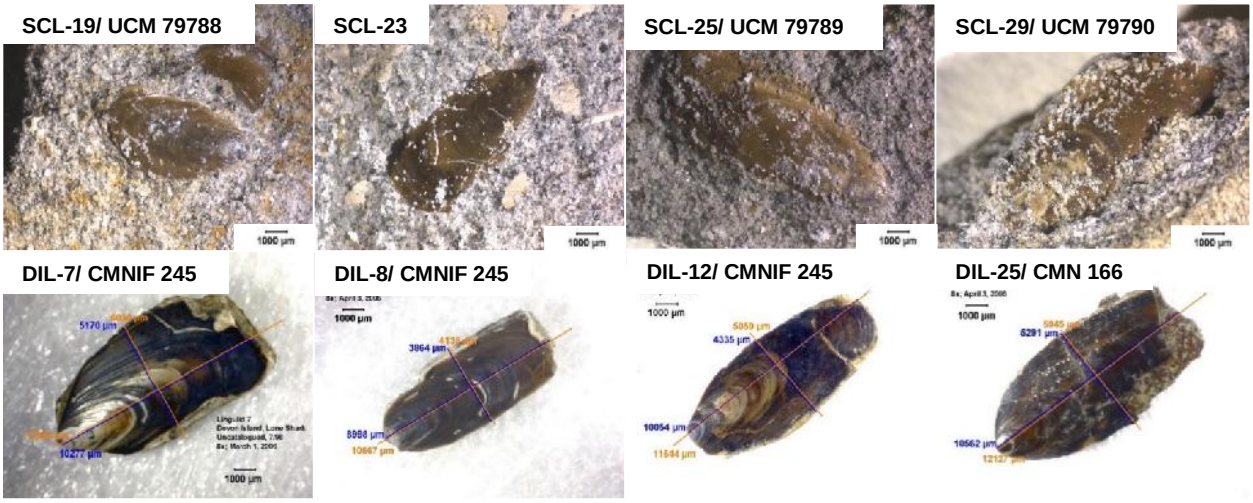

Figure 8: Reflected light microscopy of whole shells of fossil lingulids from Stewart County (SCL) and Devon Island (DIL). Images of Devon Island specimens by David Barton.

poorly-indurated sandstones, which required impregnation prior to thin-sectioning to avoid damaging the shells. A solution of 90% acetone and 10% epoxy (Struers EpoFix) was used, and samples were placed under vacuum to improve infiltration of the epoxy into the sediments. The samples were left to dry for four days, and then heated to 60°C for an additional 48 hours. This process was repeated for some shells to achieve adequate impregnation for sectioning. Modern lingulids were first embedded in epoxy within a small, plastic dish to form a solid suitable for sectioning.

Specimens were cut dorso-ventrally (z-axis) through the shell along the lateral (x-axis) midline (Fig. 1) using a Buehler Isomet slow speed saw with a diamond-edged blade. Samples were mounted to frosted glass petrographic slides with Devcon 2-Ton epoxy. The mounted specimens were thinned with a graded series of diamond-embedded platens. The resultant thin sections were analyzed with a Leica MZ 12.5 stereoscope and a Leica DMRX petrographic scope. Primary shell architecture (i.e., primary and secondary shell layers as well as stratiform shell lamina) were noted for all samples. Finally, specimens were polished with 5.0 µm aluminum oxide and a 0.05 µm alumina suspension, and were carbon coated for microprobe analysis.

Electron Probe Microanalysis

Thin sections of lingulid specimens were analyzed via a JEOL JXA-8600 electron microprobe at the University of Colorado. A beam current of 20 nanoamperes (nA) was utilized for all analyses but beam diameters varied between assemblages (5 µm for Devon Island specimens and 10 µm for Stewart County); this inconsistency was necessitated by the greater susceptibility to beam damage of the Stewart County specimens. A summary of standards and detection limits for the elements analyzed in this study may be found in Table 1. Dorso-ventral spacing was even and longitudinal (posterior to anterior) spacing was approximately even within the two areas measured in each fossil shell. Nine elements (Ca, P, Fe, Mg, Sr, F, S, Mn and Na) with potential for providing insight into lingulid shell growth, paleoenvironmental conditions and diagenesis were selected for detailed quantitative and qualitative analyses. Data were screened for instrument error, and all points with element weight percent totals less than 88% were

removed from the data set before values were converted to parts per million (ppm). Additionally, transects with fewer than four data points with weight percent totals <88% were removed. The lower limit of acceptable weight percent totals was determined by observation of element concentration consistency during microanalysis.

The quantitative electron microprobe data were analyzed for patterns of elemental concentrations and distributions within dorso-ventral transects descending inward from the shell exterior through single valves of fossil lingulids. Elemental concentration data were acquired for twenty-eight transects across three Devon Island lingulids while only six were obtained across the same number of Stewart County specimens; after data were screened, twenty-seven transects could be analyzed for Devon Island lingulids and five remained for Stewart County specimens ($N_{transects}$ = 32). The number of points per transect varied with shell thickness. Transects were located in each shell in the shell posterior (near the larval shell) and at points across the approximate longitudinal midline of the shell to evaluate whether or not elemental distributions changed substantially through ontogeny (Fig. 9). Elemental concentrations and distributions representing whole-shell chemistry were also determined by calculating the mean values of all transect analyses in individual shells.

Table 1: Analyzed elements, crystal standards and detection limits in ppm for JEOL JXA-8600 electron microprobe analytics. Detection limit data not available for Na concentrations of Devon Island lingulids (DIL). Limits vary between sample populations due to different dates of measurement.

Element	Standards	Detection limits (ppm)	
		DIL	SCL
Ca	Apt-104	246	200
P	Apt-104	187	230
Fe	P-130	191	250
Mg	Oliv-2566	50	100
Sr	Stro	185	270
F	Apt-104	635	960
S	Barite	61	80
Mn	P-130	192	260
Na	Amelia	--	120

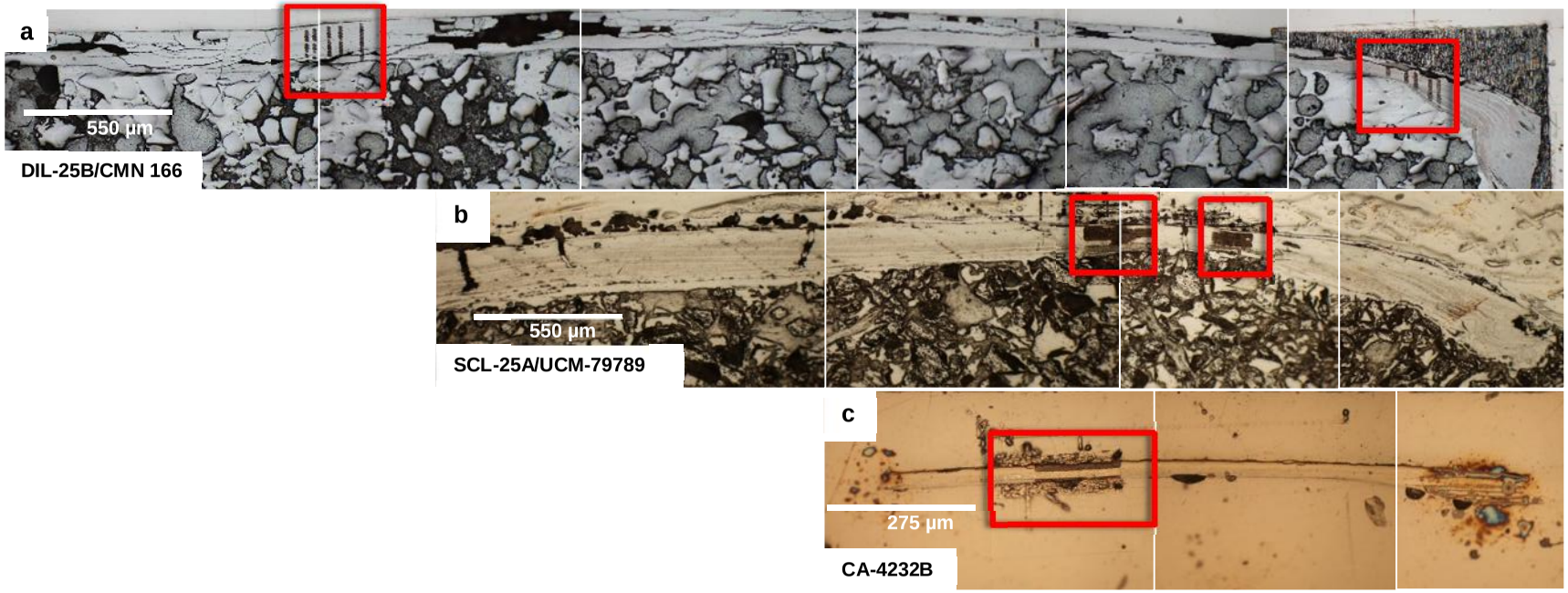

Figure 9: Transmitted light microscopy images showing electron probe microanalysis sites in boxes for two fossil lingulids (a = Devon Island; b = Stewart County) and one modern lingulid (c).

Distributions of elements within lingulid shells were also compared with elemental maps of Ca, P, Fe, Mg, Sr, S, Mn and Na, which were generated for three fossil specimens and a modern lingulid. When possible, map areas were set to overlap with point analyses. The maps were analyzed for visible trends in elemental distributions and compared with the quantitative point data so as to evaluate the effects of diagenesis on the preservation of elemental distributions.

Statistical Analyses

Quantitative microprobe data were analyzed statistically and graphically via Paleontological Statistical software (PAST) and Microsoft EXCEL. Normalcy of data distributions both within sites and among individual shells were analyzed via Shapiro-Wilk's test in PAST (Table 2). Only two elements, Mn and F, were normally distributed within the original dataset. Non-normally-distributed data were transformed via Tukey's Ladder of Powers; however, data from only one element (Fe) was normalized under these methods.

Table 2: Shapiro-Wilk's test for normal distribution. Values in bold represent those that are normally-distributed, and bolded pairs are those elements for which both fossil localities exhibited normal distributions. Asterisk (*) beside element indicates that a statistical transformation was required to obtain normality.

Locality	Ca	P	Fe*	Mg	Sr	F	S	Mn	Na
Devon Island	*p*<0.05	*p*<0.05	***p*>0.05**	*p<0.05*	*p<0.05*	***p*>0.05**	*p<0.05*	***p*>0.05**	*p<0.05*
Stewart County	*p*<0.05	*p*<0.05	***p*>0.05**	*p<0.05*	*p<0.05*	***p*>0.05**	*p<0.05*	***p*>0.05**	*p<0.05*

A Kruskal-Wallis test for equal medians was conducted for Mn, F and Fe between fossil localities, and concentrations were further analyzed via F-Test for equality of variances and Student's ***t***-Test for equality of means (Table 3). The remaining non-normally distributed elemental data (Ca, P, Mg, Sr, S and Na) were analyzed for differences of medians via Man-Whitney U Test (Table 4). Correlation coefficients (r) were calculated to numerically analyze

apparent correlations between elements in dorso-ventral transects. Element pairings were also analyzed for robustness of correlation within whole lingulid shells. Ratios of Ca/Mg and Sr/Ca were plotted for all shells and for between-site comparison, and ratios of Sr/Mn and Fe/Mn were evaluated against values reported by Brand et al. (2003) for modern, calcitic brachiopods. Lastly, ratios of Sr/Ca for fossil lingulids in this study were compared with the bioapatitic hardparts of fossil and recent mammals (Sponheimer and Lee-Thorp, 2006).

Table 3: Summary of parametric tests for significance of difference between variances and means of two sample populations (Devon Island and Stewart County lingulids). Variances are equal for the minerals iron and fluorine but are unequal for manganese. For all elements, p-values for differences between means were less than 0.05. The null hypothesis of no differences is thus rejected.

Statistic	Points (n)	Fe	F	Mn
F-test	Devon Island = 204	$p>0.05$	$p>0.05$	$p<0.05$
Student's *t*-test	Stewart County = 23	$p<0.05$	$p<0.05$	$p<0.05$

Table 4: Summary of non-parametric test for significance of difference between medians of two sample populations (Devon Island and Stewart County lingulids). For Ca, P and Sr, p-values were less than 0.05; the null hypothesis of no differences is thus rejected for these elements.

Statistic	Points (n)	Ca	P	Mg	Sr	S	Na
Mann Whitney-U	Devon Island = 204 Stewart County = 23	**$p<0.05$**	**$p<0.05$**	$p>0.05$	**$p<0.05$**	$p>0.05$	$p>0.05$

Institutional Abbreviations

Devon Island specimens utilized in this study are reposited at the Canadian Museum of Nature for the Government of Nunavut. The fossil material from Stewart County and thin sections of the modern specimens are reposited at the University of Colorado Museum of Natural History. Modern lingulids utilized in this study were acquired from the University of Chicago and are reposited at the University of Colorado.

CMN(IF): Canadian Museum of Nature Invertebrate Fossil collection, Ottawa, Canada; NUIF: Nunavut Invertebrate Fossil collection (housed at CMN, Ottawa, Canada); UCM: University of Colorado Museum of Natural History, Boulder, Colorado, USA; CSUK: Columbus

State University, Columbus, Georgia, USA. Field numbers (DIL: Devon Island Lingulid; SCL: Stewart County Lingulid) are also referenced as co-identifiers within this manuscript and supplemental materials, and the field number CA (California) is used for uncatalogued modern specimens.

Results

Fossil Descriptions

Devon Island lingulids

The Devon Island lingulids are preserved mostly as fully-articulated valves in-filled with glauconitic sandstone from the Upper Kanguk Formation (Fig. 10). There is little shell breakage or disarticulation; only three of twenty-three specimens are represented by single valves. An organic-rich periostracum and external growth features are readily apparent on all shells examined (Fig. 11). This high quality of physical preservation suggests that specimens were neither moved far from their original depositional setting nor heavily reworked after deposition. Phosphatic fossils are well-preserved within this environment; coprolites and fossil teeth and bones from fish, marine reptiles, and hesperornithiform birds were also found in the glauconitic sandstone (Chin et al., 2008; Wilson et al., 2011). Siliceous microfossils (including diatoms, silicoflagellates, and radiolarians) are evident within the coprolites and the marine shales (McCartney et al., 2011;

Figure 10: Labeled shell of an Arctic lingulid (DIL-25/ CMN 166). Dark, organic-rich periostracum well-preserved, and cementing glauconitic sandstone visible along zones of breakage. Image by David Barton.

Witkowski et al., 2011). Little carbonate is preserved in the exposure of the Kanguk Formation from which the lingulid fossils were collected (Chin et al., 2008).

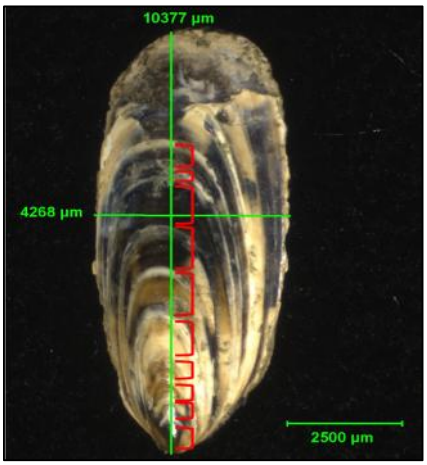

Figure 11: Labeled shell of an Arctic lingulid (DIL-9/ CMNIF 245). Width and length measurements in um; red brackets mark prominent exterior growth features.

The Arctic specimens from Devon Island exhibit a classic linguliform morphology: elongation along the axis of maximum growth (y-axis), rounding to sub-rounding of the ventral margin, and broadening from posterior to anterior with the maximum width occurring slightly anterior of the shell midline. Devon Island specimens were 1.04 cm in length on average, and ratios between measurements of length, width and height (means: w/l=0.47; h/w=0.45; Table 5) were compared to those reported by Biernat and Emig (1993) for common lingulid genera. The Devon Island specimens are most comparable to the extant genus *Glottidia* and the Mesozoic form, *Lingularia*. Both the expanded width to length ratio and greater dorso-ventral height of Devon Island lingulids relative to modern *Glottidia* suggest that these samples likely represent another high-latitude occurrence of *Lingularia* (Holmer and Nakrem, 2012). Attempts to remove the in-filling greensands and reveal the delicate interior of these specimens were not successful; therefore, no additional taxonomic indicators were utilized.

Table 5: Ranges of width to length (W/L), height to length (H/L) and height to width (H/W) ratios in the shells of fossil lingulids from Devon Island and Stewart County compared with the same measurements for shells of lingulid genera Glottidia, Lingula and Lingularia reported by Biernat and Emig (1993). L. adamsi and L. tumidula were excluded for some ratios, which capture all Lingula species other than those listed.

Locality/ Genera	n	W/L		n	H/L		n	H/W		Source
		Range	Mean		Range	Mean		Range	Mean	
Devon Island	11	0.37-0.61	0.47	8	0.15-0.31	0.20	9	0.33-0.62	0.45	This study
Stewart County	5	0.44-0.61	0.53							This study
Glottidia	35	0.32-044	0.33-0.40	35	0.09-0.11	0.09	35	0.15-0.24	0.20	Biernat & Emig (1993)
Lingula	135	0.44-0.53	0.43-0.48	95	0.06-0.12	0.1	95	0.14-0.25	0.20	Biernat & Emig (1993)
except. L. adamsi	31	0.54-0.70	0.63	19	0.11-0.18	0.13	19	0.16-0.26	0.20	Biernat & Emig (1993)
and L. tumidula	7	0.58-0.69	0.63							Biernat & Emig (1993)
Lingularia	82	0.45-0.75	0.51-0.65	17	0.12-0.23	0.16	17	0.20-0.44	0.32	Biernat & Emig (1993)

External growth features are evident as ridges radiating outward from the larval shell, and representing longitudinal growth along the marginal fold (Williams et al., 1994; Fig. 1). These ridges range from prominent (<10 per valve) to visible only microscopically (>40x). It is important to note that growth features observed on the shell exterior could not be correlated with the internal stratiform microstructure of the secondary shell layer, rendering assessment of ontogenetic ages as relative estimates. However, the small size distribution and abundance of both external growth features and internal lamina (Freeman et al., 2013) suggest that the Devon Island specimens represent mature individuals rather than a preservation bias in favor of juveniles.

Stewart County lingulids

The Stewart County specimens are disarticulated and highly fragmented. They are found in association with abundant molluscan and uncommon vertebrate (plesiosaur and shark) debris. Carbonate preservation is high at this locality but the physical degradation and abundance of fossil materials (e.g., bivalve mollusks, lingulids, and shark teeth) suggest that the Hanahatchee Creek locality of the Upper Blufftown Formation represents a condensed stratigraphic unit (Schwimmer et al., 1993).

Size parameters for the fossil lingulids from this site were also measured (mean w/l=0.53; Table 5) for comparison with values reported by Biernat and Emig (1993). However, due to the relatively poor physical preservation of these materials, only five samples could be measured for width/length (W/L) ratios (Table 5). These limited data overlap exclusively with values reported for *Lingularia* but are, on average, slightly shorter (0.99 cm in length) than Devon Island

specimens (1.04 cm). These specimens are highly fragile, and no additional taxonomic work was performed.

External growth features are less prominent on the Stewart County specimens than lingulids from Devon Island (Fig. 12). This appears to be due to differences in physical preservation rather than differences in shell growth, as the periostraca of Stewart County specimens are highly weathered. For the purposes of this study, it was assumed that both localities were represented by individuals of comparable ages due to their similar size and putative taxonomy.

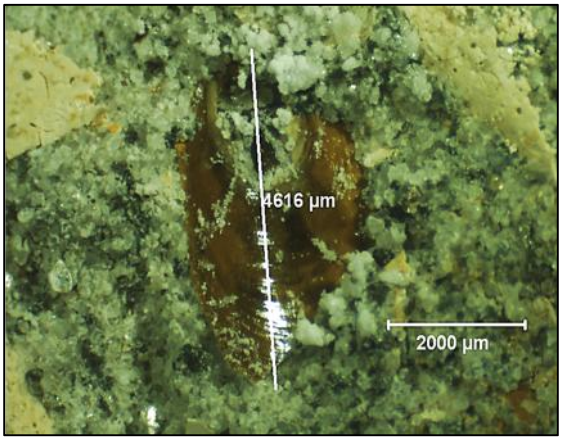

Figure 12: Labeled shell of Georgia lingulid (SCL-21). Note smaller and less prominent exterior growth features relative to the Devon Island specimen shown in Fig. 11.

Petrography

External growth features were not observed in thin section whereas stratiform shell laminae were readily apparent (Fig. 13). Laminae that occur within the shells of lingulids are repeating alternations of mineralized (apatitic) and organic (chitinous) laminae (Williams et al., 1994; Williams and

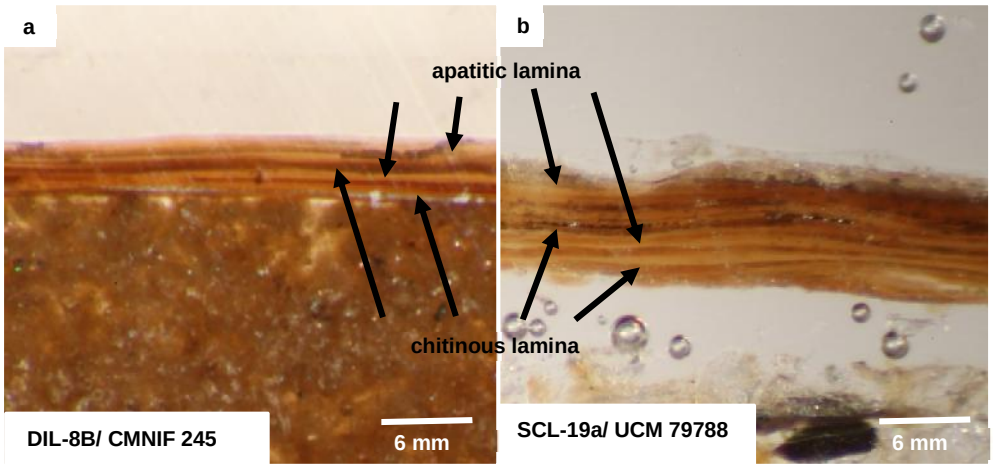

Figure 13: Reflected light views of apatitic and chitinous lamina within the secondary shell layer of Devon Island (a) and Stewart County (b) fossil lingulids.

Cusack, 1999; Kocsis et al., 2012; Zabini et al., 2012). Original apatitic laminae are beige to light-brown under reflected light, and commonly exhibit a crystalline texture. Originally chitinous laminae are brown to black and lack any determinable texture. Zones of recrystallization, commonly associated with shell damage, are blocky in texture (Fig. 14b-c).

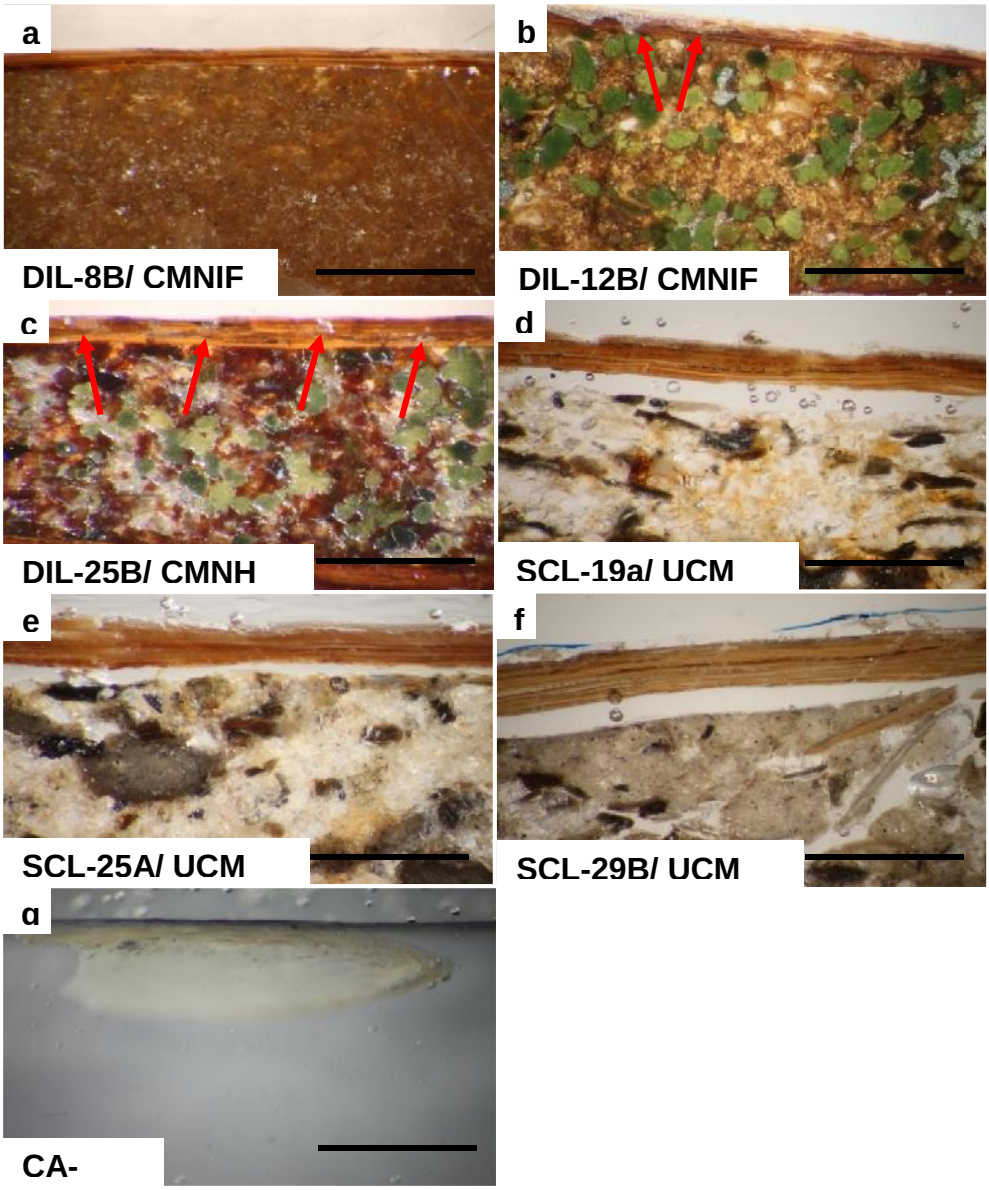

Figure 14: Reflected light microscopy of a fossil lingulids from Devon Island (a-c) showing abundant greensand grains between the valves. Zones of recrystallization (indicated with red arrows) in the valves display a blocky texture that appear to cross-cut laminar boundaries. Quartz and shell debris are associated with specimens from Stewart County (e-f). Note shell lamina (apatitic and chitinous) in specimens from both fossil localities. (g) Modern lingulid. Scale bars are 10 mm.

Under reflected light microscopy, an abundance of cemented greensand grains may be observed within the valves of the Devon Island specimens (Fig. 14b-c). Non-cemented Stewart County fossils occur in association with abundant quartz, common shell debris and rare micaceous grains (Figs. 14d, f). High magnification reflected light microscopy allowed for the correlation of electron probe microanalysis points and elemental maps with gross shell architecture. Original apatitic and chitinous laminae are less easily resolved in transmitted light but remain visible (Fig. 15).

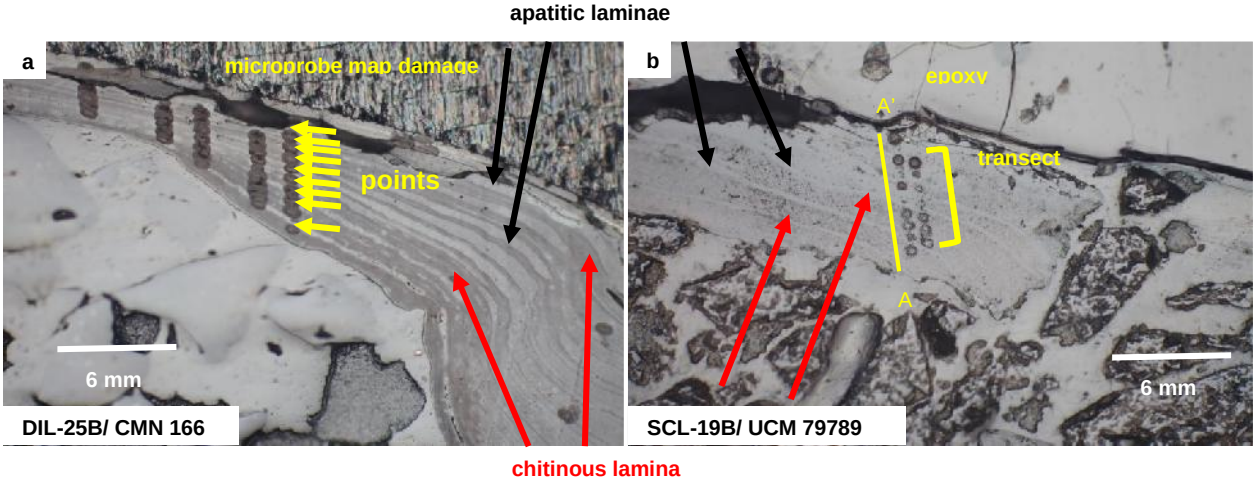

Figure 15: Transmitted light views of apatitic and chitinous lamina within the secondary shell layer of Devon Island (a) and Stewart County (b) lingulids. Electron probe microanalysis points marked by yellow arrows. Individual transects (comprised of multiple points) show by yellow arrows (a) or yellow brackets (b) brackets. Element map area (and epoxy damage also apparent. Zones of recrystallization and shell damage are visible as darker gray area that cross-cut shell grain boundaries. A'-A line in b indicates directionality (exterior descending toward the shell interior).

Gross Shell Geochemistry

Mean abundances of trace elements (Table 6) in all samples from the two sites indicate that Ca, P, and F are major elements with Fe, Mg, Sr, S, and Na occurring as trace elements. This distribution of major and trace elements suggests that the shells are composed of fluorapatite ($Ca_5(PO_4)_3F$) and not francolite [$(Ca, Mg, Sr, Na)_{10}(PO_4,SO_4,CO_3)_6F_{2-3}$].

Table 6: Mean element concentrations between fossil localities. Means are based on all spot and transect analyses. Transects with fewer than four point sums of <88 weight percent were removed from this data set; this resulted in the removal of one Stewart County shell (SCL-19/ UCM 79788).

Locality	Ca	P	Fe	Mg	Sr	F	S	Mn	Na
Devon Island	348000	152000	5985	2682	3214	37960	5180	3089	6246
Stewart County	367200	145700	4798	2700	2889	35670	5498	333	5835

Overall, the concentrations of Mg, S and Na in the shells at the two sites define relatively similar populations (Fig. 16). However, between fossil assemblages, the means of Mn, F and Fe were significantly different, with higher values of Mn and F and lower values of Fe in Devon Island specimens. Additionally, the medians of Ca, P and Sr concentrations were significantly different between populations, with lower values of P and Sr and higher values of Ca observed in Stewart County specimens.

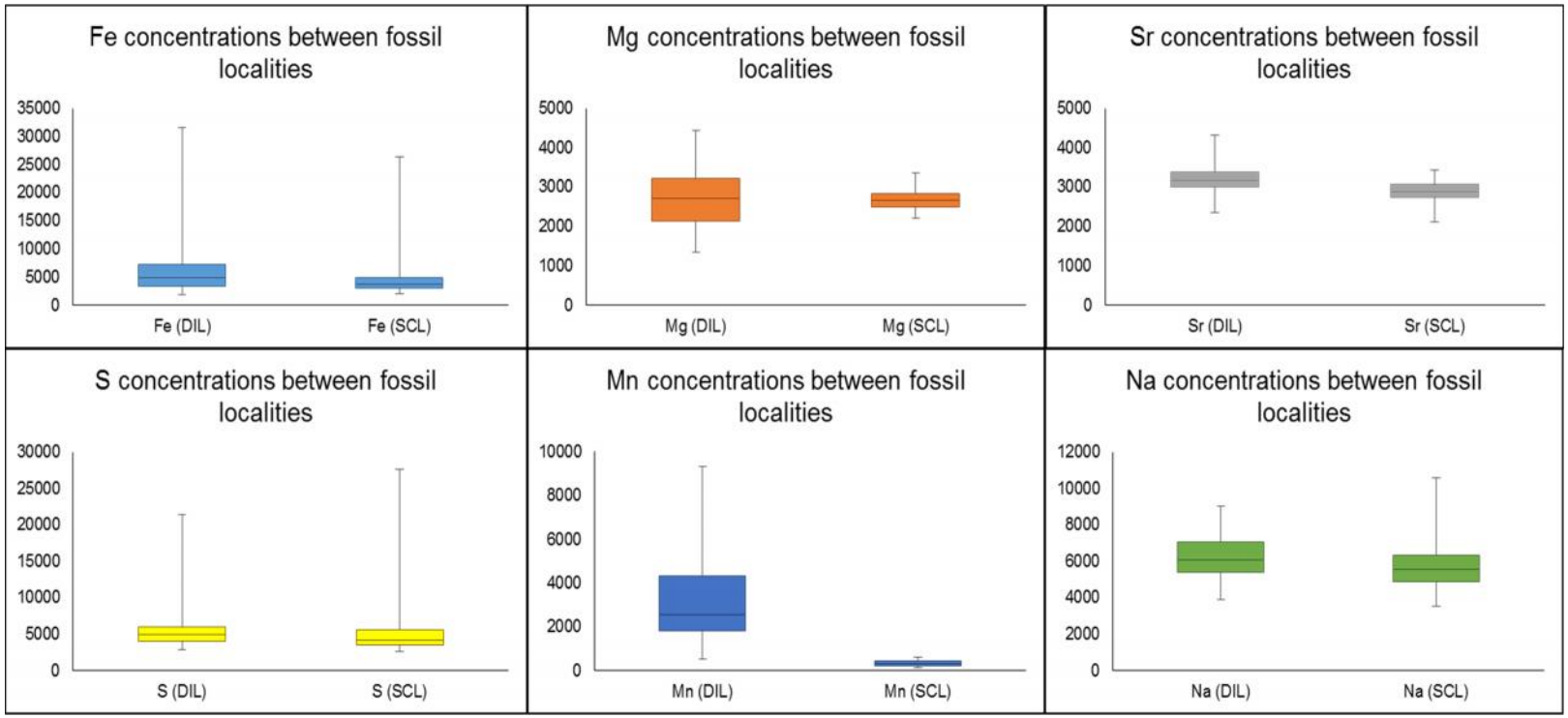

Figure 16: Box plots of mean element concentrations in ppm per fossil locality with 95% confidence intervals. All point analyses for each location were summed, and the mean determined. The means of Mn were significantly different between fossil assemblages while other elements exhibited high degrees of variance within sites and no significant differences between sites.

Element ratios between fossil sites reflect the aforementioned chemical concentrations. Ratios of Mg/Ca and Sr/Mn are markedly different between populations, with higher values observed in Stewart County and Devon Island lingulids respectively (Figs. 17-18). Mg/Fe and Sr/Mg ratios exhibit substantial overlap between populations (Figs. 19-20).

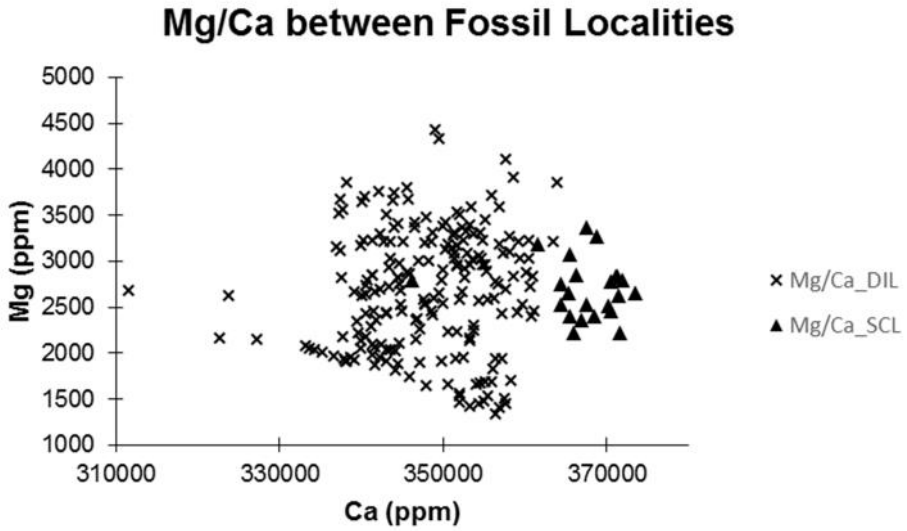

Figure 17: Absolute values of Mg and Ca from all point microanalyses as a function of sample locality. There is substantial variation in Ca concentrations within both fossil sites, but Ca values tend to overlap between the two sites. In contrast, the Arctic and Georgia lingulids are differentiated in Mg values with Georgia lingulids exhibiting higher overall Mg concentrations

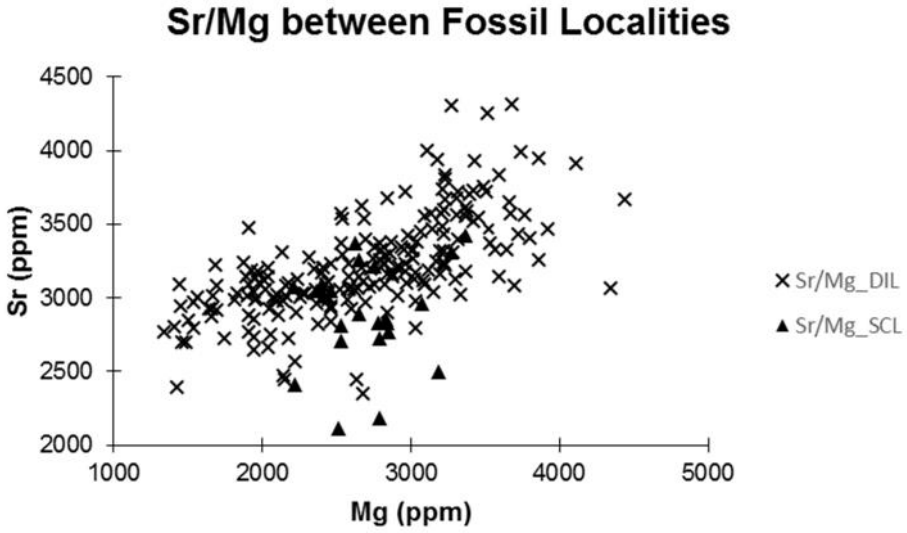

Figure 18: Absolute values of Sr and Mg from all point microanalyses for all transects. There is substantial overlap between fossil assemblages.

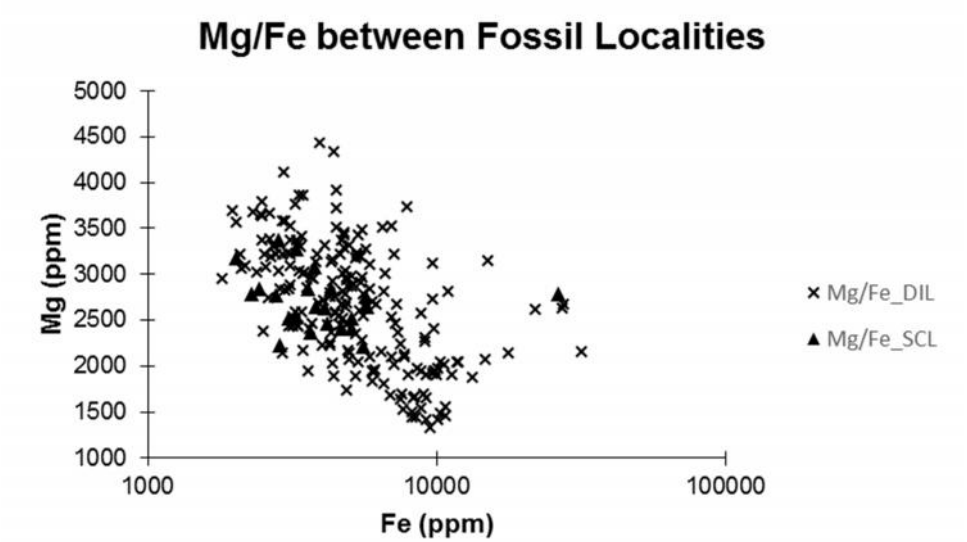

Figure 19: Absolute values of Mg and Fe from all point microanalyses for all transects. There is greater variation in Fe concentrations within Devon Island specimens, and ratios overlap between fossil assemblages.

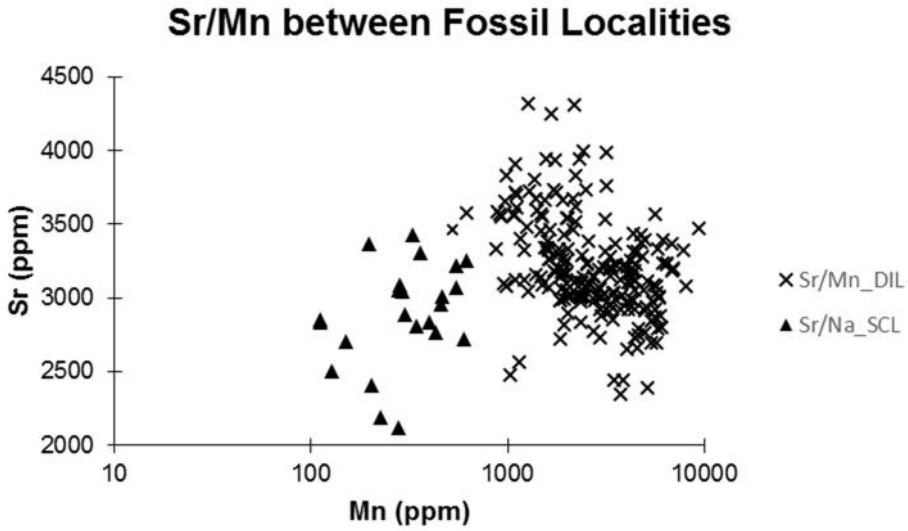

Figure 20: Absolute values of Sr and Mn from all point microanalyses for all transects. Fossil assemblages appear highly differentiated, with Sr values overlapping but Mn concentrations significantly lower in Stewart County specimens.

Qualitative Shell Geochemical Heterogeneity

Element maps were generated in order to detect spatial heterogeneity in elemental concentrations to determine 1) whether elemental zonation is present and 2) if elemental distributions differed between sample populations. Maps were made for three fossil specimens (one from Devon Island and two from Stewart County) and for one modern lingulid. Major and trace elements were mapped for two zones in each fossil shell. Zone 1 overlaps with the larval shell and zone 2 is near the longitudinal midline. Maps of both zones for a representative Devon Island and Stewart County sample are shown in Figures 21-27. The relatively poor quality of the modern lingulid allowed for only one map along the midline (Fig. 27) as the larval shell area was highly-fragmented. Within samples from each locality, patterns of element concentration were fairly consistent; however, the relative distributions of several trace elements in shells from the two fossil sites and the modern sample differed. Overall, the analyzed Devon Island specimen was found to be more similar to fossils from Stewart County than fossil specimens from either site were to the modern lingulid.

Major elements (Ca, F and P)

Major element distributions in all of the maps help to establish some basic mineralogical patterns. In the Devon Island shell, Ca, F, and P occur throughout the maps, indicating increased phosphatization of the originally chitinous laminae. In contrast, the shells of Stewart County lingulids and the modern sample, Ca, P, and F show chemical zonation with some laminae containing relatively little if any (in the case of F) of these elements and others exhibiting very high abundances (e.g. F concentrated in the interior-most region of the secondary shell layer in the modern lingulid). These observations are consistent with the expected distribution of the

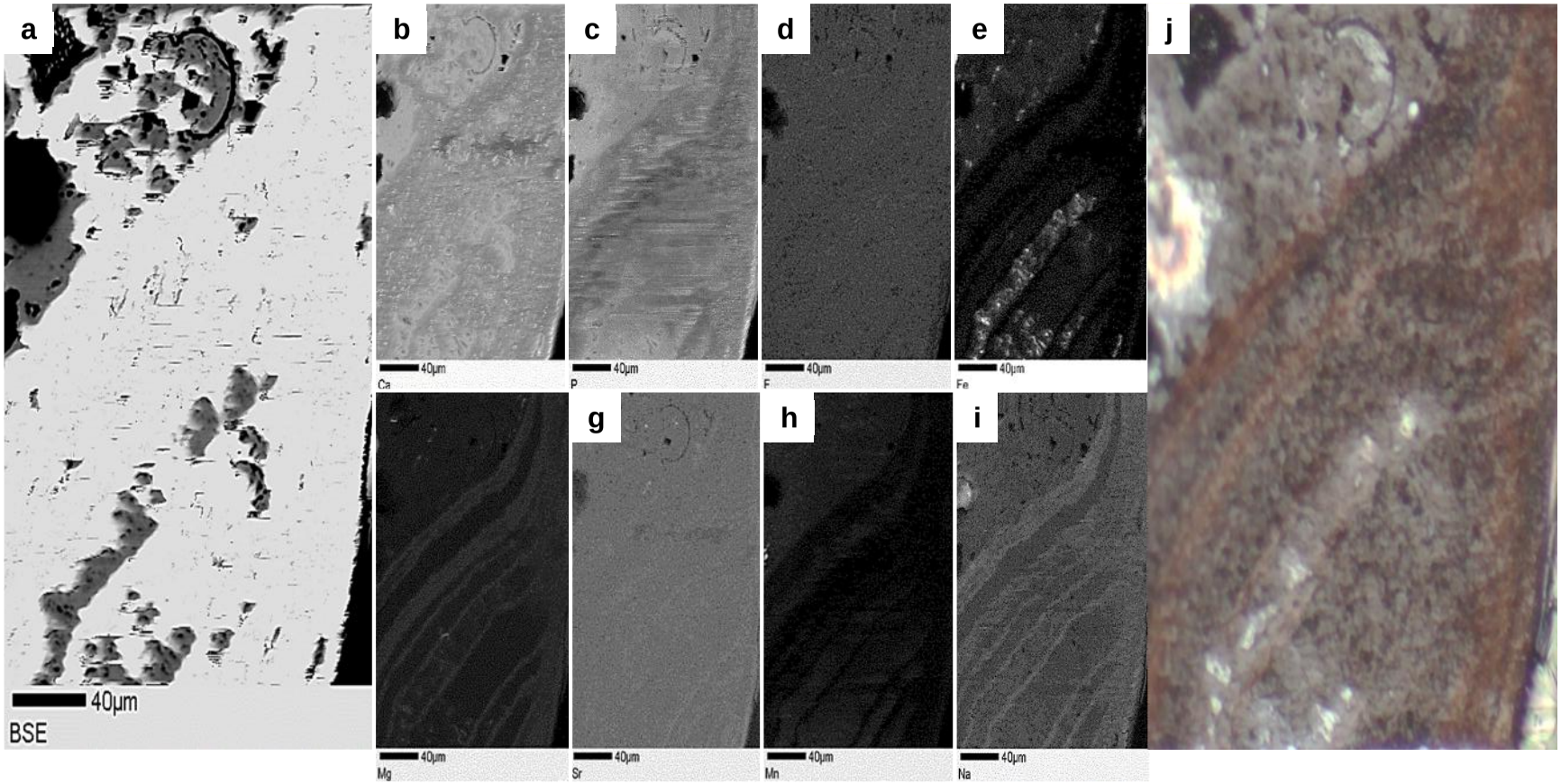

Figure21: Devon Island lingulid (DIL-12B/CMNIF 245), backscattered electron image (a), and elemental maps for of Ca, P, F, Fe, Mg, Sr, Mn and Na (b-i) via JEOL JXA-8600 electron microprobe. Scale bar is 40 µm. Transmitted light image (j) of same zone allowing for correlation of elements with shell layers.

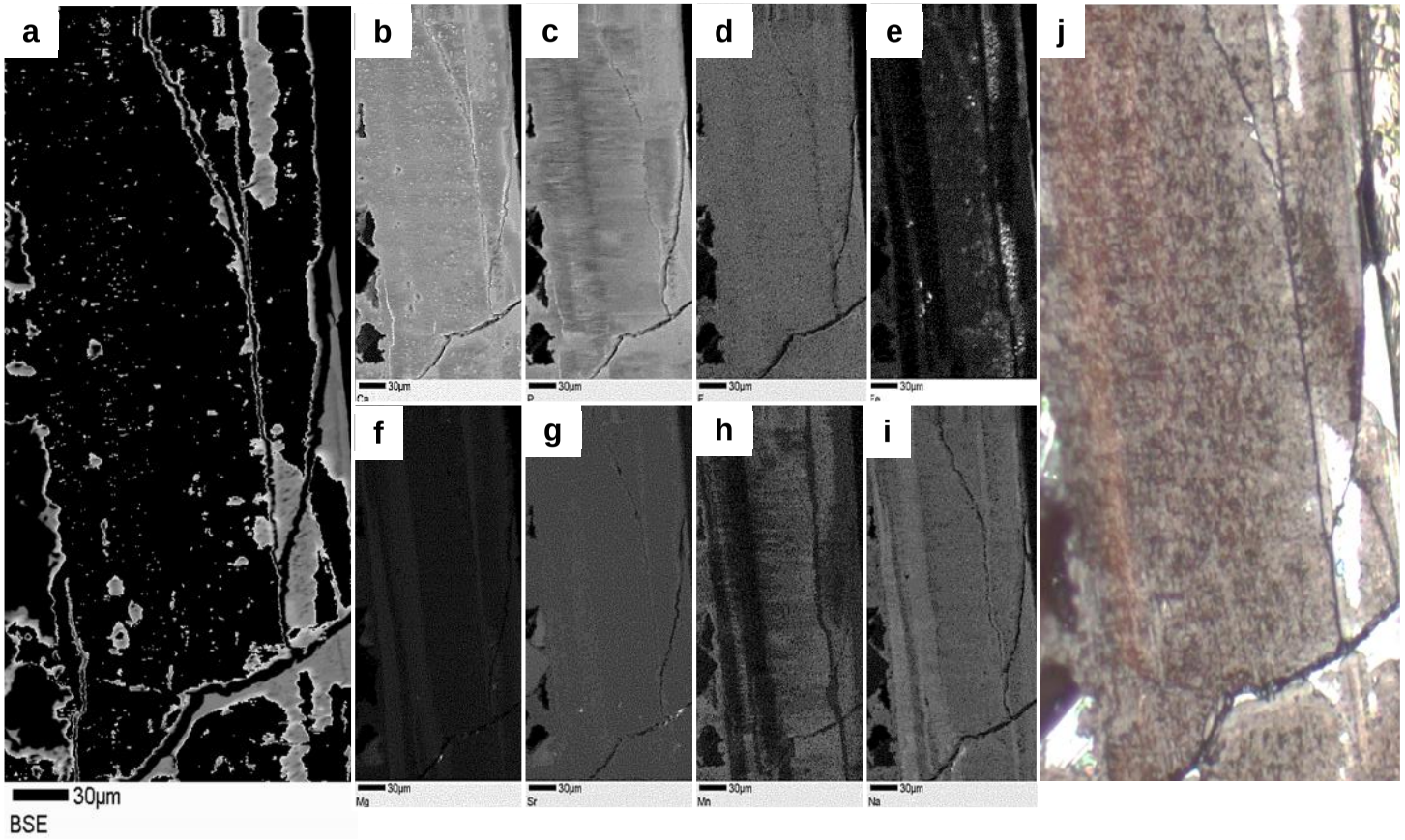

Figure 22: Devon Island lingulid (DIL-12B/CMNIF 245) backscattered electron image (a), and elemental maps for of Ca, P, F, Fe, Mg, Sr, Mn and Na (b-i) via JEOL JXA-8600 electron microprobe. Scale bar is 30 µm. Transmitted light image (j) of same zone allowing for correlation of elements with shell layers.

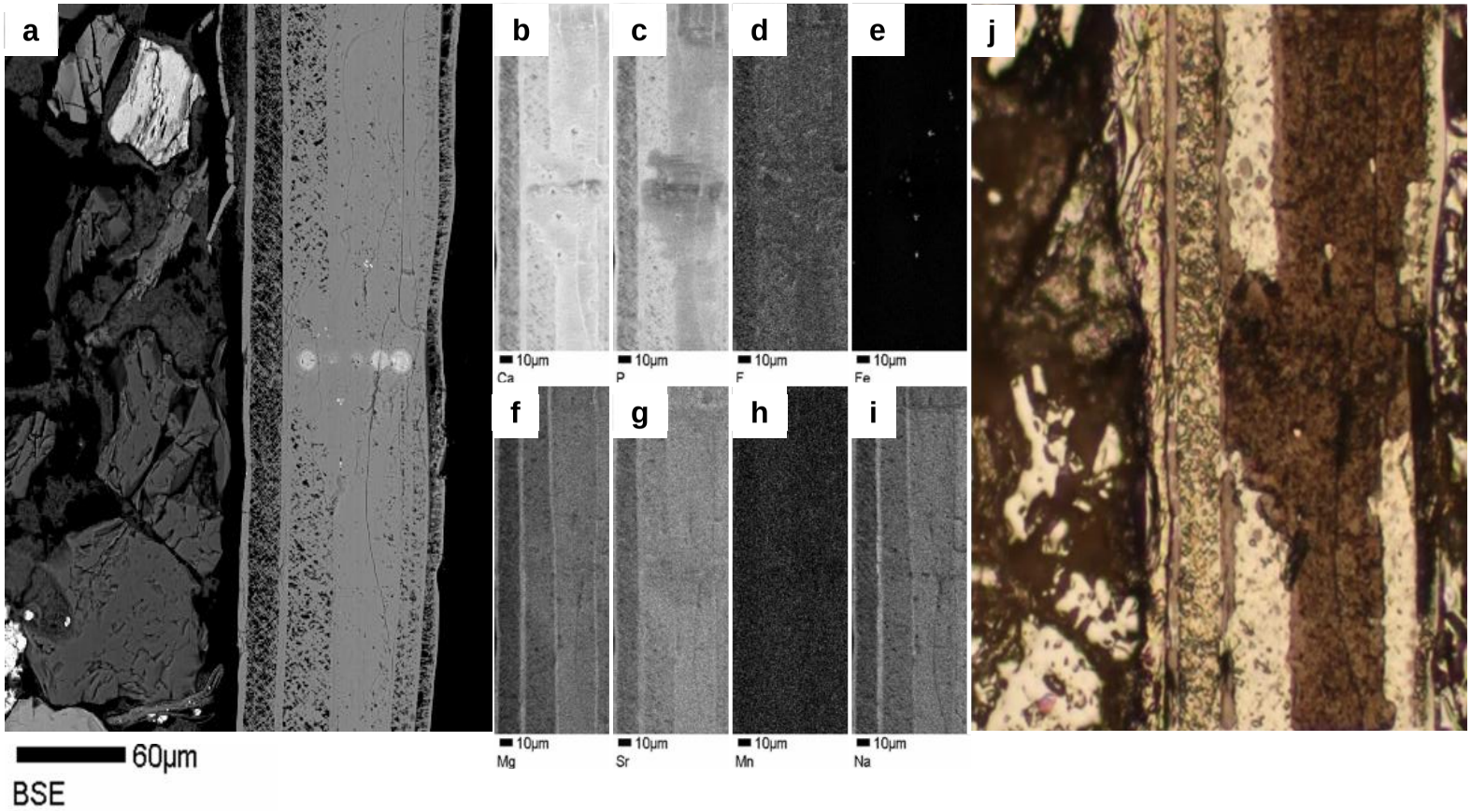

Figure 23: Stewart County lingulid (SCL 25A/ UCM 78789), backscattered electron image (a), and elemental maps for of Ca, P, F, Fe, Mg, Sr, Mn and Na (b-i) via JEOL JXA-8600 electron microprobe. Scale bar is 10 µm. Transmitted light image (j) of same zone allowing for correlation of elements with shell layers.

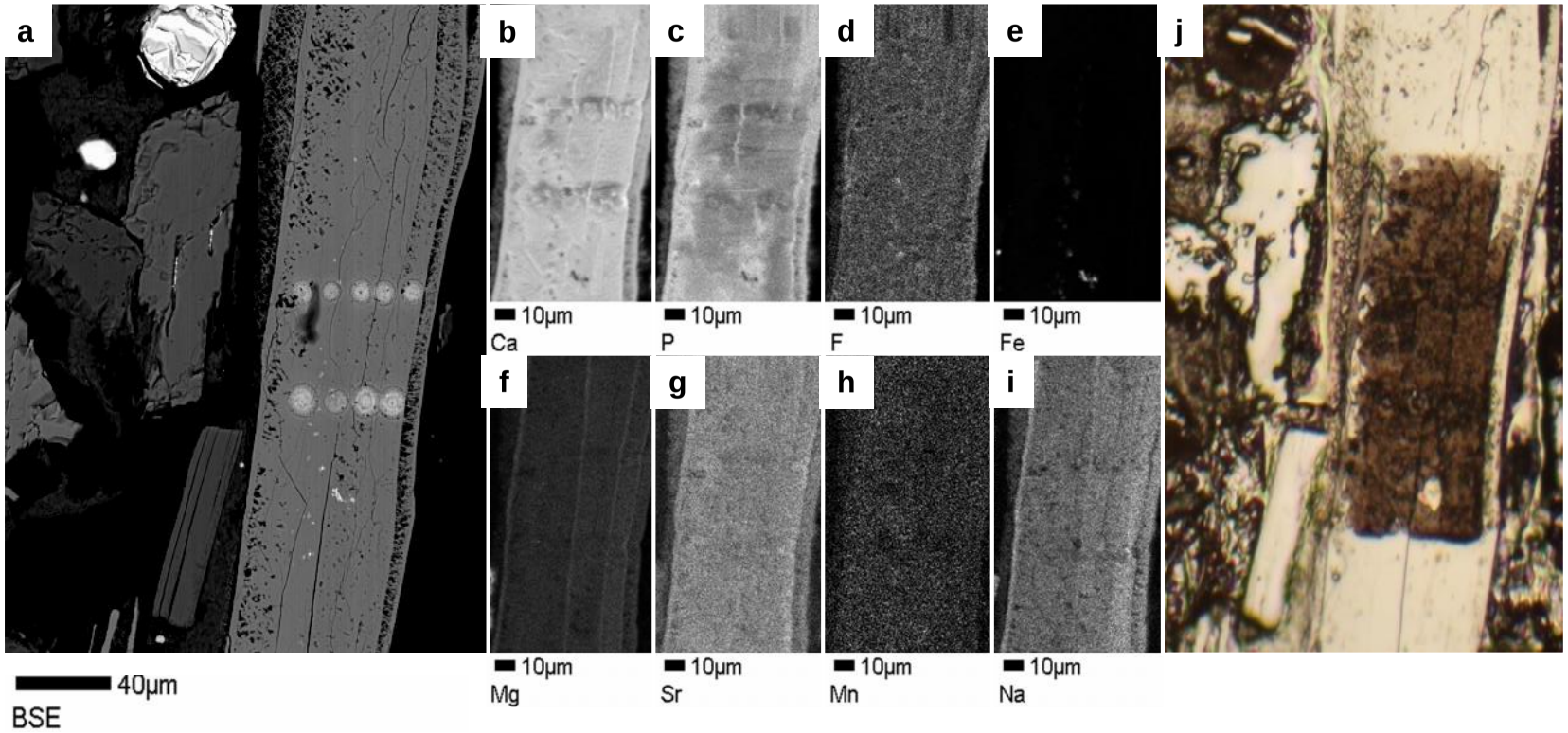

Figure 24: Stewart County lingulid (SCL 25A/ UCM 78789), backscattered electron image (a), and elemental maps for of Ca, P, F, Fe, Mg, Sr, Mn and Na (b-i) via JEOL JXA-8600 electron microprobe. Scale bar is 10 µm. Transmitted light image (j) of same zone allowing for correlation of elements with shell layers.

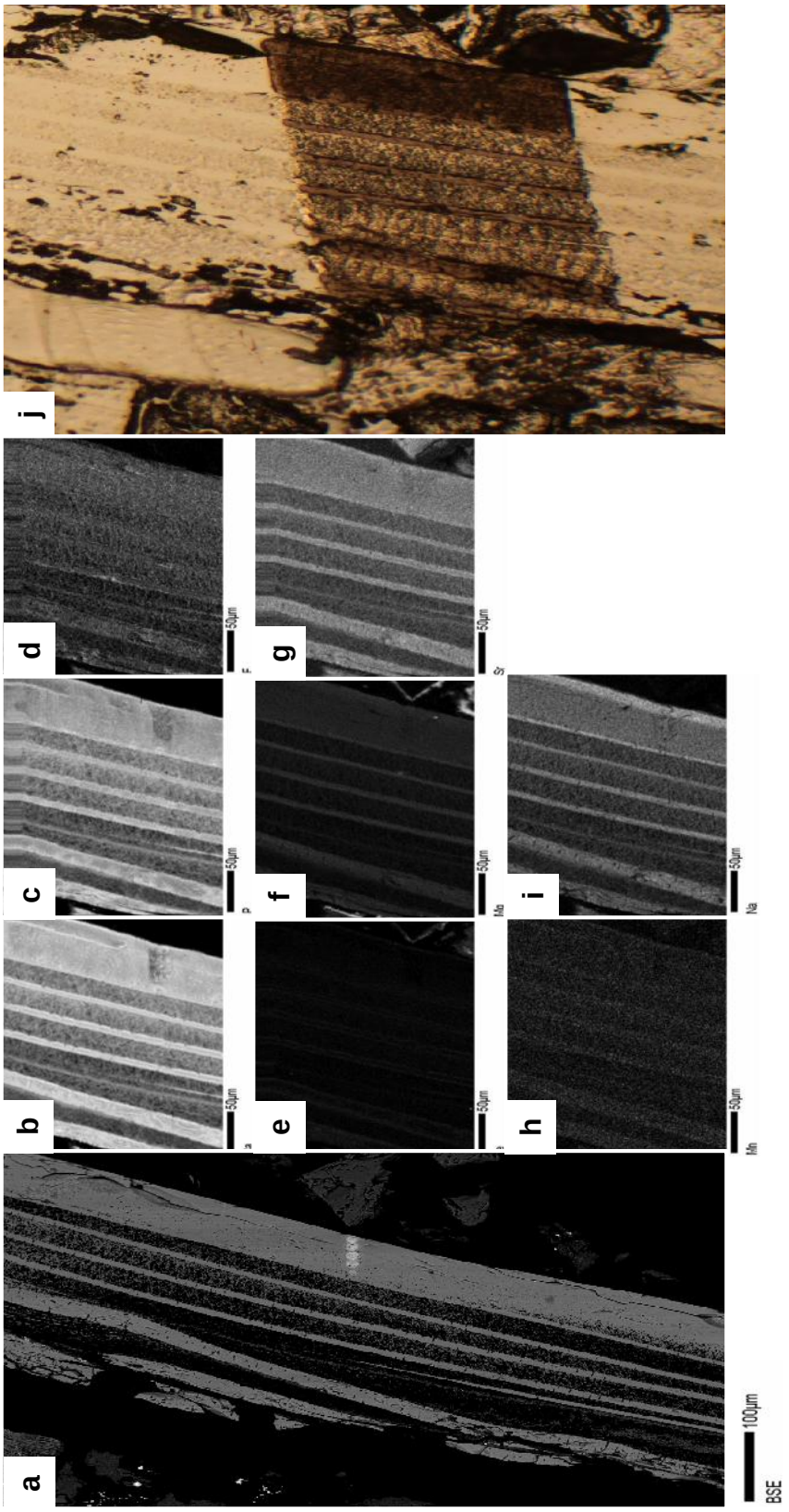

Figure 25: Stewart County lingulid (SCL 29B/ UCM 78790), backscattered electron image (a), and elemental maps for of Ca, P, F, Fe, Mg, Sr, Mn and Na (b-i) via JEOL JXA-8600 electron microprobe. Scale bar is 50 µm. Transmitted light image (j) of same zone allowing for correlation of elements with shell layers.

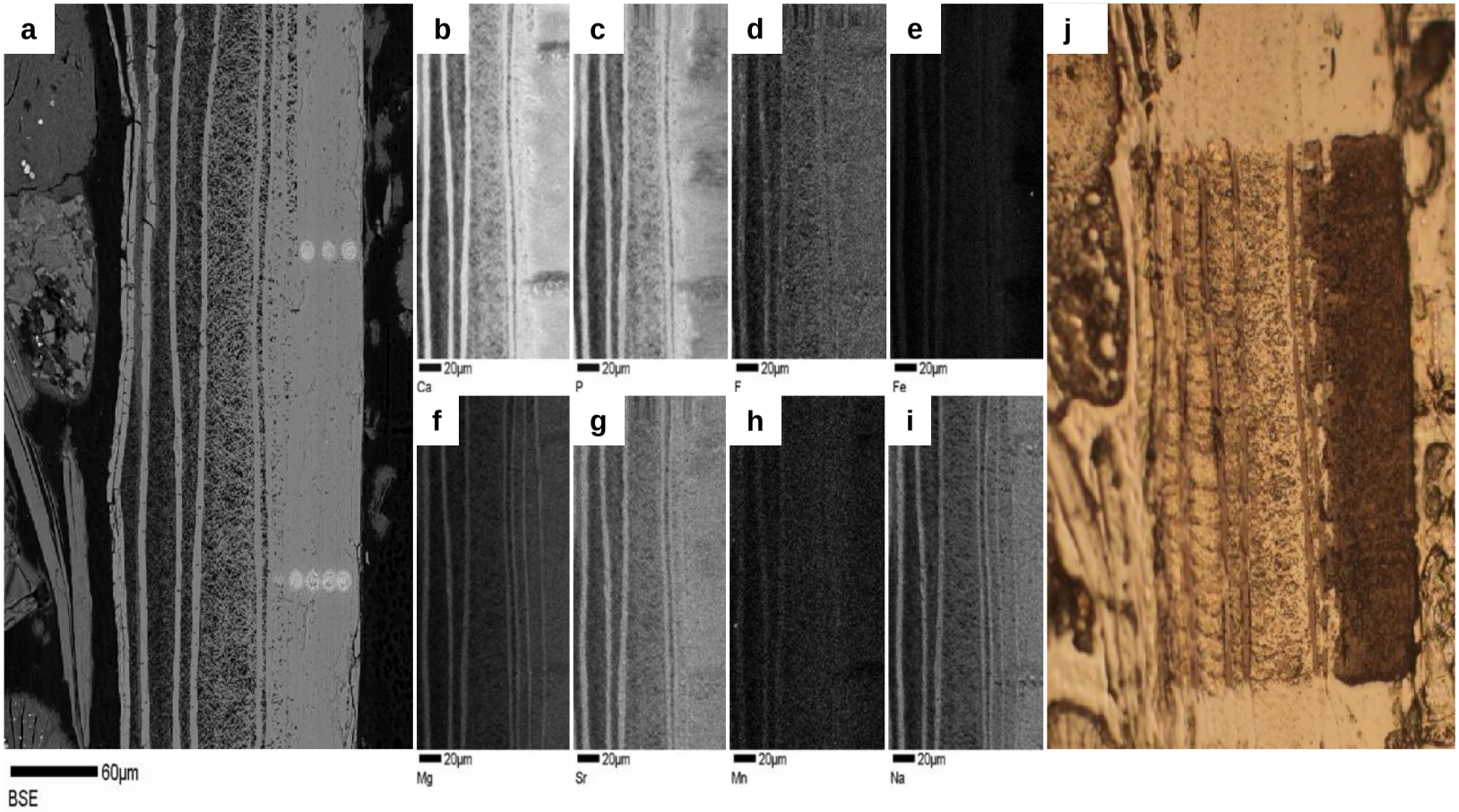

Figure 26: Stewart County lingulid (SCL 29B/ UCM 78790), backscattered electron image (a), and elemental maps for of Ca, P, F, Fe, Mg, Sr, Mn and Na (b-i) via JEOL JXA-8600 electron microprobe. Scale bar is 20 µm. Transmitted light image (j) of same zone allowing for correlation of elements with shell layers.

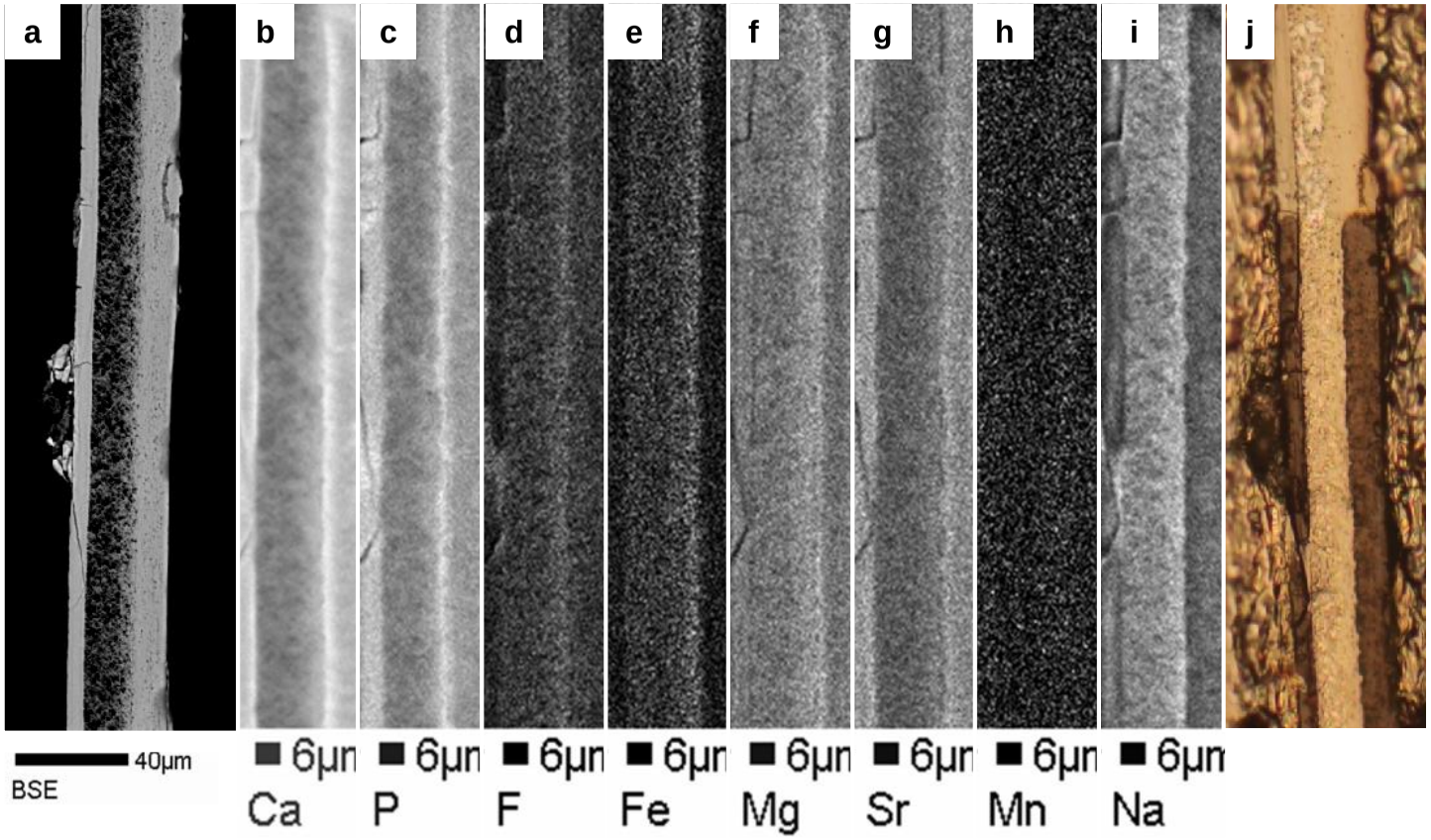

Figure 27: Modern lingulid (CA-4282B), backscattered electron image (a), and elemental maps for of Ca, P, F, Fe, Mg, Sr, Mn and Na (b-i) via JEOL JXA-8600 electron microprobe. Scale bar is 6 µm. Transmitted light image (j) of same zone allowing for correlation of elements with shell layers.

original mineralized and chitinous laminae in these samples. Variations in the concentrations of F may reflect differences in apatite mineralogy.

Ca and P are ubiquitous in the Devon Island sample, and no consistent patterns of heterogeneities in abundance (i.e., zonation) were observed (Figs., 21-22). A discretely zoned pattern of Ca and P heterogeneity among laminae is seen in one Stewart County lingulid (SCL-29B; Figs. 23-24), which suggests variable mineralization of chitinous laminae (i.e., differences in diagenetic alteration). However, no zonation was observed in the other Stewart County specimen (SCL-25A; Figs. 25-26); this suggests that the Stewart County lingulids have experienced differential amounts of diagenesis.

Trace elements (Fe, Mg, Sr, Mn and Na)

Trace elements are commonly zoned within the shells of both the fossil and modern lingulids examined in this study (Figs. 21-27). Moreover, a few major trends in zonation may be observed. In all fossil lingulids examined, Mg and Na are concentrated within the more mineralized laminae; Sr is also commonly zoned in this manner. However, in the modern lingulid, these elements are concentrated within the interior-most portion of the secondary shell layer rather than zoned along boundaries of alternating shell material.

Magnesium is highly concentrated within original apatitic laminae and is limited within originally chitinous laminae for analyzed specimens from both fossil assemblages. Sodium concentrates preferentially within original apatitic lamina of fossil lingulids, and within the interior of the secondary shell layer of the modern lingulid. Strontium appears most abundant in fossil lingulids from Stewart County in which it typically concentrates within original apatitic

lamina, while the Devon Island lingulid exhibits a nearly uniform distribution. The modern lingulid also exhibits higher concentrations in more mineralized zones of the secondary and primary shell layers. Very little sulfur can be observed in element maps, and the sulfur that is present occurs almost exclusively along zones of shell damage.

In Devon Island lingulids, Fe and Mn are concentrated within the originally chitinous laminae, while Mn is uniformly distributed throughout shell laminae of both the modern lingulid and fossils from Stewart County. Within the shells from Stewart County, Fe is also uniformly distributed, while it is concentrated in the interior-most secondary shell layer in the modern lingulid.

Quantitative Element Distributions among Dorso-ventral Transects

Microprobe point analyses provide quantitative data that can be compared with the zonations and heterogeneities revealed in the elemental maps. Comparisons of dorso-ventral transect data between the two fossil assemblages are made with the potential for sample-size errors in mind; the small Stewart County data set may not reliably capture the chemical trends.

In Devon Island lingulids, the most commonly observed distributional patterns are the increasing Na and Mg and decreasing Fe towards the interior shell wall (Figs. 28-30). Stewart County lingulids exhibit the reverse of this pattern with Na and Mg decreasing and Fe becoming relatively enriched towards the interior shell wall (Figs. 31-32). These dorso-ventral trends also may have superimposed oscillations in concentrations, which may relate to the zonation seen in the elemental maps. However, as point analyses are not correspondent with these zones, any potential correlation between elemental zonation and concentration data could not be evaluated. Other trace-element distributions generally exhibit no consistent pattern or trend, or rarely, an

oscillatory pattern. The abundances of several elements, however, seem to either positively or negatively correspond with other elements.

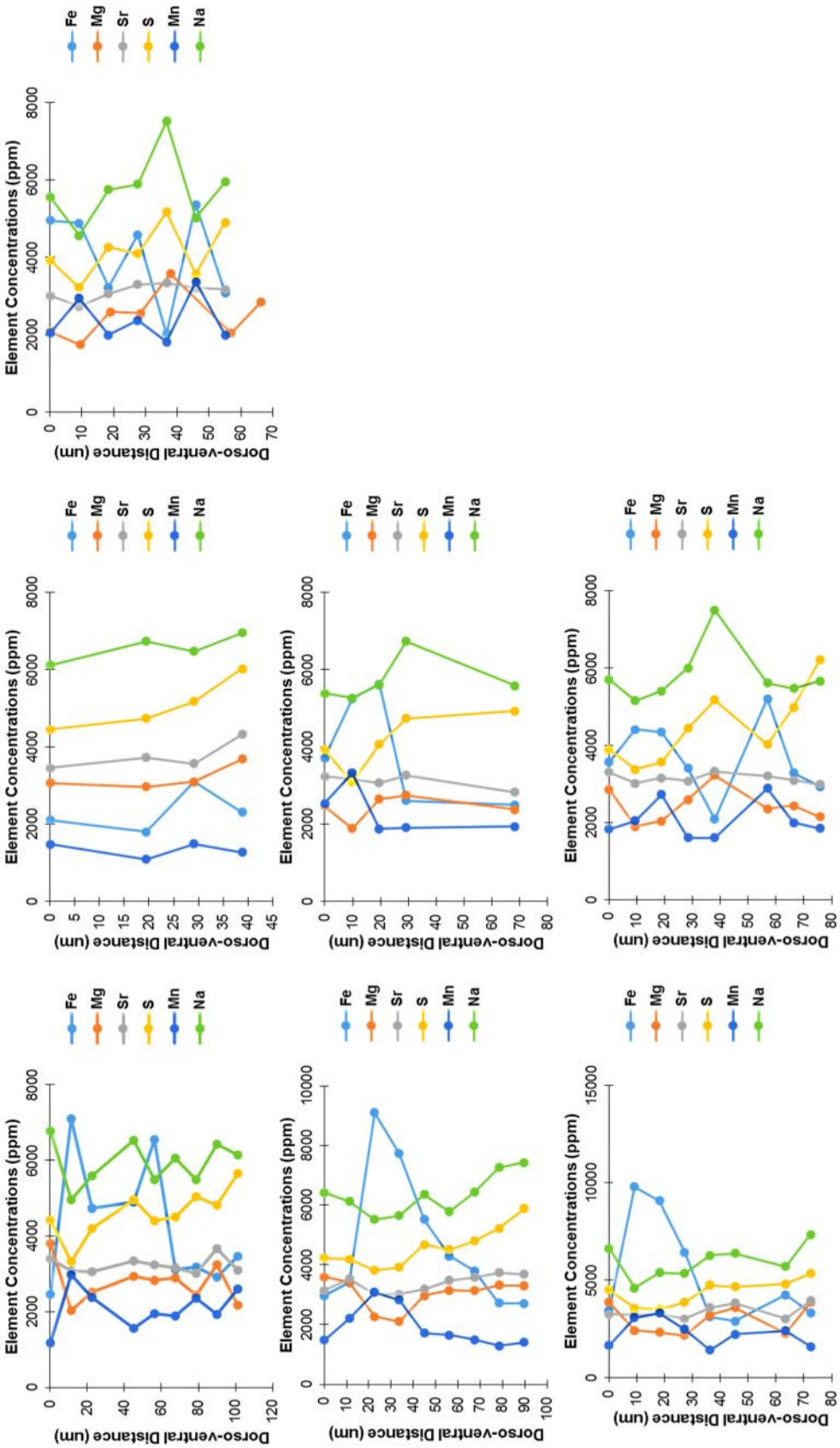

Figure 21: Seven dorso-ventral transects of trace elements Fe, Mg, Sr, S, Mn and Na through the shell of Devon Island lingulid DIL 8B/ CMNIF 245. Element concentrations are in ppm and distance through the shell is plotted in millimeters with the first point of each transect corresponding with the uppermost microanalyzed point (typically less than 40 microns from the shell exterior). Transects descend at a constant longitudinal (x-axis) position toward the shell interior but do not intersect with cementing sediments. In all transects within this specimen, Mg, Sr, S and Na behave similarly whereas Mn and Fe appear anti-correspondent with the other four elements.

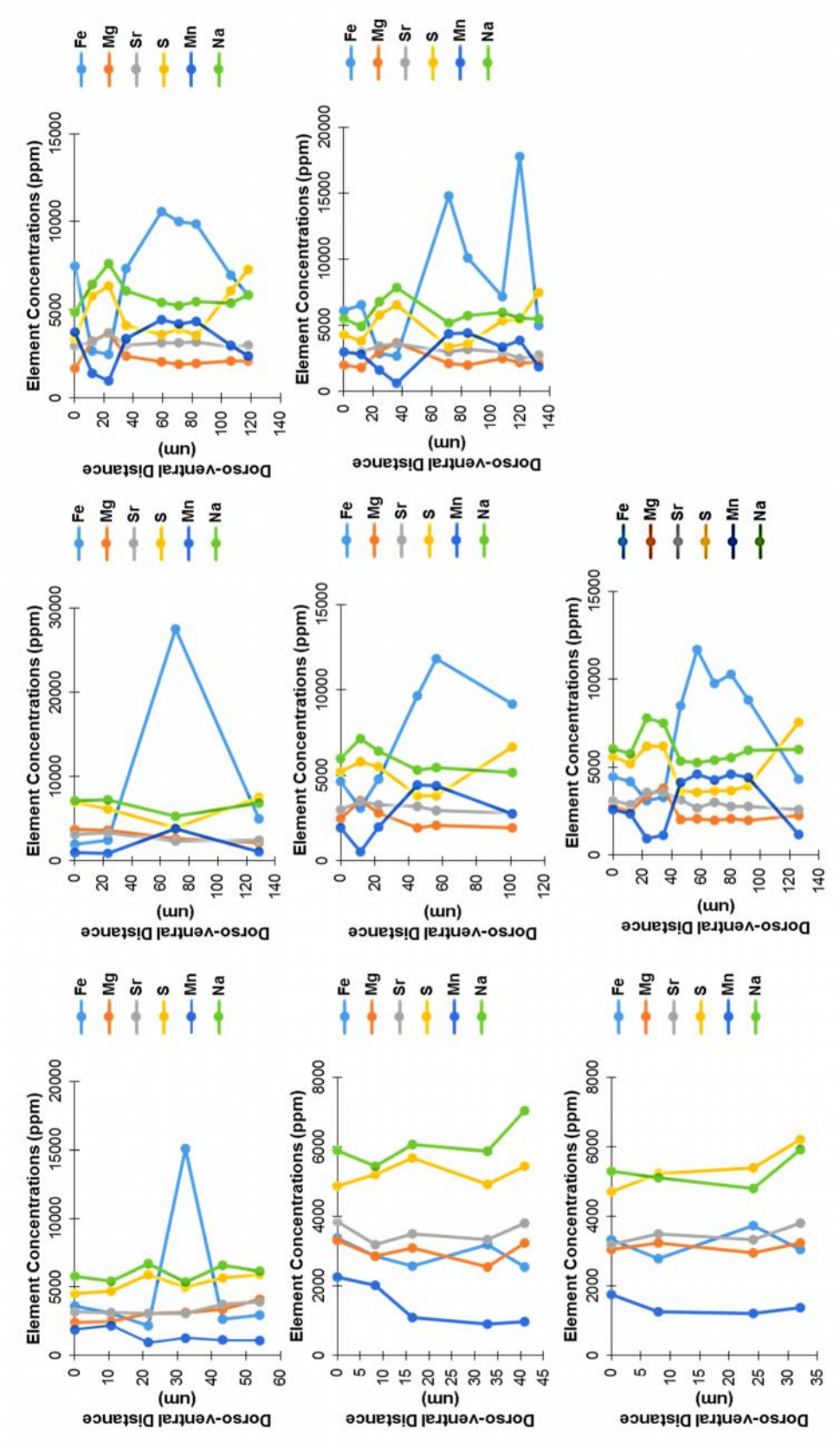

Figure 22: Eight dorso-ventral transects of trace elements Fe, Mg, Sr, S, Mn and Na through the shell of Devon Island lingulid (DIL) 12B/ CMNIF 245. Element concentrations are in ppm and distance through the shell is plotted in millimeters with the first point of each transect corresponding with the uppermost microanalyzed point (typically less than 40 microns from the shell exterior. Transects descend at a constant longitudinal (x-axis) position toward the shell interior but do not intersect with cementing sediments. In most (b-f) transects in the specimen, Mg, Sr, S and Na behave similarly. Sr diverges slightly from this pattern in two transects (g-h) and Mg diverges in one transect (a). In five transects (d-h), Fe and Mn behave similarly but this trend does not emerge in the three remaining transects (a-c). In

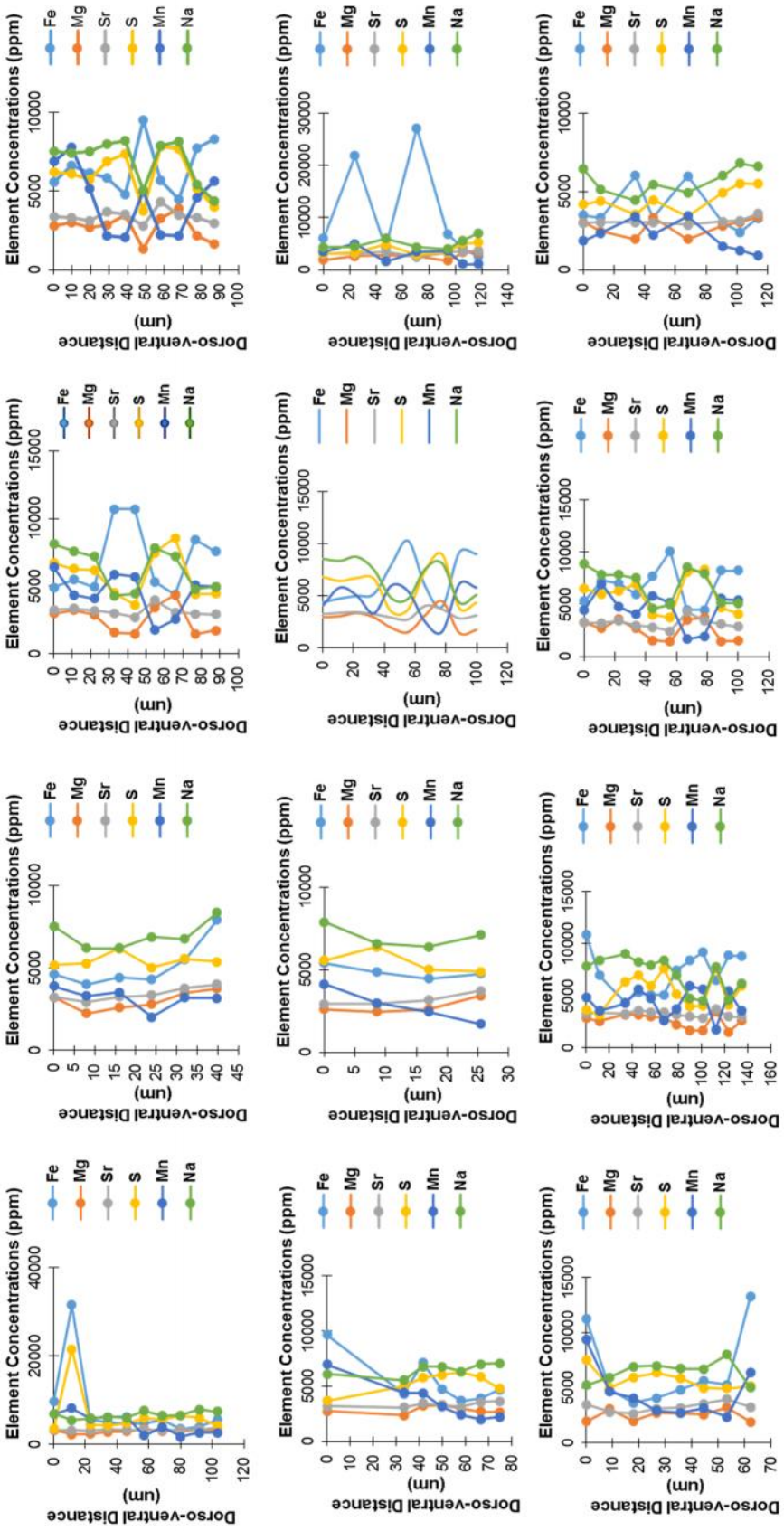

Figure 30: Twelve dorso-ventral transects of trace elements Fe, Mg, Sr, S, Mn and Na through the shell of Devon Island lingulid (DIL) 25B/ CMN 166. Element concentrations are in ppm and distance through the shell is plotted in millimeters with the first point of each transect corresponding with the uppermost microanalyzed point (typically less than 40 microns from the shell exterior. Transects descend at a constant longitudinal (x-axis) position toward the shell interior but do not intersect with cementing sediments. In most (c-k) transects in the specimen, Mg, Sr, S and Na behave similarly. Sr diverges slightly from this pattern in three transects (a-b, l). In all transects, Fe and Mn behave similarly, and Fe appears anti-correspondent with Mg and Na. In one transect (a) Fe, Mn and S appear to positively correspond.

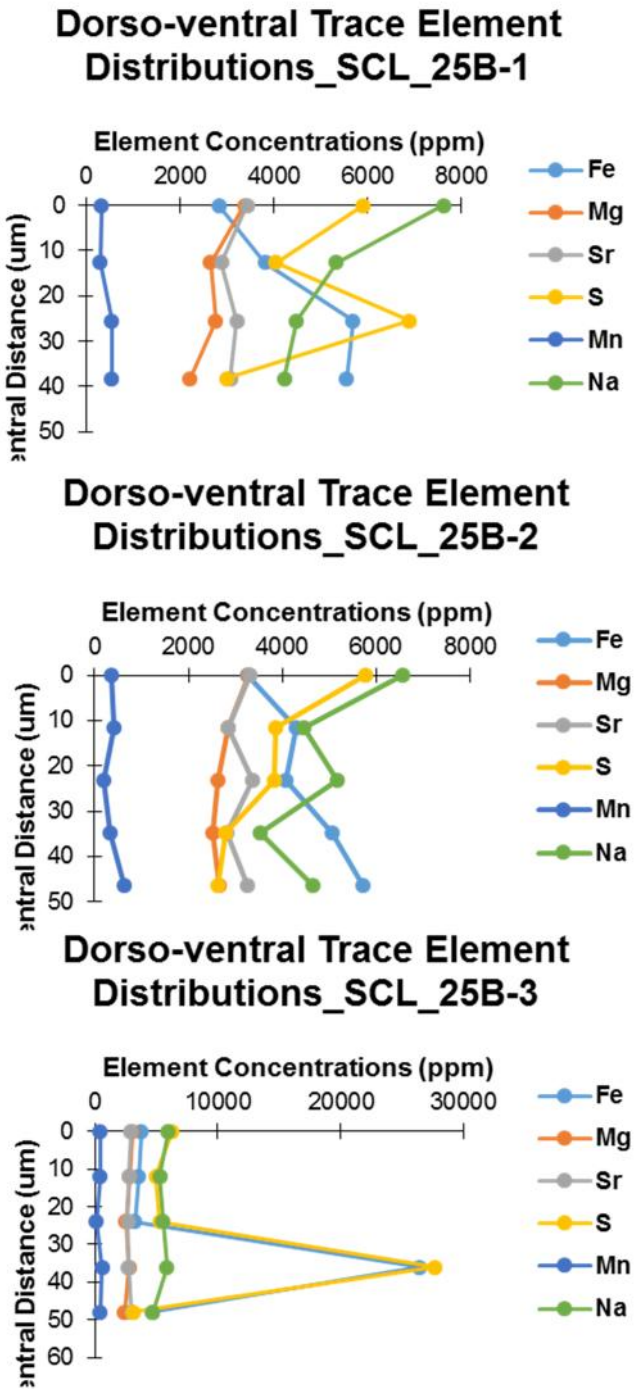

Figure 31: Three dorso-ventral transects of trace elements Fe, Mg, Sr, S, Mn and Na through the shell of Stewart County lingulid (SCL) 25A/ UCM 79789. Element concentrations are in ppm and distance through the shell is plotted in millimeters with the first point of each transect corresponding with the uppermost microanalyzed point (typically less than 40 microns from the shell exterior. Transects descend at a constant longitudinal (x-axis) position toward the shell interior but do not intersect with cementing sediments. In one transect (b), Na and S behave similarly, with Sr and Mg loosely corresponding. In two transects (a-b), Fe and Na appear anti-correspondent.

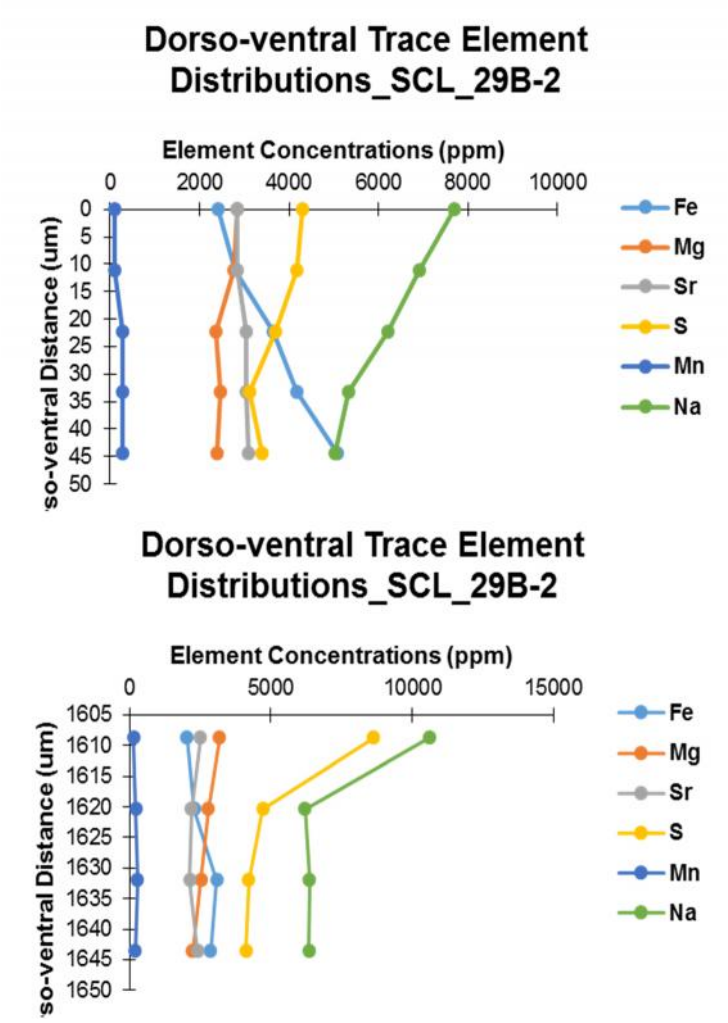

Figure 32: Two dorso-ventral transects of trace elements Fe, Mg, Sr, S, Mn and Na through the shell of Stewart County lingulid (SCL) 29B/ UCM 79790. Element concentrations are in ppm and distance through the shell is plotted in millimeters with the first point of each transect corresponding with the uppermost microanalyzed point (typically less than 40 microns from the shell exterior. Transects descend at a constant longitudinal (x-axis) position toward the shell interior but do not intersect with cementing sediments. Mg, S and Na behave similarly in both transects but Sr exhibits no clear correspondence. No clear relationship between Fe and Mn emerges, but in both transects, Fe and Na appear anti-correspondent.

Element correspondences along transects

The elements Mg, Sr, S and Na were observed to correspond in 81.5% of all transects (twenty-two out of twenty-seven) in the Devon Island shells. The apparent correspondence of Mg, Sr and Na, in particular, is unsurprising given their propensity for ionic substitution with Ca in the apatite lattice (Grossman et al., 1996; Elliot et al. 2002). Among ~63% of the Devon Island transects (seventeen of twenty-seven), Mn and Fe were also observed to co-vary. Mn and Mg were found to be anti-correspondent. Fe and S were seen to correspond in only one Devon Island transect (Fig. 29a).

Among the Stewart County lingulids, positive correspondences were observed among Na, S and Mg, between Fe and S, and among Na, S and Sr in different transects, Negative correspondences were observed between Fe and S, Fe and Na, and Na, S and Mg. The most common elemental covariances observed among Stewart County shells are a positive correspondence between Na and S, and a negative correspondence between Fe and Na, with both occurring 60% of the time (three of five transects).

Pearson's r correlation

Element correspondences suggested by the transects in Figures 28-32 were analyzed by Pearson's r values in order to test whether observed trends were numerically robust (i.e., $-0.7 < r > 0.7$). Pearson's r values were calculated for eight element pairs: Fe–Mn, Sr–Mg, Na–Mg, Mg–Fe, Mn–Na, Na–Ca, Sr–Ca and Mg–Ca. Results for each element pair both for whole shells and along individual dorso-ventral transects are given in Tables 7 and 8. For whole shells, all point data for a shell were evaluated as a continuous dataset. Among the eight pairings examined, the most robust positive correlations were found between Na—Mg (80% of all shells) and Fe—Mn

(60% of all shells). Mn—Na were negatively correlated in 40% of all shells, and the remaining pairs exhibited weak or no correlation.

Among all twenty-seven Devon Island transects, five pairings exhibited r values above the 0.7 limit for numerical importance in >50% of the transects: Fe—Mn (52%), Sr—Mg (63%), Na–Mg (63%), Mg–Fe (52%), and Mn—Na (56%). The first three of these element pairs were positively correlated, and the latter two were negatively correlated. The remaining three element pairs were highly-correlated in less than 20% of all transects.

Table 7: Pearson's r values for element pairings between transects of fossil lingulids. Bolded numbers indicate strong correlation. The pairings Fe – Mn, Sr – Mg, Na – Mg, Mg – Fe and Mn – Na exhibited strong correlations in all most (≥40%) of all transects; additionally, Mg – Ca was strongly correlated in Stewart County specimens.

Locality	Specimen-Transect #	Fe-Mn	Sr-Mg	Na-Mg	Mg-Fe	Mn-Na	Na-Ca	Sr-Ca	Mg-Ca
Devon Island	25B-1	0.63	0.43	**0.90**	-0.62	**-0.75**	0.42	0.18	0.59
Devon Island	25B-2	**0.89**	0.16	0.49	0.13	-0.59	-0.20	-0.56	0.58
Devon Island	25B-3	**0.80**	0.26	0.65	-0.61	**-0.85**	0.31	-0.60	0.27
Devon Island	25B-4	0.06	**0.91**	**0.83**	**0.83**	0.05	**-0.95**	-0.68	**-0.89**
Devon Island	25B-5	**0.81**	**0.97**	0.19	-0.16	0.59	-0.22	**-0.95**	**-0.96**
Devon Island	25B-6	0.32	**0.87**	**0.88**	-0.60	-0.52	-0.61	**-0.80**	-0.66
Devon Island	25B-7	0.56	0.60	**0.87**	**-0.88**	-0.49	-0.16	-0.24	-0.36
Devon Island	25B-8	0.63	**0.81**	**0.87**	**-0.92**	-0.57	-0.17	0.04	-0.40
Devon Island	25B-9	**0.74**	**0.76**	**0.94**	**-0.86**	-0.51	-0.36	-0.23	-0.22
Devon Island	25B-10	0.46	0.70	**0.91**	**-0.96**	-0.41	0.24	0.39	0.18
Devon Island	25B-11	0.70	0.44	**0.81**	-0.11	**-0.85**	0.33	**0.79**	-0.14
Devon Island	25B-12	**0.89**	0.58	**0.80**	**-0.83**	**-0.93**	-0.28	-0.60	-0.58
Devon Island	12B-13	-0.08	**0.80**	0.45	0.00	**-0.71**	0.19	0.33	-0.19
Devon Island	12B-14	0.52	-0.02	0.48	-0.21	-0.56	-0.51	-0.14	**-0.94**
Devon Island	12B-15	0.05	**0.78**	0.68	**-0.94**	0.31	**0.75**	0.31	**0.71**
Devon Island	12B-16	**1.00**	**0.89**	0.48	-0.42	**-0.99**	**0.98**	0.66	0.33
Devon Island	12B-17	**0.93**	**0.82**	**0.99**	**-0.86**	**-0.84**	0.18	0.11	0.13
Devon Island	12B-18	**0.95**	**0.84**	**0.92**	**-0.78**	**-0.80**	0.48	0.51	0.55
Devon Island	12B-19	**0.98**	**0.79**	**0.96**	**-0.84**	**-0.84**	0.15	-0.02	0.30
Devon Island	12B-20	**0.82**	0.69	**0.98**	-0.52	**-0.72**	0.28	0.55	0.24
Devon Island	8B-21	0.46	**0.76**	**0.77**	-0.52	**-0.81**	0.05	-0.15	0.23
Devon Island	8B-22	**0.90**	0.66	0.63	**-0.95**	**-0.78**	-0.02	-0.11	0.37
Devon Island	8B-23	**0.89**	**0.78**	**0.87**	**-0.72**	**-0.83**	-0.06	-0.26	0.07
Devon Island	8B-25	0.68	**0.90**	0.62	0.12	**-0.72**	-0.69	**-0.94**	**-1.00**
Devon Island	8B-26	0.45	0.16	0.69	-0.36	-0.58	-0.61	-0.55	-0.59
Devon Island	8B-28	**0.84**	**0.79**	**0.85**	-0.64	-0.49	-0.19	**-0.70**	-0.40
Devon Island	8B-29	**0.76**	**0.73**	**0.97**	**-0.92**	**-0.74**	-0.60	-0.35	-0.53
Stewart County	25B-1	**0.93**	**0.74**	**0.91**	**-0.77**	**-0.74**	0.23	-0.61	0.03
Stewart County	25B-2	0.64	0.31	**0.86**	**-0.77**	-0.15	0.21	-0.03	0.17
Stewart County	25B-3	0.64	-0.02	**0.74**	0.11	0.10	-0.56	0.54	-0.19
Stewart County	29B-2	**0.88**	**-0.97**	**0.85**	**-0.84**	**-0.90**	0.65	**-0.76**	**0.78**
Stewart County	29B-3	**0.80**	0.31	**0.81**	**-0.87**	**-0.86**	**-0.99**	-0.66	**-0.80**

Among the five Stewart County transects, three pairings exceeded the 0.70 limit in 50% or more transects: Fe—Mn (60%) and Na—Mg (100%), and Mg-Fe (80%). In 40% of all transects, Sr—Mg, Mn—Na, and Mg—Ca were well correlated. Fe—Mn, Sr—Mg, Na—Mg, and Mg—Ca exhibited positive correlations in these specimens, while

Mg—Fe and Mn—Na were negatively correlated. Weaker relationships emerged between Na—Ca and Sr—Ca, with each correlated in 20% of Stewart County transects.

Table 8: Pearson's r values for element pairings within whole shells of fossil lingulids. Correlations were consistently strong in three element pairs: Fe – Mn, Na – Mg and Mn – Na.

Locality	Specimen-Transect #	Fe-Mn	Sr-Mg	Na-Mg	Mg-Fe	Mn-Na	Na-Ca	Sr-Ca	Mg-Ca
Devon Island	DIL-25B	0.49	0.64	**0.77**	-0.37	-0.32	-0.02	-0.10	-0.15
Devon Island	DIL-12B	**0.70**	0.67	0.70	-0.50	-0.63	0.07	0.57	0.34
Devon Island	DIL-8B	**0.71**	**0.74**	**0.82**	-0.53	**-0.74**	-0.01	0.05	0.17
Stewart County	SCL-25B	0.49	0.36	**0.79**	-0.07	-0.24	-0.14	0.33	-0.01
Stewart County	SCL-29B	**0.73**	-0.22	**0.82**	-0.67	**-0.72**	-0.52	-0.24	-0.36

Elemental ratios along longitudinal axes

The 7 to 12 dorso-ventral transects in the Devon Island lingulids mean that generalized elemental trends along the longitudinal growth axes of those shells could also be analyzed. Conversely, the 2 to 3 transects through Stewart County specimens may offer less reliable representations of such trends. The longitudinal profiles were generated by calculating the mean concentration of an element for each transect and then plotting those values as a function of absolute distance between transects. The result is a "moving-average" corresponding to longitudinal shell growth along the marginal fold of the fossil shells.

For all Devon Island lingulids, Mg/Ca (Fig. 33) decreased sharply at approximately 100 microns distance from the initial, posterior-most transect (i.e., within or near the larval shell). Following this initial decrease, Mg/Ca ratios declined with shell length (i.e., age). For Stewart County lingulids, Mg/Ca (Fig. 34) increased, though, in SCL-25, a substantially smaller longitudinal area was surveyed. Ratios of Sr/Ca in all Devon Island specimens were broadly constant at around 0.0095 ppm but rapidly declined after 4 mm to approximately 0.0092 ppm (Fig. 35). Stewart County specimens also exhibited decreasing Sr/Ca ratios with age (Fig. 36).

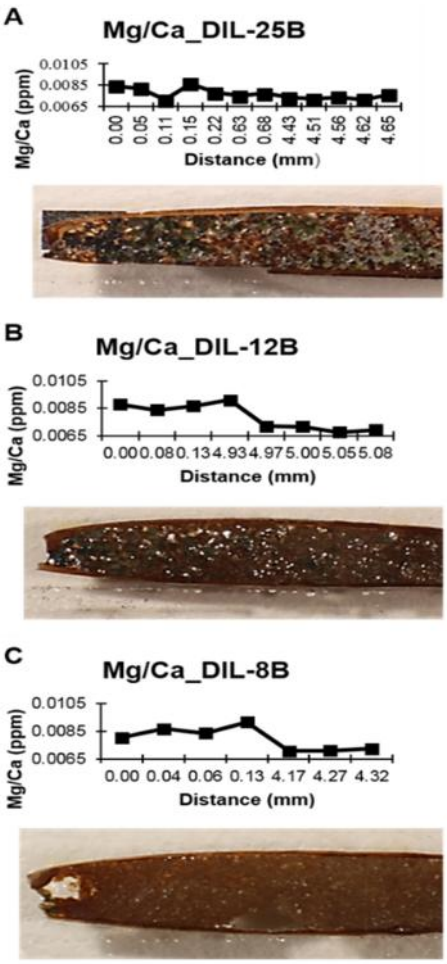

Figure 33: Mean Mg/Ca ratios plotted against longitudinal (posterior to anterior) position for lingulid fossils from Devon Island (DIL 25B/ CMN 166, DIL 12B/ CMNIF 245 and DIL 8B/ CMNIF 245). Mean Mg and Ca values were calculated per transect before ratios were determined, and a moving average was then plotted against length in the y-direction (i.e., age or growth along the marginal fold). In all shells, Mg/Ca decreases substantially at around 100 microns from the start of the transect (most posterior) before rebounding and then decreasing toward the ventral margin.

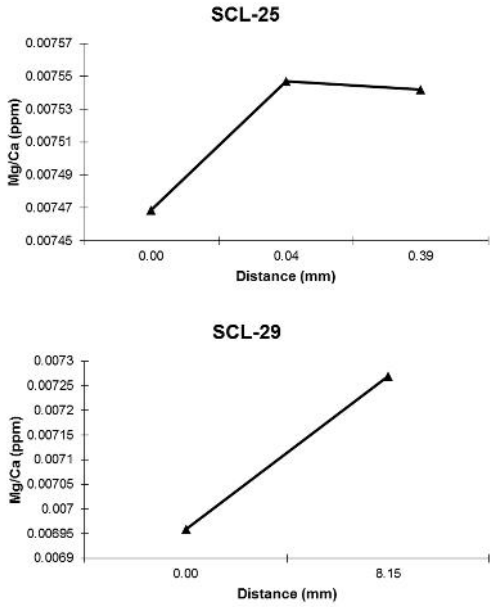

Figure 34: Mean Mg/Ca ratios plotted against longitudinal (posterior to anterior) position in millimeters for lingulid fossils from Stewart County (SCL 25/ UCM 79789 and SCL 29/ UCM 79790). Mean Mg and Ca values were calculated per transect before ratios were determined, and a moving average was then plotted against length in the y-direction (i.e., age or growth along the marginal fold). In all shells, Mg/Ca increases with age.

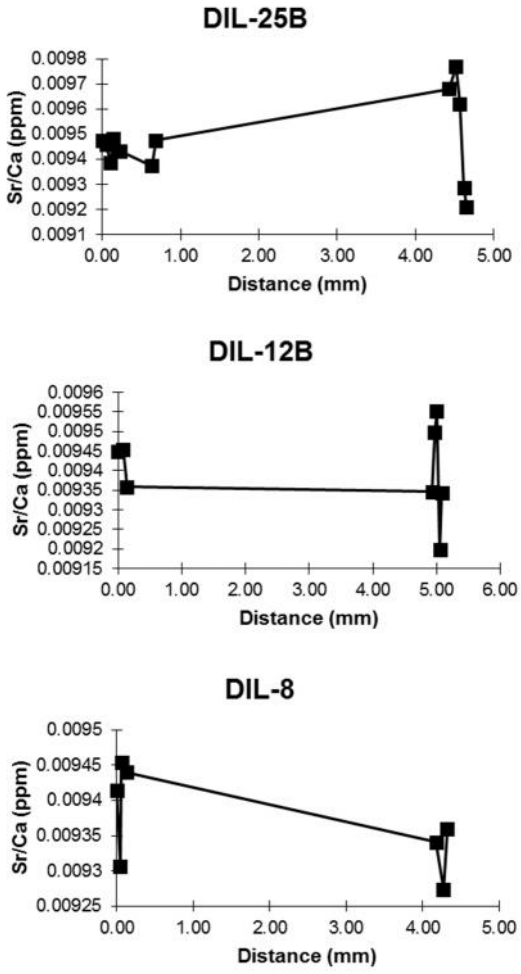

Figure 35: Mean Sr/Ca ratios plotted against longitudinal (posterior to anterior) position in millimeters for lingulid fossils from Devon Island (DIL 25B/ CMN 166, DIL 12B/ CMNIF 245 and DIL 8B/ CMNIF 245). Mean Sr and Ca values were calculated per transect before ratios were determined, and a moving average was then plotted against length in the y-direction (i.e., age or growth along the marginal fold). In two shells (25B and 12B), Sr/Ca decreases after reaching its maximum value at approximate 5 mm from the posterior most transect. In the remaining lingulid (8B), the maximum value is reached at approximately 10 µm, and decreases after this point.

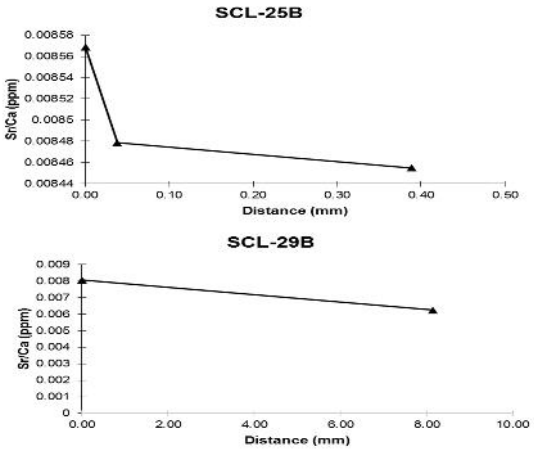

Figure 36: Mean Sr/Ca ratios plotted against longitudinal (posterior to anterior) position in millimeters for lingulid fossils from Stewart County (SCL 25/ UCM 79789 and SCL 29/ UCM 79790). Mean Sr and Ca values were calculated per transect before ratios were determined, and a moving average was then plotted against length in the y-direction (i.e., age or growth along the marginal fold). In both shells, Sr/Ca is observed to decrease with distance from the shell posterior.

Discussion

In this study, the distribution of major and trace elements within lingulid shells from two, coeval fossil localities were shown to be markedly consistent within individual shells (Figs. 28-32), but reveal differences in spatial patterns (both qualitative and quantitative) between lingulids from the two sites as well as between fossil lingulids and a modern glottidian (Figs. 21-28). These differences may reflect site-specific: 1) seawater element abundances indicative of environmental conditions, 2) concentrations derived from their respective geologic settings (i.e., provenance), 3) differential incorporation during shell growth, or 4) diagenetic effects (Dodd and Crisp, 1982; Popp et al., 1986; Grossman et al., 1996; England et al., 2007; Freitas et al., 2006; Kocsis et al., 2012). Moreover, elements exhibiting little to no variance in concentration or distributional patterns between fossil brachiopods may represent those controlled by taxon-specific vital effects rather than (paleo) environmental conditions (Lowenstam, 1961; Grossman et al., 1996; England et al., 2007). Diagenetic effects overprint the primary signals represented by all of the other possible causes of geochemical variability, thus diagenetic effects are evaluated first.

Diagenetic effects

Several studies have demonstrated the effects of diagenetic alteration in fossil brachiopods (Grossman et al., 1996; Rodland et al., 2003; Kocsis et al., 2012). Differences in elemental distributions, correlations and concentrations between fossil and modern lingulids, and between fossil lingulid assemblages in this study may also be attributable to variable degrees of chemical alteration. Major element (Ca, F and P) distributions were more similar between Stewart County specimens and the modern lingulid than between the two fossil assemblages

(Figs. 21-27). While pronounced zonations were observed in both Stewart County specimens and the modern lingulid, fossils from Devon Island exhibited no discernible zones. This suggests that in Devon Island specimens, originally chitinous laminae in which these elements are less abundant became more mineralized. Trace elements were commonly zoned within the original mineralized laminae of the fossil lingulids. In particular, all lingulids in this study exhibited zones of increased Mg, Na and Sr along these micro-structural and mineralogic boundaries. In contrast, distributions of Fe and Mn were once again more similar between Stewart County lingulids and the modern specimen. While elemental maps reveal greater qualitative similarities in element distributions between Stewart County specimens and the modern lingulid, some elements (Mg, Na and Sr) appear to be distributed similarly within shells of all analyzed lingulids, suggesting that these distributions may reflect original incorporation during shell growth (Grossman et al., 1996).

Among all fossil lingulids, several patterns of elemental correlation through dorso-ventral transects emerged. The most important of these in the context of diagenesis is the robust pairing (60% of all shells exhibited, $r > 0.7$) of the redox sensitive elements, Fe and Mn. Both of these elements may be concentrated in biogenic hard parts during chemical alteration (Zabini et al., 2012). It seems probable then that the strong positive correlation observed between these elements is suggestive of diagenetic mineral formation in the fossil lingulids.

Elevated concentrations of Fe and Mn in calcitic shells of articulated brachiopods are routinely interpreted to indicate diagenetic alteration (Lowenstam, 1961; Popp et al., 1986; Grossman et al., 1996). In the fossil lingulids examined in this study, concentrations of these elements were found to be one to three orders of magnitude greater than those reported for modern calcitic brachiopods (Brand et al., 2003). While some of the discrepancy between these

may be attributable to different shell chemistry and vital effects, the potential role of diagenesis must also be considered. One argument for diagenesis controlling these differences may be made by considering plots of Mg/Fe and Sr/Mn for modern brachiopods from the Brand et al. (2003) study and the fossil lingulids from this study (Fig. 37). In these plots, the significant

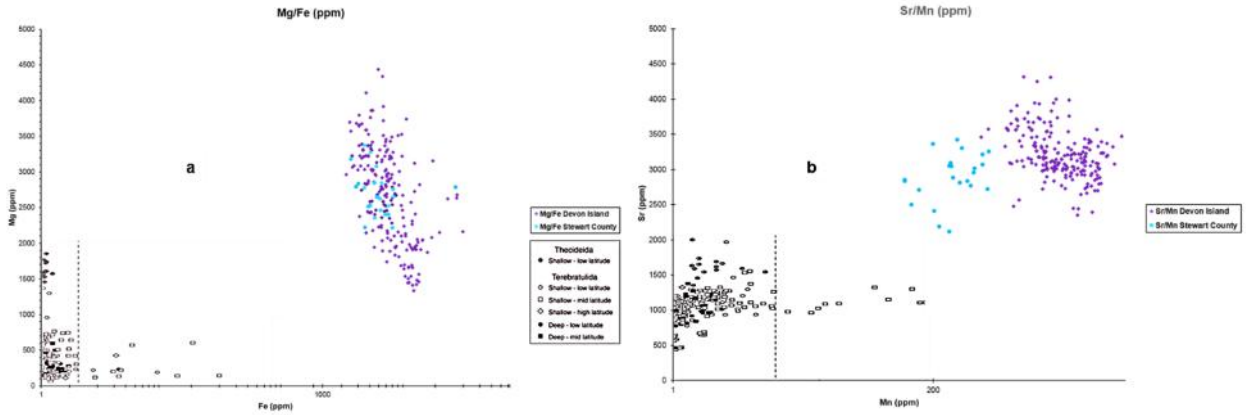

Figure 34: Comparison of Mg/Fe and Sr/Mn ratios between data from extant articulated brachiopod fossils (Brand et al., 2003) with those from Devon Island and Stewart County lingulids. There is substantial overlap in Mg/Fe between lingulid assemblage with Sr/Mn ratios appear in two, roughly discrete populations. Sr values are consistent between fossil lingulid assemblages; however, Mn concentrations are significantly higher in Devon Island specimens, suggesting increased geochemical alteration. Note that lingulid samples do not overlap with data from extant articulated brachiopods. After Brand et al. (2003).

difference in Fe and Mn concentrations is readily apparent while values for both Mg and Sr exhibit some degree of overlap between modern calcitic and fossil apatitic assemblages. This suggests not only that concentrations of Fe and Mn in fossil lingulids are controlled by diagenetic processes but also, and quite conversely, that Mg and Sr concentrations may be robust to such effects. All of these data, including qualitative trends and absolute concentrations, suggest that the fossil lingulids examined in this study have been subject to chemical diagenesis. It would also seem useful to compare their relative degrees of alteration as a means of developing some criteria against which we might examine their utility in paleoenvironmental reconstructions.

Lingulid fossils from Devon Island exhibit higher average concentrations of diagenetically-mediated elements (Fe and Mn) than shells from Stewart County. When considered with the previous argument for alteration in all fossil shells examined, one may infer from the significantly higher concentrations of Mn that Devon Island lingulids (mean [Mn] = 3089 ppm) are more geochemically altered than lingulids from Stewart County (mean [Mn] = 333 ppm) (Table 3). Furthermore, while the degree of physical preservation is high among Devon Island lingulids, zones of recrystallization that cross-cut shell lamina (i.e., are post-mortem), and the heterogenous but unzoned distribution of Ca, F and P in element maps support the implications of the quantitative chemical data that these Devon Island specimens have undergone chemical alteration. Collectively these data support the findings of previous studies (Popp et al., 1986; Grossman et al., 1996) that infer that variations in trace element concentrations (particularly those of Fe and Mn) of brachiopod shells reflect exposure to diagenetic processes, and argue that the Devon Island shells have undergone more chemical alteration than those from Stewart County.

Controls on Mg, Na and Sr concentrations: environmental conditions vs. vital effects

Zonation of Mg, Na and Sr is consistent among all lingulids examined in this study (Fig. 21-27). Additionally, the absolute concentration of Mg overlaps with values reported by Brand et al. (2003) for unaltered, modern brachiopods (Fig. 37). Finally, ratios of Sr/Ca suggest that no diagenetic homogenization of these elements has occurred as Sr/Ca ratios in fossil lingulids were found to be significantly different than those reported from bone apatite of both modern and fossil mammals (Sponheimer and Lee-Thorp, 2006; Fig. 38). These data suggest that these

elements are likely preserved in their original distribution and order of magnitude concentration for all fossil lingulids in this study.

Magnesium, sodium and strontium are common trace elements within normal seawater, and are observed to precipitate in biominerals at near-equilibrium with prevailing seawater chemistry (Dodd and Crisp, 1982). Freitas et al. (2006) observed that concentrations of Mg and Sr within the shells of bivalve mollusks may be controlled by changes in temperature and rate of mineral precipitation. The authors found that with decreasing temperatures and rates of biomineralization, concentrations of Mg increased. Conversely, Sr concentrations increased with increased temperatures and biomineralization. In their study, these trends could be linked with seasonality, suggesting that higher values of Mg should represent winter shell growth and increased Sr values should represent summer (Freitas et al., 2006).

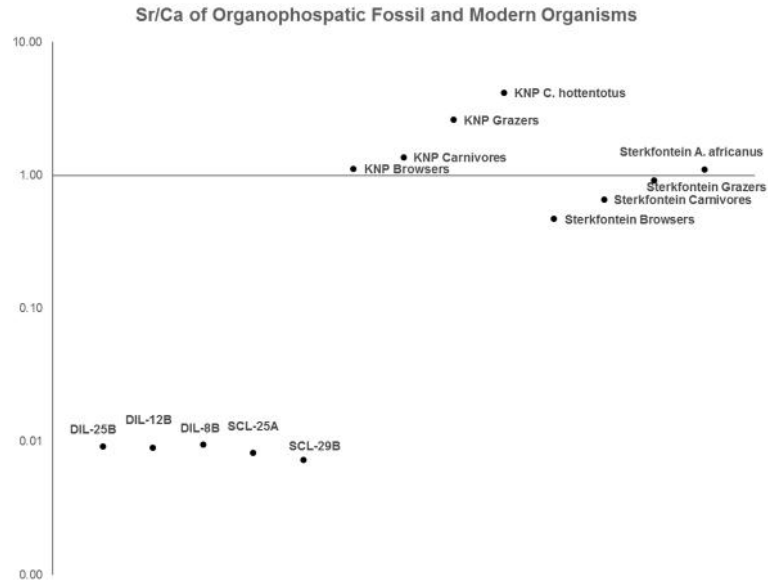

Figure 35: Sr/Ca ratios for fossil lingulids (this study) and fossil (Sterkfontein) and extant (KNP) mammals (Sponheimer and Lee-Thorp, 2006). Ratios for fossil lingulids and mammals are more similar than either fossil group is the ratios found in modern bioapatite.

In this study, average concentrations of Mg and Na within shells at each locality vary little between sites (Table 6). Due to the high paleo-latitudinal position of Devon Island lingulids (Tarduno et al., 1998), the null hypothesis is that Mg concentrations should be higher among Devon Island lingulids relative to the Stewart County lingulids due to lower temperatures and rates of biomineralization. However, the data (Table 3; Fig. 16) do not indicate any

substantial difference in the concentration of Mg between fossil locales. At the lower latitude fossil site, average Mg concentrations were nearly equal to those found in Devon Island specimens. Given the paleo-latitudinal differences, it seems unlikely that temperatures were warmer at Devon Island than Stewart County during the Late Cretaceous. Rates of biofractionation and subsequently, biomineralization may have varied independently of temperature between fossil localities. One potential cause for the observed variation in element abundances within the shells of fossil lingulids is site-specific differences in food supply, with lower food supplies slowing rates of biomineralization (Brockington and Clarke, 2002). However, more data would be needed to test these hypotheses as a lack of geochemical data from the associated sediments precludes inferences at this time.

In addition to the environmental control-mechanisms for Mg and Sr precipitation proposed by Freitas et al. (2006), Lowenstam (1961) and England et al. (2007) suggest a biological control upon the incorporation of Mg within the shells of bio-calcite. According to their findings, Mg concentrations should be reduced through both biofractionation in shell calcite relative to prevailing seawater Mg concentrations as well as through exposure to diagenetic fluids (Popp et al. 1986). Recalling the substitution between Ca and Mg, Sr and (rarely) Na within the apatite crystal lattice, one might consider that fractionation between Mg/Ca and Sr/Ca for bio-calcite and bio-apatite may behave similarly (Elliot et al., 2002). The role of vital effects on the relative concentrations of Mg and Sr may be evaluated by considering whether or not they change with ontogeny. If ratios exhibited little long-term directionality, one might assume that the concentrations of their component elements were governed by environmental conditions (i.e., one would expect cyclicity rather than directionality). In the case of both Mg/Ca and Sr/Ca, directionality is apparent along the longitudinal axis of whole shells (Figs. 33-36), and both

ratios decrease with time. One potential cause for these trends may be that rates of biofractionation change through ontogeny (Lee et al., 2004), with lingulids rejecting elemental impurities at an increased rate later in life. Coupled with the positive correlation observed between Mg and Sr, which should be inversely correlated if controlled by environmental factors, it would seem that element signatures in lingulids examined in this study record vital effects more reliably than those due to environment.

Implications for paleoenvironmental analyses

Observed differences in elemental concentrations and distributions of trace elements between fossil lingulids from Devon Island and Stewart County do not provide unequivocal evidence for differences in paleoenvironment. Diagenesis, which affected samples at both sites, and those at Devon Island to a greater extent, makes it difficult to extract unequivocal primary trace-element signals, with the potential exceptions of Mg, Na and Sr, which appear to be dominantly controlled by vital effects. However, if the effects of diagenesis and rates of biofractionation are understood, it seems likely that lingulid shells could be used in paleoenvironmental reconstructions. Moreover, the distributions of elements within fossil shells appear useful in evaluating chemical diagenesis.

Conclusions

This study examined the potential utility of elemental variability in organophosphatic brachiopods from the family Lingulidae to provide insights into paleoenvironmental conditions, growth and/or diagenetic alteration. Distributions of Mg, Na and Sr were fairly consistent between analyzed fossil and modern lingulid shells. These elements appear to be governed largely by vital effects, though environmental effects could not be unequivocally rejected.

While the directionality of these elements in lingulid shells along the axis of maximum growth suggests that rates of biofractionation change through ontogeny, these rates may also be controlled by prevailing temperatures and food availability, which may vary on inter-annual scales (Brockington and Clarke, 2002).

Concentrations of Mn were substantially elevated in all fossil lingulids relative to modern calcitic brachiopods, though their concentrations of Mg and Sr were similar (Brand et al., 2003). Additionally, the concentrations of these elements were elevated in Devon Island specimens relative to lingulids from Stewart County. The Arctic specimens also reveal that their chitinous laminae are more highly mineralized, but such laminae are partially to well preserved in the different Georgia samples. Stewart County specimens lacked clear petrographic evidence for recrystallization while such evidence is common in Devon Island lingulids. Based upon these data, I infer that all fossil lingulids in this study have been subject to chemical alterations, and that Devon Island specimens have undergone substantially more alteration than Stewart County lingulids.

To utilize the shells of organophosphatic brachiopods as proxy records of paleoenvironment, the effects of diagenesis must be well understood. The fossil lingulids analyzed in this study were subject to different degrees of geochemical alteration. This alteration changed the original concentrations of some elements, and may have influenced the concentrations of others, including those that have the potential to offer insights into paleoenvironmental conditions.

References

Angiolini, L., Stephenson, M., Leng, M.J., Jadoul, F., Millward, D., Aldridge, A., Andrews, J., Chenery, S., Williams, G., 2012. Heterogeneity, cyclicity and diagenesis in the Mississippian brachiopod shell of palaeoequatorial Britain. Terra Nova 24, 16-26.

Biernat, G., Emig, C.C., 1993. Anatomical distinctions of the Mesozoic lingulide brachiopods. Acta Palaeontologica Polonica 8, 1-20.

Blakey, R., Mollewide map of Late Cretaceous (90 Ma), Colorado Plateau Geosystems, Arizona, USA. <http:www2.nau.edu/rcb7/globaltext2.html>.

Brand, U., Logan, A., Hiller, N., Richardson, J., 2003. Geochemistry of modern brachiopods: Applications and implications for oceanography and paleoceanography. Chemical Geology 198, 305-334.

Brand, U., Webster, G.D., Azmy, K., Logan, A., 2007. Bathymetry and productivity of the southern Great Basin seaway, Nevada, USA: An evaluation of isotope and trace element chemistry in mid-Carboniferous and modern brachiopods. Palaeogeography, Palaeoclimatology, Palaeoecology 256, 273-297.

Brockington, S., Clarke, A., 2001. The relative influence of temperature on the metabolism of marine invertebrates. Journal of Experimental Marine Biology and Ecology 258, 87-99.

Carroll, M.L., Johnson, B.J., Henkes, G.A., McMahon, K.W., Voronkov, A., Ambrose, W.G., Jr., Denisenko, S.G., 2009. Bivalves as indicators of environmental variation and potential anthropogenic impacts in the southern Barents Sea. Marine Pollution Bulletin 59, 193-206.

Case, G.R., Schwimmer, D.R., 1988. Late Cretaceous fish from the Blufftown Formation (Campanian) in western Georgia. Journal of Paleontology 62, 290-301.

Chin, K., Block, J., Sweet, A., Tweet, J., Eberle, J., Cumbaa, S., Witkowski, J., Harwood, D., 2008. Life in a temperate Polar sea: A unique taphonomic window on the structure of a Late Cretaceous Arctic marine ecosystem. Proceedings of the Royal Society B 275: 2675-2685.

Dodd, J.R., Crisp, E.L., 1982. Non-linear variation with salinity of Sr/Ca and Mg/Ca ratios in water and aragonitic bivalve shells: Implications for paleosalinity studies. Palaeogeography, Palaeoclimatology, Palaeoecology 38, 45-56,

Elliot, J.C., Wilson, R.M., Dowker, S.E.P., 2002. Apatite structures. Advances in X-ray Analysis 45, 172-181.

England, J., Cusack, M., Lee, M.R., 2007. Magnesium and sulphur in the calcite shells of two brachiopods, *Terebratulina retusa* and *Novocrania anomala*. Lethaia 40, 2-10.

Fortier, Y.O., & Geological Survey of Canada, 1963. Geology of the north-central part of the the Arctic Achipelego, Northwest Territories (Operation Franklin). Department of Mines and Technical Surveys Canada.

Freeman, R.L., Dattilo, F., Morse, A., Blair, M., Felton, S., Pojeta, J., Jr., 2013. The “curse of the *Rafinesquina*:” Negative taphonomic feedback exerted by strophomenid shells on the storm-buried lingulids in the Cincinnatian series (Katian, Ordovician) of Ohio. Palaios 28, 359-372.

Freitas, P.S., Clarke, L.J., Kennedy, H., Richardson, C.A., Abrantes, F., 2006. Environmental and biological controls on elemental (Mg/Ca, Sr/Ca, Mn/Ca) ratios in shells of the king scallop *Pecten maximus*. Geochemica et Cosmochemica Acta 70, 5119-5133.

Grossman, E.L., Mii, H.S., Zhang, C., Yancey, T.E., 1996. Chemical variation in Pennsylvanian brachiopod shells – Diagenetic, taxonomic, microstructural and seasonal effects. Journal of Sedimentary Research 66, 1011-1022.

Holmer, L.E., Nakrem, H.A., 2012. The lingulid brachiopod Lingularia from lowermost Cretaceous hydrocarbon seep bodies, Sassenfjorden area, central Spitsbergen, Svalbard. Norwegian Journal of Geology 92, 167-174.

Jones, D.S., Williams, D.F., Arthur, M.A., Krantz, D.E., 1984. Interpreting the paleoenvironmental, paleoclimatic and life history records in mollusk shells. Geobios, Mém. Special 9, 333-339.

Jones, D.S., Quitmyer, I.R., 1996. Marking time with bivalve shells: Oxygen isotopes and season of annual increment formation. Palaios 11, 340-346.

Kocsis, L., Dulai, A., Bitner, M.A., Vennemann, T., Cooper, M., 2012. Geochemical compositions of Neogene phosphatic brachiopods: Implications for ancient environmental marine conditions. Palaeogeography, Palaeoclimatology, Palaeoecology 326-328, 66-77.

Kowaleski, M., Dyreson, E., Marcot, J.D., Vargas. J.A., Flessa, K.W., Hallman, D.P., 1997. Phenetic discrimination of biometric simpletons: Paleobiological implications of morphospecies in the lingulide brachiopod *Glottidia*. Paleobiology 23, 444-469.

Lécuyer, C., Reynard, B., Grandjean, P., 2004. Rare earth element evolution of Phanerozoic seawater recorded in biogenic apatites. Chemical Geology 204, 63-102.

Lee, X., Hi, R., Brand, U., Zhou, H., Liu, X., Yuan, H., Yan, C., Cheng, H., 2004. Ontogenetic trace element distribution in brachiopod shells: An indicator of original seawater chemistry. Chemical Geology 209, 49-65.

Lowenstam, H.A., 1961. Mineralogy, δ18O/δ16O ratios, and strontium and magnesium contents of recent and fossil brachiopods and their bearing on the history of the oceans. The Journal of Geology 69, 241-260.

Mayr, U., de Freitas, T., Beauchamp, B., 1998. The geology of Devon Island north of 76°, Canadian Arctic Archipelago. Geological Survey of Canada Bulletin 526.

McCartney, K., Witkowski, J., Harwood, D.M., 2011. Unusual assemblages of Late Cretaceous silicoflagellates from the Canadian Archipelago. Revue de micropaléontologie 54, 31-58.

Pérez-Huerta, A., Cusack, M., Jeffries, T.E., Williams, C.T., 2008. High resolution distribution of magnesium and strontium and the evaluation of Mg/Ca thermometry in recent brachiopod shells. Chemical Geology 247, 229-241.

Picard, S., Lécuyer, C., Barrat, J.A., Garcia, J.P., Dromart, G., Sheppard, S.M.F., 2002. Rare earth element contents of Jurassic fish and reptile teeth and their potential relation to sweater composition (Anglo-Paris Basin, France and England). Chemical Geology 186, 1-16.

Popp, B.N., Anderson, T.F., Sandberg, P.A., 1986. Brachiopods as indicators of original isotopic compositions in some Paleozoic limestones. Geological Society of America Belletin 10, 1262-1269.

Powell, M.G., Schöne, B.R., Jacob, D.E., Tropical marine climate during the Late Paleozoic ice age using trace element analyses of brachiopods. Palaeogeography, Palaeoclimatology, Palaeoecology 280, 143-149.

Putnis, A., 2009. Mineral replacement reactions. Reviews in Mineralogy & Geochemistry 70, 87-124.

Rigby, J.K., Chin, K., Bloch, J.D., Tweet, J.S., 2007. A new hexactinellid sponge from the Cretaceous of Devon Island, Canadian High Arctic. Canadian Journal of Earth Sciences 44, 1235-1242.

Rodland, D.L., Kowaleski, M., Dettman, D.L., Flessa, K.W., Atudorei, V., Sharp, Z.D., 2003. High-resolution analysis of δ18O in the biogenic phosphate of modern and fossil lingulid brachiopods. The Journal of Geology 111, 441-453.

Schöne, B.R., Lega, J., Flessa, K.W., Goodwin, D.H., Dettman, D.L., 2002. Reconstructing daily temperatures from growth rates of the intertidal bivalve mollusk *Chione cortezi* (north Gulf of California, Mexico. Palaeogeography, Palaeoclimatology, Palaeoecology 184, 131-146.

Schöne, B.R., Fiebig, J., Pfeiffer, M., Gleb, R., Hickson, J., Johnson, A.L.A., Dreyer, W., Oschmann, W., 2005. Climate records from a bivalve Methuselah (*Arctica islandica*, Mollusca; Iceland). Palaeogeography, Palaeoclimatology, Palaeoecology 228, 130-148.

Schöne, B.R., Rodland., D.L., Fiebig, J., Oschmann, W., Goodwin, D., Flessa, K.W., Dettman, D., 2006. Reliability of multitaxon, multiproxy reconstructions of environmental conditions from accretionary biogenic skeletons. The Journal of Geology 114, 267-285.

Schwimmer, D.R., Williams, G.D., Dobie, J.L., Siesser, W.G., 1993. Late Cretaceous dinosaurs from the Blufftown Formation in western Georgia and eastern Alabama. Journal of Paleontology 67, 288-296.

Sponheimer, M., Lee-Thorp, J.A., 2006. Enamel diagenesis at South African Australopith sites: Implications for paleoecological reconstruction with trace elements. Geochemica et Cosmochemica Acta 70, 1644-1654.

Sturesson, U., Popov, L.E., Holmer, L.E., Bassett, M.G., Felitsyn, S., Belyatsky, B., 2005. Neodymium isotopic composition of Cambrian-Ordovician biogenic apatite in the Baltoscandian Basin: Implications for palaeogeographical evolution and patterns of biodiversity. Geology Magazine 142, 419-439.

Tarduno, J.A., Brinkman, D.B., Renne, P.R., Cottrell, R.D., Scher, H., Castillo, P., 1998. Evidence for extreme climatic warmth from Late Cretaceous Arctic vertebrates. Science 282, 2241-2244.

Williams, A., Cusack, M., Mackay, S., 1994. Collagenous chitinophosphatic shell of the brachiopod *Lingula*. Philosophical Transactions of the Royal Society B 346, 223-266.

Williams, A., Cusack, M., 1999. Evolution of rhythmic lamination on the organophosphatic shells of brachiopods. Journal of Structural Biology 126, 227-240.

Williams, A., Holmer, L.E., Cusack, M., 2004. Chemico-structure of the organophosphatic shells of siphonotreide brachiopods. Paleontology 47, 1313-1337.

Wilson, L.E., Chin, K., Cumbaa, S., Dyke, G., 2011. A high latitude hesperornithoform (Aves) from Devon Island: Palaeobiogeography and size distribution of the North American hesperornithoforms. Journal of Systematic Palaeontology 9, 9-23.

Witkowski, J., Harwood, D.M., Chin, K., 2011. Taxonomic composition, paleoecology and biostratigraphy of Late Cretaceous diatoms from Devon Island, Nunavut Canadian High Arctic. Cretaceous Research 32, 277-300.

Zabini, C., Schiffbauer, J.D., Xiao, S., Kowaleski, M., 2012. Biomineralization, taphonomy and diagenesis of Paleozoic lingulide brachiopod shells preserved in silicified mudstone concretions. Palaeogeography, Palaeoclimatology, Palaeoecology 326-328, 118-127.

Appendix A: Fossil materials from Devon Island and Stewart County

Thin Sections

Locality	Formation	Age	Field #	Museum #
Eidsbotn Graben, Devon Island	Upper Kanguk	Campanian-Santonian	DIL-7a	CMNIF 245
Eidsbotn Graben, Devon Island	Upper Kanguk	Campanian-Santonian	DIL-8a	CMNIF 245
Eidsbotn Graben, Devon Island	Upper Kanguk	Campanian-Santonian	DIL-8b	CMNIF 245
Eidsbotn Graben, Devon Island	Upper Kanguk	Campanian-Santonian	DIL-12a	CMNIF 245
Eidsbotn Graben, Devon Island	Upper Kanguk	Campanian-Santonian	DIL-12b	CMNIF 245
Eidsbotn Graben, Devon Island	Upper Kanguk	Campanian-Santonian	DIL-25a	CMN 166
Eidsbotn Graben, Devon Island	Upper Kanguk	Campanian-Santonian	DIL-25b	CMN 166
Hanahatchee Creek, Stewart County	Upper Blufftown	Early Campanian	GA/ SCL-19a	UCM 79788
Hanahatchee Creek, Stewart County	Upper Blufftown	Early Campanian	GA/ SCL-19b-1	UCM 79788
Hanahatchee Creek, Stewart County	Upper Blufftown	Early Campanian	GA/ SCL-19b-2	UCM 79788
Hanahatchee Creek, Stewart County	Upper Blufftown	Early Campanian	GA/ SCL-23-b	
Hanahatchee Creek, Stewart County	Upper Blufftown	Early Campanian	GA/ SCL-25a-1	UCM 79789
Hanahatchee Creek, Stewart County	Upper Blufftown	Early Campanian	GA/ SCL-25a-2	UCM 79789
Hanahatchee Creek, Stewart County	Upper Blufftown	Early Campanian	GA/ SCL-25-b	UCM 79789
Hanahatchee Creek, Stewart County	Upper Blufftown	Early Campanian	GA/ SCL-29a	UCM 79790
Hanahatchee Creek, Stewart County	Upper Blufftown	Early Campanian	GA/ SCL-29b	UCM 79790
San Pedro, Gulf of California	N/A	Recent	CA-4232a	
San Pedro, Gulf of California	N/A	Recent	CA-4232b	
San Pedro, Gulf of California	N/A	Recent	CA-4282a	
San Pedro, Gulf of California	N/A	Recent	CA-4282b	

Hand Samples

Locality	Formation	Age	Field #	Museum #
Eidsbotn Graben, Devon Island	Upper Kanguk	Campanian-Santonian	DIL-1	NUIF-25
Eidsbotn Graben, Devon Island	Upper Kanguk	Campanian-Santonian	DIL-2	NUIF-25
Eidsbotn Graben, Devon Island	Upper Kanguk	Campanian-Santonian	DIL-3	NUIF-25
Eidsbotn Graben, Devon Island	Upper Kanguk	Campanian-Santonian	DIL-4	CMNIF 245
Eidsbotn Graben, Devon Island	Upper Kanguk	Campanian-Santonian	DIL-9	CMNIF 245
Eidsbotn Graben, Devon Island	Upper Kanguk	Campanian-Santonian	DIL-10	CMNIF 245
Eidsbotn Graben, Devon Island	Upper Kanguk	Campanian-Santonian	DIL-11	CMNIF 245
Eidsbotn Graben, Devon Island	Upper Kanguk	Campanian-Santonian	DIL-13	CMNIF 245
Eidsbotn Graben, Devon Island	Upper Kanguk	Campanian-Santonian	DIL-14	CMNIF 245
Eidsbotn Graben, Devon Island	Upper Kanguk	Campanian-Santonian	DIL-16	CMNIF 245
Eidsbotn Graben, Devon Island	Upper Kanguk	Campanian-Santonian	DIL-17	CMNIF 245
Eidsbotn Graben, Devon Island	Upper Kanguk	Campanian-Santonian	DIL-18	CMNIF 245
Eidsbotn Graben, Devon Island	Upper Kanguk	Campanian-Santonian	DIL-19	NUIF-25
Eidsbotn Graben, Devon Island	Upper Kanguk	Campanian-Santonian	DIL-21	NUIF-25
Eidsbotn Graben, Devon Island	Upper Kanguk	Campanian-Santonian	DIL-22	NUIF-25
Eidsbotn Graben, Devon Island	Upper Kanguk	Campanian-Santonian	DIL-23	NUIF-22
Eidsbotn Graben, Devon Island	Upper Kanguk	Campanian-Santonian	DIL-24	NUIF-22
Eidsbotn Graben, Devon Island	Upper Kanguk	Campanian-Santonian	DIL-26	NUIF-25
Eidsbotn Graben, Devon Island	Upper Kanguk	Campanian-Santonian	DIL-27	NUIF-25
Hanahatchee Creek, Stewart County	Upper Blufftown	Early Campanian	GA/ SCL-1	
Hanahatchee Creek, Stewart County	Upper Blufftown	Early Campanian	GA/ SCL-2	
Hanahatchee Creek, Stewart County	Upper Blufftown	Early Campanian	GA/ SCL-3	
Hanahatchee Creek, Stewart County	Upper Blufftown	Early Campanian	GA/ SCL-4	
Hanahatchee Creek, Stewart County	Upper Blufftown	Early Campanian	GA/ SCL-5	

Hanahatchee Creek, Stewart County	Upper Blufftown	Early Campanian	GA/ SCL-6
Hanahatchee Creek, Stewart County	Upper Blufftown	Early Campanian	GA/ SCL-7
Hanahatchee Creek, Stewart County	Upper Blufftown	Early Campanian	GA/ SCL-8
Hanahatchee Creek, Stewart County	Upper Blufftown	Early Campanian	GA/ SCL-9
Hanahatchee Creek, Stewart County	Upper Blufftown	Early Campanian	GA/ SCL-10
Hanahatchee Creek, Stewart County	Upper Blufftown	Early Campanian	GA/ SCL-11
Hanahatchee Creek, Stewart County	Upper Blufftown	Early Campanian	GA/ SCL-12
Hanahatchee Creek, Stewart County	Upper Blufftown	Early Campanian	GA/ SCL-13
Hanahatchee Creek, Stewart County	Upper Blufftown	Early Campanian	GA/ SCL-14
Hanahatchee Creek, Stewart County	Upper Blufftown	Early Campanian	GA/ SCL-15
Hanahatchee Creek, Stewart County	Upper Blufftown	Early Campanian	GA/ SCL-16
Hanahatchee Creek, Stewart County	Upper Blufftown	Early Campanian	GA/ SCL-17
Hanahatchee Creek, Stewart County	Upper Blufftown	Early Campanian	GA/ SCL-18
Hanahatchee Creek, Stewart County	Upper Blufftown	Early Campanian	GA/ SCL-20
Hanahatchee Creek, Stewart County	Upper Blufftown	Early Campanian	GA/ SCL-21
Hanahatchee Creek, Stewart County	Upper Blufftown	Early Campanian	GA/ SCL-22
Hanahatchee Creek, Stewart County	Upper Blufftown	Early Campanian	GA/ SCL-24
Hanahatchee Creek, Stewart County	Upper Blufftown	Early Campanian	GA/ SCL-26
Hanahatchee Creek, Stewart County	Upper Blufftown	Early Campanian	GA/ SCL-27
Hanahatchee Creek, Stewart County	Upper Blufftown	Early Campanian	GA/ SCL-28
Hanahatchee Creek, Stewart County	Upper Blufftown	Early Campanian	GA/ SCL-30
Hanahatchee Creek, Stewart County	Upper Blufftown	Early Campanian	GA/ SCL-31
Hanahatchee Creek, Stewart County	Upper Blufftown	Early Campanian	GA/ SCL-32
Hanahatchee Creek, Stewart County	Upper Blufftown	Early Campanian	GA/ SCL-33
Hanahatchee Creek, Stewart County	Upper Blufftown	Early Campanian	GA/ SCL-34

Hanahatchee Creek, Stewart County	Upper Blufftown	Early Campanian	GA/ SCL-35	
Hanahatchee Creek, Stewart County	Upper Blufftown	Early Campanian	GA/ SCL-36	
Hanahatchee Creek, Stewart County	Upper Blufftown	Early Campanian	CSU-1	CSUK-09-04a
Hanahatchee Creek, Stewart County	Upper Blufftown	Early Campanian	CSU-2	CSUK-09-04b
Hanahatchee Creek, Stewart County	Upper Blufftown	Early Campanian	CSU-2	CSUK-09-04
San Pedro, Gulf of California	N/A	Recent	CA-4080	
San Pedro, Gulf of California	N/A	Recent	CA-4232	
San Pedro, Gulf of California	N/A	Recent	CA-4282	
San Pedro, Gulf of California	N/A	Recent	CA-4366	

Appendix B: Element concentration data reported in weight percent and ppm for fossil lingulids

All Devon Island samples were analyzed via a 5 µm beam diameter; Stewart County samples were via a 10 µm beam diameter. Dwell times were consistently 20 seconds for all fossils analyzed.

All transects start from the exterior-most secondary shell layer (point 1) and proceed dorso-ventrally through the shell toward the shell interior; maximum point numbers vary from 4 to 11. Transects are coded to each sample, such that transects 1, 2, 3, etc for sample DIL-25B are coded as 25B-1, 25B-2, 25B-3, etc.

Measured values, in weight percent (wt. %) were converted to ppm (parts *per* million) for each element according to the following formula:

ppm Ca = wt% Ca x (1×10^4)
ppm P = wt% P x (1×10^4)
ppm Fe = wt% Fe x (1×10^4)
ppm Mg = wt% Mg x (1×10^4)
ppm Sr = wt% Sr x (1×10^4)
ppm F = wt% F x (1×10^4)
ppm S = wt% S x (1×10^4)
ppm Mn = wt% Mn x (1×10^4)
ppm Na = wt% Na x (1×10^4)

Measured weight percent are reported below for each analysis, followed by the same table with values converted to ppm.

			Element Concentrations in Weight %								
Field #	**Transect**	**Point**	**Ca**	**P**	**Fe**	**Mg**	**Sr**	**F**	**S**	**Mn**	**Na**
DIL-25B	25B-1	1	33.74	15.70	0.96	0.31	0.32	2.92	0.34	0.68	0.68
		2	32.26	15.36	3.15	0.22	0.31	3.73	2.15	0.80	0.54
		3	34.12	15.72	0.55	0.23	0.30	3.32	0.44	0.57	0.59
		4	34.22	15.61	0.49	0.27	0.34	3.57	0.41	0.61	0.61
		5	34.44	15.81	0.47	0.28	0.32	3.77	0.47	0.61	0.59
		6	34.40	15.61	0.47	0.34	0.32	3.60	0.58	0.19	0.75
		7	34.99	15.42	0.54	0.29	0.30	3.45	0.56	0.38	0.64
		8	34.83	15.51	0.34	0.30	0.33	3.74	0.64	0.16	0.65
		9	34.27	15.72	0.39	0.32	0.32	3.56	0.59	0.26	0.78
		10	34.36	16.36	0.54	0.32	0.37	3.45	0.42	0.25	0.74
	25B-2	1	34.34	15.65	0.97	0.27	0.32	3.46	0.37	0.70	0.61
		5	34.66	15.75	0.43	0.24	0.31	3.44	0.50	0.44	0.56
		6	34.86	15.75	0.71	0.32	0.34	3.64	0.58	0.44	0.68

	7	35.12	15.39	0.48	0.33	0.33	3.67	0.60	0.31	0.68
	8	35.33	15.52	0.37	0.30	0.31	3.66	0.63	0.24	0.63
	9	34.48	15.89	0.39	0.27	0.35	3.47	0.58	0.20	0.70
	10	33.91	16.05	0.47	0.27	0.36	3.24	0.48	0.22	0.71
25B-3	1	33.82	15.57	1.13	0.19	0.35	4.12	0.75	0.93	0.52
	2	35.14	15.61	0.48	0.30	0.28	3.71	0.50	0.46	0.59
	3	35.15	15.46	0.36	0.19	0.26	3.71	0.59	0.40	0.69
	4	36.06	15.44	0.41	0.27	0.31	3.65	0.63	0.29	0.70
	5	34.95	15.59	0.48	0.27	0.31	4.06	0.58	0.27	0.67
	6	35.00	16.01	0.56	0.25	0.35	3.57	0.49	0.31	0.67
	7	33.99	16.33	0.52	0.32	0.39	3.29	0.49	0.23	0.80
	8	34.17	15.60	1.32	0.19	0.32	4.09	0.52	0.64	0.50
25B-4	1	34.51	15.60	0.46	0.32	0.32	3.81	0.52	0.39	0.75
	2	35.16	15.60	0.40	0.22	0.29	3.96	0.53	0.33	0.62
	3	35.20	15.52	0.44	0.26	0.32	3.60	0.62	0.35	0.62
	4	34.98	15.95	0.43	0.28	0.33	3.44	0.50	0.20	0.69
	5	34.79	16.15	0.55	0.35	0.38	3.57	0.55	0.32	0.68
	6	34.40	16.21	0.79	0.37	0.40	3.05	0.54	0.32	0.83
25B-5	1	35.62	15.38	0.54	0.26	0.29	3.80	0.56	0.41	0.79
	2	36.11	15.46	0.49	0.25	0.29	3.93	0.64	0.30	0.66
	3	35.54	15.85	0.45	0.26	0.31	3.51	0.50	0.24	0.64
	4	34.65	16.39	0.48	0.34	0.37	3.45	0.49	0.17	0.71
25B-6	1	34.44	15.93	1.09	0.28	0.33	3.53	0.36	0.48	0.78
	2	34.78	16.30	0.70	0.25	0.34	3.19	0.32	0.35	0.84
	4	35.16	15.85	0.44	0.32	0.33	3.62	0.63	0.42	0.90
	5	34.77	15.68	0.53	0.32	0.36	3.74	0.69	0.56	0.82
	6	34.46	15.62	0.51	0.30	0.34	3.65	0.59	0.48	0.79
	7	34.58	15.59	0.51	0.29	0.34	3.88	0.76	0.26	0.84
	8	35.05	15.36	0.75	0.22	0.31	4.27	0.51	0.37	0.69
	9	35.45	15.27	0.84	0.17	0.30	4.09	0.40	0.59	0.48
	10	35.06	14.96	0.92	0.17	0.29	4.38	0.40	0.57	0.45
	11	34.31	15.85	0.65	0.35	0.37	3.97	0.76	0.18	0.78
	12	35.20	15.20	0.88	0.15	0.30	4.23	0.41	0.54	0.46
	13	35.43	15.32	0.88	0.26	0.30	4.41	0.59	0.35	0.62
25B-7	2	35.16	15.63	0.49	0.30	0.32	3.56	0.67	0.64	0.81
	3	35.69	15.61	0.55	0.32	0.33	4.05	0.63	0.43	0.76
	4	36.02	15.44	0.49	0.29	0.32	4.08	0.62	0.41	0.72
	5	35.20	15.15	1.07	0.16	0.30	3.94	0.45	0.58	0.43
	6	35.20	14.86	1.07	0.15	0.27	3.81	0.36	0.57	0.44
	7	35.03	15.27	0.53	0.34	0.39	3.89	0.75	0.17	0.78
	8	34.95	15.38	0.44	0.43	0.31	4.21	0.85	0.25	0.72
	9	35.76	15.22	0.84	0.14	0.29	4.54	0.44	0.51	0.47

	10	35.82	15.15	0.75	0.17	0.29	4.21	0.44	0.50	0.49
25B-8	1	35.26	15.78	0.43	0.29	0.32	3.81	0.68	0.40	0.85
	2	35.36	15.48	0.47	0.30	0.33	4.14	0.64	0.58	0.83
	3	35.45	15.47	0.50	0.33	0.34	3.67	0.67	0.50	0.87
	4	35.53	15.29	0.51	0.29	0.32	4.03	0.66	0.33	0.75
	5	34.98	15.05	0.79	0.19	0.29	4.09	0.35	0.59	0.48
	6	35.49	14.79	1.02	0.15	0.27	4.14	0.37	0.54	0.47
	7	35.81	15.37	0.59	0.31	0.40	3.76	0.74	0.24	0.76
	8	34.90	15.42	0.39	0.44	0.37	4.00	0.89	0.15	0.81
	9	35.69	15.10	0.91	0.14	0.28	3.99	0.38	0.61	0.43
	10	35.59	15.17	0.90	0.17	0.31	4.19	0.43	0.57	0.50
25B-9	1	35.25	15.59	0.53	0.32	0.32	3.59	0.65	0.45	0.89
	2	34.17	14.89	0.72	0.27	0.32	3.48	0.60	0.69	0.78
	3	35.16	15.46	0.70	0.35	0.34	4.00	0.63	0.48	0.78
	4	35.77	15.33	0.60	0.27	0.30	4.46	0.69	0.40	0.75
	5	35.54	15.10	0.77	0.15	0.28	4.13	0.40	0.58	0.46
	6	35.32	14.88	1.01	0.14	0.24	4.21	0.37	0.51	0.50
	7	35.20	15.47	0.45	0.35	0.43	4.13	0.81	0.17	0.86
	8	35.59	15.42	0.45	0.37	0.34	4.28	0.83	0.19	0.79
	9	35.43	15.13	0.82	0.14	0.31	4.31	0.47	0.55	0.52
	10	35.75	15.08	0.82	0.15	0.28	4.10	0.40	0.54	0.51
25B-10	1	35.64	15.45	0.56	0.28	0.34	3.96	0.62	0.69	0.75
	2	34.70	15.50	0.66	0.30	0.33	3.82	0.61	0.78	0.74
	3	35.23	15.31	0.62	0.27	0.31	3.89	0.57	0.51	0.75
	4	36.10	15.33	0.59	0.28	0.37	3.81	0.69	0.22	0.80
	5	35.51	15.31	0.48	0.35	0.35	3.86	0.74	0.20	0.82
	6	35.63	14.88	0.95	0.13	0.28	3.93	0.37	0.50	0.50
	7	35.81	15.40	0.57	0.33	0.43	3.74	0.78	0.22	0.79
	8	35.86	15.30	0.45	0.39	0.35	4.05	0.77	0.21	0.82
	9	35.32	15.14	0.77	0.21	0.33	3.92	0.52	0.46	0.54
	10	35.41	15.13	0.83	0.17	0.29	3.90	0.40	0.56	0.44
25B-11	1	35.60	14.43	0.60	0.18	0.30	4.13	0.32	0.35	0.44
	3	34.01	13.67	2.18	0.26	0.31	3.43	0.32	0.49	0.44
	5	35.67	14.46	0.42	0.28	0.33	3.77	0.48	0.16	0.60
	7	32.38	13.34	2.71	0.26	0.24	3.52	0.29	0.35	0.44
	9	35.51	14.32	0.69	0.17	0.32	4.03	0.34	0.36	0.39
	10	35.14	14.52	0.41	0.33	0.36	3.49	0.50	0.11	0.56
	11	35.23	14.81	0.25	0.34	0.36	3.71	0.52	0.11	0.70
25B-12	1	35.46	14.29	0.35	0.30	0.30	3.95	0.42	0.18	0.64
	2	35.72	14.34	0.33	0.24	0.30	3.77	0.44	0.24	0.51
	4	35.71	14.31	0.60	0.19	0.30	4.05	0.35	0.34	0.44
	5	35.27	14.37	0.33	0.33	0.30	3.81	0.44	0.22	0.55

		7	35.64	14.39	0.60	0.19	0.29	3.80	0.34	0.34	0.49
		9	35.26	14.49	0.30	0.28	0.31	3.82	0.49	0.15	0.60
		10	35.93	14.50	0.24	0.30	0.31	3.98	0.55	0.12	0.68
		11	34.99	14.70	0.33	0.34	0.36	3.90	0.55	0.09	0.66
DIL-12B	12B-13	2	36.07	14.33	0.36	0.24	0.32	4.17	0.45	0.19	0.58
		3	35.90	14.21	0.31	0.24	0.31	3.84	0.47	0.22	0.54
		4	35.14	14.44	0.22	0.31	0.31	3.75	0.59	0.10	0.67
		5	33.70	13.85	1.51	0.32	0.30	3.64	0.50	0.13	0.54
		6	35.33	14.48	0.26	0.34	0.37	3.82	0.57	0.11	0.66
		7	35.77	14.54	0.29	0.41	0.39	3.96	0.59	0.11	0.61
	12B-14	1	35.37	14.37	0.34	0.33	0.31	3.89	0.49	0.23	0.59
		2	35.86	14.17	0.28	0.28	0.29	4.07	0.52	0.20	0.54
		3	35.73	14.31	0.26	0.31	0.31	3.89	0.57	0.11	0.61
		5	35.97	14.65	0.32	0.25	0.36	3.92	0.49	0.09	0.59
		6	35.48	14.67	0.25	0.32	0.38	3.95	0.54	0.10	0.70
	12B-15	1	36.04	14.32	0.33	0.30	0.32	3.31	0.47	0.17	0.53
		2	35.92	14.31	0.28	0.32	0.35	3.81	0.52	0.12	0.51
		4	35.17	14.35	0.37	0.30	0.33	3.89	0.54	0.12	0.48
		5	36.05	14.41	0.30	0.32	0.38	3.96	0.62	0.14	0.59
	12B-16	1	34.04	15.19	0.20	0.37	0.31	3.77	0.69	0.10	0.72
		3	34.01	15.45	0.25	0.36	0.33	4.16	0.61	0.09	0.73
		7	31.15	14.12	2.75	0.27	0.23	3.64	0.39	0.38	0.53
		12	33.99	15.03	0.50	0.21	0.25	4.23	0.75	0.10	0.69
	12B-17	2	34.31	15.10	0.46	0.24	0.30	3.86	0.52	0.19	0.60
		3	33.73	15.39	0.31	0.35	0.35	3.81	0.58	0.05	0.71
		4	34.07	15.01	0.48	0.28	0.33	4.08	0.55	0.20	0.64
		6	33.91	15.03	0.96	0.19	0.32	3.99	0.38	0.44	0.53
		7	33.37	14.88	1.18	0.20	0.29	4.03	0.38	0.44	0.54
		11	33.81	15.17	0.92	0.19	0.28	3.85	0.67	0.27	0.51
	12B-18	1	34.46	14.90	0.44	0.28	0.31	3.82	0.56	0.26	0.60
		2	34.86	15.10	0.42	0.25	0.28	3.62	0.52	0.23	0.58
		3	34.65	15.68	0.31	0.34	0.36	3.62	0.62	0.09	0.78
		4	34.21	15.25	0.32	0.38	0.36	3.69	0.62	0.11	0.75
		5	34.14	14.84	0.85	0.20	0.31	3.68	0.36	0.41	0.53
		6	33.43	14.84	1.17	0.20	0.27	3.92	0.35	0.46	0.52
		7	33.87	15.33	0.98	0.19	0.30	3.85	0.37	0.42	0.54
		8	33.99	15.28	1.03	0.21	0.28	3.58	0.36	0.46	0.55
		9	33.79	15.23	0.88	0.19	0.27	3.86	0.39	0.44	0.60
		12	33.96	15.11	0.43	0.22	0.26	4.21	0.75	0.11	0.60
	12B-19	1	34.79	15.02	0.75	0.16	0.29	3.64	0.33	0.37	0.48
		2	35.06	15.29	0.26	0.32	0.32	3.81	0.58	0.14	0.64
		3	34.39	15.38	0.25	0.37	0.37	3.55	0.64	0.10	0.76

		4	34.18	14.99	0.73	0.24	0.30	3.61	0.41	0.33	0.61
		6	33.52	14.87	1.05	0.20	0.31	3.68	0.36	0.44	0.54
		7	34.30	14.99	1.00	0.19	0.31	3.92	0.39	0.42	0.52
		8	34.22	15.30	0.99	0.19	0.31	4.07	0.35	0.43	0.54
		10	34.46	15.42	0.69	0.21	0.29	3.73	0.61	0.30	0.54
		11	34.24	15.46	0.58	0.21	0.30	3.92	0.73	0.23	0.58
	12B-20	1	35.25	15.31	0.61	0.20	0.30	3.37	0.43	0.30	0.54
		2	34.42	15.04	0.65	0.18	0.30	3.90	0.38	0.28	0.49
		3	34.36	15.54	0.28	0.30	0.34	4.08	0.58	0.16	0.68
		4	34.57	15.47	0.26	0.37	0.36	3.67	0.66	0.06	0.79
		7	33.31	14.76	1.47	0.21	0.30	3.99	0.34	0.43	0.52
		8	33.67	15.06	1.01	0.20	0.32	3.53	0.36	0.44	0.57
		10	34.15	15.43	0.71	0.25	0.29	3.78	0.53	0.33	0.60
		11	32.72	14.79	1.77	0.21	0.24	3.76	0.54	0.39	0.55
		12	34.06	15.47	0.49	0.22	0.27	3.76	0.75	0.19	0.55
DIL-8B	8B-21	1	34.55	15.80	0.25	0.38	0.34	3.74	0.44	0.12	0.68
		2	34.42	15.30	0.71	0.20	0.31	3.79	0.33	0.30	0.49
		3	34.48	15.23	0.47	0.25	0.31	3.33	0.42	0.24	0.56
		5	34.34	15.41	0.49	0.29	0.33	3.58	0.50	0.15	0.65
		6	33.76	15.33	0.65	0.28	0.32	4.00	0.44	0.19	0.55
		7	34.55	15.24	0.31	0.29	0.31	3.41	0.45	0.19	0.61
		8	34.30	15.21	0.32	0.24	0.30	3.72	0.50	0.24	0.55
		9	34.02	15.51	0.29	0.32	0.37	3.49	0.48	0.19	0.64
		10	33.77	15.18	0.35	0.22	0.31	3.72	0.56	0.26	0.61
	8B-22	1	35.34	15.62	0.30	0.36	0.31	3.82	0.42	0.15	0.64
		2	34.45	15.44	0.34	0.34	0.35	4.31	0.42	0.22	0.61
		3	34.72	14.89	0.91	0.23	0.30	3.49	0.38	0.31	0.55
		4	34.13	15.07	0.77	0.21	0.30	3.75	0.39	0.28	0.57
		5	35.48	15.41	0.55	0.30	0.32	3.89	0.47	0.17	0.63
		6	35.11	15.30	0.43	0.31	0.35	3.70	0.45	0.16	0.58
		7	35.02	15.50	0.38	0.31	0.36	3.71	0.48	0.15	0.64
		8	34.87	15.46	0.27	0.33	0.37	3.55	0.52	0.13	0.73
		9	34.22	15.59	0.27	0.33	0.37	4.04	0.59	0.14	0.74
	8B-23	1	36.39	15.04	0.35	0.39	0.33	3.72	0.45	0.16	0.66
		2	34.87	14.88	0.98	0.24	0.32	3.79	0.36	0.31	0.46
		3	35.37	14.74	0.91	0.23	0.33	3.50	0.35	0.33	0.54
		4	35.32	14.85	0.64	0.22	0.30	3.45	0.39	0.25	0.53
		5	36.35	15.10	0.31	0.32	0.36	3.78	0.47	0.14	0.63
		6	35.69	15.44	0.29	0.36	0.38	3.35	0.47	0.22	0.64
		8	35.37	15.16	0.42	0.23	0.30	3.74	0.48	0.24	0.57
		9	33.82	15.72	0.33	0.39	0.39	3.77	0.53	0.16	0.73
	8B-25	3	35.43	14.69	0.21	0.31	0.35	3.78	0.44	0.15	0.61

		5	35.51	14.55	0.18	0.30	0.37	3.61	0.47	0.11	0.67
		6	35.29	14.63	0.31	0.31	0.36	3.71	0.52	0.15	0.65
		7	33.74	15.16	0.23	0.37	0.43	4.01	0.60	0.13	0.69
	8B-26	1	34.49	15.33	0.37	0.25	0.32	3.69	0.39	0.25	0.54
		2	34.44	15.07	0.52	0.19	0.31	3.42	0.31	0.33	0.53
		3	34.06	14.95	0.56	0.26	0.31	3.85	0.41	0.19	0.56
		4	34.05	15.45	0.26	0.27	0.33	3.88	0.47	0.19	0.67
		8	34.68	14.98	0.25	0.24	0.28	4.07	0.49	0.19	0.56
	8B-28	1	34.13	15.38	0.36	0.29	0.33	3.59	0.39	0.18	0.57
		2	34.72	15.38	0.44	0.19	0.30	3.51	0.34	0.20	0.52
		3	34.35	15.45	0.43	0.20	0.31	3.88	0.36	0.27	0.54
		4	34.88	15.52	0.34	0.26	0.31	3.77	0.44	0.16	0.60
		5	34.14	15.81	0.21	0.32	0.33	3.63	0.52	0.16	0.75
		7	33.94	15.23	0.52	0.24	0.32	3.45	0.40	0.29	0.56
		8	34.05	15.34	0.33	0.24	0.31	4.08	0.50	0.20	0.55
		9	34.67	15.28	0.29	0.21	0.30	3.93	0.62	0.18	0.57
	8B-29	1	34.16	15.31	0.50	0.21	0.30	3.81	0.39	0.20	0.56
		2	34.59	15.31	0.49	0.17	0.27	3.75	0.32	0.29	0.46
		3	34.76	15.57	0.32	0.26	0.31	3.74	0.43	0.20	0.57
		4	34.77	15.38	0.46	0.25	0.33	3.71	0.41	0.24	0.59
		5	33.77	15.96	0.20	0.36	0.33	3.49	0.52	0.18	0.75
		6	34.31	15.07	0.54	0.20	0.32	3.55	0.36	0.34	0.50
		7	34.14	15.16	0.31	0.28	0.32	3.78	0.49	0.20	0.59
SCL-25B	25B-1	1	36.75	14.49	0.28	0.34	0.34	3.75	0.59	0.03	0.76
		2	37.34	15.10	0.38	0.26	0.29	3.57	0.40	0.03	0.53
		3	36.44	14.84	0.57	0.28	0.32	3.23	0.69	0.05	0.45
		4	36.60	15.04	0.56	0.22	0.31	3.51	0.30	0.05	0.42
	25B-2	1	36.88	14.73	0.33	0.33	0.33	3.92	0.58	0.04	0.66
		2	37.11	14.81	0.43	0.28	0.28	3.80	0.39	0.04	0.45
		3	37.14	14.76	0.41	0.26	0.34	3.61	0.38	0.02	0.52
		4	36.75	14.71	0.51	0.25	0.28	3.40	0.28	0.03	0.35
		5	36.53	14.89	0.57	0.27	0.33	3.39	0.26	0.06	0.47
	25B-3	1	36.55	14.53	0.38	0.31	0.30	3.64	0.63	0.05	0.60
		2	36.63	14.64	0.36	0.28	0.28	3.23	0.50	0.04	0.53
		3	36.44	14.52	0.33	0.25	0.27	3.55	0.53	0.02	0.56
		4	34.62	14.03	2.64	0.28	0.27	3.37	2.77	0.06	0.59
		5	36.85	14.94	0.47	0.24	0.30	3.33	0.31	0.05	0.47
SCL-29B	29B-2	1	37.13	14.61	0.24	0.28	0.29	3.59	0.43	0.01	0.77
		2	37.05	14.74	0.28	0.28	0.28	3.63	0.42	0.01	0.69
		3	36.69	14.65	0.36	0.24	0.31	3.39	0.37	0.03	0.62
		4	37.05	14.82	0.42	0.25	0.30	3.59	0.31	0.03	0.53
		5	36.54	14.71	0.51	0.24	0.31	3.76	0.34	0.03	0.50

	29B-3	1	36.16	14.31	0.20	0.32	0.25	3.36	0.86	0.01	1.06
		2	37.19	13.85	0.23	0.28	0.22	3.72	0.47	0.02	0.62
		3	37.02	13.81	0.31	0.25	0.21	3.83	0.42	0.03	0.64
		4	37.16	13.69	0.29	0.22	0.24	3.88	0.41	0.02	0.63

Element Concentrations in PPM

Field #	Transect	Point	Ca	P	Fe	Mg	Sr	F	S	Mn	Na
DIL-25B	25B-1	1	337400	157000	9646	3120	3186	29175	3418	6797	6849
		2	322600	153600	31500	2161	3079	37300	21469	8031	5378
		3	341200	157200	5528	2285	3034	33200	4389	5704	5863
		4	342200	156100	4858	2693	3397	35700	4146	6131	6061
		5	344400	158100	4716	2820	3233	37700	4727	6124	5911
		6	344000	156100	4660	3366	3179	36000	5848	1894	7479
		7	349900	154200	5424	2913	3017	34500	5568	3823	6363
		8	348300	155100	3423	3010	3263	37400	6430	1626	6525
		9	342700	157200	3861	3220	3239	35600	5924	2551	7791
		10	343600	163600	5418	3211	3735	34500	4162	2506	7369
	25B-2	1	343400	156500	9675	2727	3194	34600	3670	6957	6085
		5	346600	157500	4301	2361	3055	34400	5010	4402	5558
		6	348600	157500	7113	3221	3436	36400	5753	4369	6787
		7	351200	153900	4766	3283	3312	36700	6022	3136	6764
		8	353300	155200	3653	2966	3103	36600	6295	2380	6318
		9	344800	158900	3883	2683	3540	34700	5829	2001	6995
		10	339100	160500	4669	2671	3621	32400	4807	2206	7066
	25B-3	1	338200	155700	11250	1908	3472	41200	7513	9325	5207
		2	351400	156100	4805	3033	2794	37100	4986	4631	5939
		3	351500	154600	3592	1942	2648	37100	5942	4043	6895
		4	360600	154400	4068	2719	3075	36500	6346	2908	6971
		5	349500	155900	4821	2652	3143	40600	5833	2720	6704
		6	350000	160100	5585	2542	3538	35700	4941	3129	6687
		7	339900	163300	5236	3179	3943	32900	4905	2327	7984
		8	341700	156000	13219	1872	3240	40900	5150	6392	4989
	25B-4	1	345100	156000	4626	3220	3222	38100	5170	3890	7507
		2	351600	156000	3990	2230	2903	39600	5253	3278	6202
		3	352000	155200	4422	2583	3230	36000	6169	3523	6204
		4	349800	159500	4277	2794	3329	34400	5004	2020	6877
		5	347900	161500	5502	3486	3757	35700	5540	3184	6753
		6	344000	162100	7882	3739	3989	30500	5370	3170	8337
	25B-5	1	356200	153800	5406	2599	2924	38000	5561	4128	7888
		2	361100	154600	4861	2457	2922	39300	6381	2964	6572
		3	355400	158500	4455	2585	3145	35100	4995	2434	6376
		4	346500	163900	4760	3422	3733	34500	4881	1703	7108

25B-6	1	344400	159300	10871	2820	3280	35300	3607	4838	7809
	2	347800	163000	6966	2531	3370	31900	3181	3547	8425
	4	351600	158500	4360	3169	3253	36200	6336	4236	9006
	5	347700	156800	5294	3204	3569	37400	6936	5607	8227
	6	344600	156200	5085	2978	3427	36500	5912	4761	7930
	7	345800	155900	5071	2869	3382	38800	7606	2577	8398
	8	350500	153600	7451	2238	3126	42700	5119	3746	6931
	9	354500	152700	8370	1669	3012	40900	3982	5900	4789
	10	350600	149600	9178	1659	2871	43800	4019	5658	4495
	11	343100	158500	6467	3508	3720	39700	7621	1765	7785
	12	352000	152000	8843	1537	2973	42300	4089	5449	4605
	13	354300	153200	8807	2573	2990	44100	5925	3539	6215
25B-7	2	351600	156300	4876	2963	3230	35600	6702	6389	8086
	3	356900	156100	5464	3191	3316	40500	6266	4347	7565
	4	360200	154400	4927	2876	3160	40800	6155	4052	7189
	5	352000	151500	10702	1563	3002	39400	4494	5849	4272
	6	352000	148600	10700	1463	2700	38100	3589	5685	4423
	7	350300	152700	5320	3430	3934	38900	7466	1730	7827
	8	349500	153800	4373	4340	3067	42100	8547	2524	7181
	9	357600	152200	8440	1447	2942	45400	4399	5053	4748
	10	358200	151500	7528	1697	2913	42100	4421	4953	4940
25B-8	1	352600	157800	4333	2919	3213	38100	6775	4034	8506
	2	353600	154800	4714	3012	3329	41400	6383	5762	8319
	3	354500	154700	4953	3313	3394	36700	6685	4957	8700
	4	355300	152900	5147	2898	3204	40300	6590	3282	7463
	5	349800	150500	7914	1906	2883	40900	3464	5937	4761
	6	354900	147900	10228	1484	2697	41400	3681	5382	4697
	7	358100	153700	5869	3108	3998	37600	7370	2439	7553
	8	349000	154200	3930	4437	3668	40000	8927	1538	8068
	9	356900	151000	9139	1411	2803	39900	3774	6092	4322
	10	355900	151700	8965	1691	3083	41900	4299	5741	5048
25B-9	1	352500	155900	5288	3226	3225	35900	6482	4465	8866
	2	341700	148900	7232	2670	3204	34800	5968	6927	7815
	3	351600	154600	6993	3529	3374	40000	6258	4773	7841
	4	357700	153300	5982	2695	2968	44600	6908	4037	7527
	5	355400	151000	7655	1535	2795	41300	3977	5825	4577
	6	353200	148800	10083	1422	2391	42100	3710	5114	4991
	7	352000	154700	4465	3511	4250	41300	8069	1661	8567
	8	355900	154200	4476	3720	3430	42800	8286	1924	7893
	9	354300	151300	8211	1446	3090	43100	4671	5531	5151
	10	357500	150800	8224	1506	2847	41000	4046	5366	5075
25B-10	1	356400	154500	5571	2785	3368	39600	6212	6882	7512

		2	347000	155000	6642	3007	3322	38200	6083	7769	7398
		3	352300	153100	6150	2674	3113	38900	5742	5148	7525
		4	361000	153300	5850	2843	3673	38100	6911	2164	7995
		5	355100	153100	4763	3454	3542	38600	7351	2034	8190
		6	356300	148800	9493	1337	2767	39300	3726	4992	5026
		7	358100	154000	5687	3275	4308	37400	7830	2191	7884
		8	358600	153000	4466	3916	3468	40500	7667	2144	8169
		9	353200	151400	7709	2134	3313	39200	5174	4580	5416
		10	354100	151300	8315	1657	2922	39000	4009	5639	4351
	25B-11	1	356000	144300	5981	1834	3034	41300	3158	3493	4363
		3	340100	136700	21823	2620	3053	34300	3239	4934	4430
		5	356700	144600	4242	2752	3341	37700	4825	1587	5964
		7	323800	133400	27113	2632	2446	35200	2859	3470	4362
		9	355100	143200	6897	1684	3223	40300	3389	3584	3916
		10	351400	145200	4092	3310	3561	34900	5026	1069	5623
		11	352300	148100	2475	3366	3613	37100	5216	1117	6984
	25B-12	1	354600	142900	3484	3029	2982	39500	4172	1848	6443
		2	357200	143400	3308	2434	3015	37700	4388	2353	5104
		4	357100	143100	6016	1940	3040	40500	3523	3398	4424
		5	352700	143700	3284	3332	3021	38100	4441	2242	5463
		7	356400	143900	5973	1945	2856	38000	3406	3413	4920
		9	352600	144900	2970	2823	3092	38200	4924	1490	6024
		10	359300	145000	2388	3026	3124	39800	5510	1221	6813
		11	349900	147000	3279	3376	3588	39000	5484	890	6582
DIL-12B	12B-13	2	360700	143300	3631	2402	3173	41700	4539	1883	5789
		3	359000	142100	3058	2443	3106	38400	4724	2180	5402
		4	351400	144400	2176	3088	3095	37500	5912	952	6681
		5	337000	138500	15063	3152	3041	36400	5002	1267	5374
		6	353300	144800	2647	3391	3702	38200	5689	1111	6564
		7	357700	145400	2946	4107	3912	39600	5910	1096	6135
	12B-14	1	353700	143700	3361	3301	3123	38900	4864	2255	5883
		2	358600	141700	2847	2838	2896	40700	5189	2014	5438
		3	357300	143100	2562	3082	3120	38900	5675	1097	6052
		5	359700	146500	3179	2528	3573	39200	4914	910	5868
		6	354800	146700	2526	3225	3834	39500	5434	979	7031
	12B-15	1	360400	143200	3330	3031	3174	33100	4701	1745	5291
		2	359200	143100	2772	3216	3484	38100	5228	1248	5107
		4	351700	143500	3722	2953	3327	38900	5377	1207	4794
		5	360500	144100	3045	3227	3806	39600	6201	1372	5916
	12B-16	1	340400	151900	1952	3697	3082	37700	6895	986	7160
		3	340100	154500	2478	3643	3329	41600	6142	868	7273
		7	311500	141200	27484	2680	2349	36400	3870	3766	5290

		12	339900	150300	4953	2143	2476	42300	7509	1026	6860
	12B-17	2	343100	151000	4624	2446	2991	38600	5209	1921	5974
		3	337300	153900	3098	3527	3460	38100	5803	530	7144
		4	340700	150100	4793	2790	3256	40800	5509	1983	6432
		6	339100	150300	9646	1926	3184	39900	3792	4437	5316
		7	333700	148800	11834	2049	2923	40300	3785	4388	5429
		11	338100	151700	9152	1908	2773	38500	6676	2720	5146
	12B-18	1	344600	149000	4429	2757	3096	38200	5576	2555	6022
		2	348600	151000	4169	2457	2837	36200	5211	2335	5757
		3	346500	156800	3090	3369	3555	36200	6198	923	7756
		4	342100	152500	3248	3761	3566	36900	6154	1082	7476
		5	341400	148400	8498	1982	3103	36800	3630	4121	5346
		6	334300	148400	11694	2040	2661	39200	3521	4574	5229
		7	338700	153300	9769	1949	2991	38500	3655	4237	5381
		8	339900	152800	10288	2052	2750	35800	3647	4601	5537
		9	337900	152300	8822	1941	2730	38600	3935	4395	5958
		12	339600	151100	4279	2222	2567	42100	7534	1144	6007
	12B-19	1	347900	150200	7458	1641	2924	36400	3341	3739	4844
		2	350600	152900	2649	3193	3161	38100	5765	1386	6445
		3	343900	153800	2463	3657	3654	35500	6359	972	7606
		4	341800	149900	7320	2362	2959	36100	4098	3335	6080
		6	335200	148700	10545	2014	3114	36800	3579	4447	5393
		7	343000	149900	9974	1908	3094	39200	3893	4211	5227
		8	342200	153000	9854	1949	3139	40700	3541	4320	5443
		10	344600	154200	6942	2103	2883	37300	6066	2968	5357
		11	342400	154600	5836	2101	2974	39200	7276	2342	5849
	12B-20	1	352500	153100	6111	1959	3000	33700	4313	2989	5443
		2	344200	150400	6533	1810	2984	39000	3799	2777	4935
		3	343600	155400	2830	3035	3384	40800	5787	1592	6793
		4	345700	154700	2629	3673	3574	36700	6550	614	7860
		7	333100	147600	14746	2080	2983	39900	3369	4331	5184
		8	336700	150600	10090	1973	3178	35300	3595	4376	5690
		10	341500	154300	7146	2461	2946	37800	5322	3321	5995
		11	327200	147900	17741	2149	2444	37600	5411	3859	5505
		12	340600	154700	4938	2173	2723	37600	7483	1855	5453
DIL-8B	8B-21	1	345500	158000	2466	3797	3407	37400	4419	1158	6768
		2	344200	153000	7095	2022	3061	37900	3314	2966	4949
		3	344800	152300	4735	2525	3055	33300	4193	2383	5576
		5	343400	154100	4885	2934	3343	35800	4950	1549	6536
		6	337600	153300	6539	2816	3231	40000	4390	1941	5482
		7	345500	152400	3102	2877	3146	34100	4502	1881	6064
		8	343000	152100	3176	2430	3002	37200	5025	2363	5484

	9	340200	155100	2912	3225	3668	34900	4810	1915	6429
	10	337700	151800	3453	2177	3097	37200	5641	2596	6147
8B-22	1	353400	156200	2964	3589	3142	38200	4223	1468	6415
	2	344500	154400	3410	3416	3521	43100	4184	2204	6110
	3	347200	148900	9095	2269	3031	34900	3801	3085	5515
	4	341300	150700	7714	2100	3019	37500	3904	2823	5652
	5	354800	154100	5516	2962	3181	38900	4678	1709	6347
	6	351100	153000	4288	3141	3468	37000	4501	1641	5775
	7	350200	155000	3799	3135	3569	37100	4788	1482	6425
	8	348700	154600	2714	3315	3723	35500	5221	1281	7251
	9	342200	155900	2710	3303	3674	40400	5875	1391	7418
8B-23	1	363900	150400	3450	3861	3262	37200	4501	1640	6623
	2	348700	148800	9784	2411	3208	37900	3562	3075	4593
	3	353700	147400	9061	2311	3279	35000	3519	3317	5385
	4	353200	148500	6437	2158	3013	34500	3873	2472	5347
	5	363500	151000	3105	3218	3596	37800	4741	1405	6274
	6	356900	154400	2904	3589	3831	33500	4667	2212	6379
	8	353700	151600	4244	2252	3008	37400	4799	2397	5689
	9	338200	157200	3327	3860	3945	37700	5340	1577	7339
8B-25	3	354300	146900	2105	3064	3452	37800	4446	1482	6112
	5	355100	145500	1796	2960	3719	36100	4732	1088	6731
	6	352900	146300	3089	3088	3555	37100	5176	1488	6467
	7	337400	151600	2306	3681	4317	40100	6015	1267	6949
8B-26	1	344900	153300	3710	2461	3230	36900	3921	2528	5379
	2	344400	150700	5245	1890	3148	34200	3076	3317	5257
	3	340600	149500	5624	2641	3062	38500	4057	1879	5596
	4	340500	154500	2607	2742	3264	38800	4735	1908	6726
	8	346800	149800	2496	2376	2820	40700	4928	1936	5582
8B-28	1	341300	153800	3562	2857	3302	35900	3887	1831	5705
	2	347200	153800	4404	1896	3017	35100	3374	2045	5151
	3	343500	154500	4336	2037	3148	38800	3559	2719	5399
	4	348800	155200	3400	2592	3072	37700	4438	1611	5996
	5	341400	158100	2084	3223	3321	36300	5169	1604	7498
	7	339400	152300	5208	2350	3197	34500	4018	2885	5614
	8	340500	153400	3283	2430	3096	40800	4985	1997	5471
	9	346700	152800	2932	2146	2982	39300	6209	1846	5658
8B-29	1	341600	153100	4950	2073	3001	38100	3922	2039	5556
	2	345900	153100	4878	1742	2727	37500	3215	2935	4557
	3	347600	155700	3223	2586	3058	37400	4261	1990	5741
	4	347700	153800	4580	2543	3292	37100	4087	2369	5883
	5	337700	159600	2015	3570	3330	34900	5162	1812	7518
	6	343100	150700	5358	2042	3206	35500	3564	3358	5018

		7	341400	151600	3080	2844	3164	37800	4901	1990	5943
SCL-25B	25B-1	1	367500	144900	2833	3371	3427	37500	5911	327	7608
		2	373400	151000	3808	2648	2887	35700	4047	299	5331
		3	364400	148400	5681	2754	3217	32300	6895	547	4476
		4	366000	150400	5555	2215	3071	35100	2995	547	4219
	25B-2	1	368800	147300	3263	3273	3306	39200	5778	358	6564
		2	371100	148100	4285	2840	2834	38000	3852	401	4459
		3	371400	147600	4091	2626	3367	36100	3832	198	5177
		4	367500	147100	5061	2526	2810	34000	2783	343	3529
		5	365300	148900	5720	2653	3258	33900	2641	621	4658
	25B-3	1	365500	145300	3768	3076	2959	36400	6300	456	5967
		2	366300	146400	3584	2847	2770	32300	5003	428	5300
		3	364400	145200	3260	2528	2708	35500	5291	150	5570
		4	346200	140300	26422	2789	2723	33700	27672	602	5894
		5	368500	149400	4676	2406	3014	33300	3087	465	4719
SCL-29B	29B-2	1	371300	146100	2424	2835	2853	35900	4301	112	7694
		2	370500	147400	2783	2778	2834	36300	4175	112	6925
		3	366900	146500	3638	2362	3050	33900	3701	278	6220
		4	370500	148200	4182	2465	3048	35900	3110	289	5344
		5	365400	147100	5069	2402	3093	37600	3396	284	5033
	29B-3	1	361600	143100	2022	3182	2501	33600	8630	128	10606
		2	371900	138500	2287	2792	2187	37200	4720	225	6207
		3	370200	138100	3081	2515	2117	38300	4219	278	6367
		4	371600	136900	2856	2222	2410	38800	4122	203	6340